

Reliability-Based Maintenance Strategies for Heat Exchanges Subject to Fouling

by

Manzoor-ul-Haq

A Thesis Presented to the

FACULTY OF THE COLLEGE OF GRADUATE STUDIES

KING FAHD UNIVERSITY OF PETROLEUM & MINERALS

DHAHRAN, SAUDI ARABIA

In Partial Fulfillment of the
Requirements for the Degree of

MASTER OF SCIENCE

In

MECHANICAL ENGINEERING

April, 1995

INFORMATION TO USERS

This manuscript has been reproduced from the microfilm master. UMI films the text directly from the original or copy submitted. Thus, some thesis and dissertation copies are in typewriter face, while others may be from any type of computer printer.

The quality of this reproduction is dependent upon the quality of the copy submitted. Broken or indistinct print, colored or poor quality illustrations and photographs, print bleedthrough, substandard margins, and improper alignment can adversely affect reproduction.

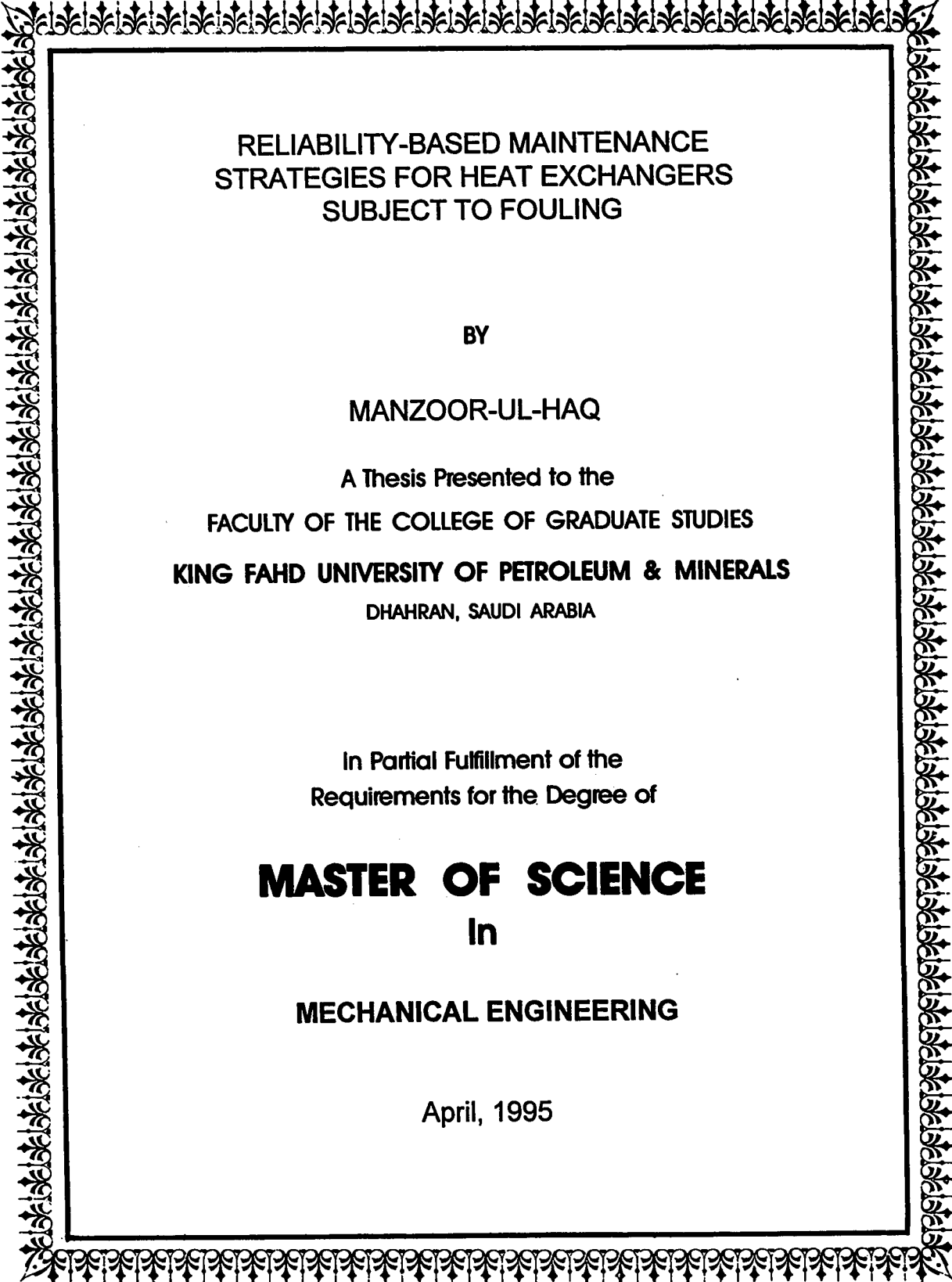
In the unlikely event that the author did not send UMI a complete manuscript and there are missing pages, these will be noted. Also, if unauthorized copyright material had to be removed, a note will indicate the deletion.

Oversize materials (e.g., maps, drawings, charts) are reproduced by sectioning the original, beginning at the upper left-hand corner and continuing from left to right in equal sections with small overlaps. Each original is also photographed in one exposure and is included in reduced form at the back of the book.

Photographs included in the original manuscript have been reproduced xerographically in this copy. Higher quality 6" x 9" black and white photographic prints are available for any photographs or illustrations appearing in this copy for an additional charge. Contact UMI directly to order.

UMI

A Bell & Howell Information Company
300 North Zeeb Road, Ann Arbor, MI 48106-1346 USA
313/761-4700 800/521-0600



RELIABILITY-BASED MAINTENANCE
STRATEGIES FOR HEAT EXCHANGERS
SUBJECT TO FOULING

BY

MANZOOR-UL-HAQ

A Thesis Presented to the
FACULTY OF THE COLLEGE OF GRADUATE STUDIES
KING FAHD UNIVERSITY OF PETROLEUM & MINERALS
DHAHRAN, SAUDI ARABIA

In Partial Fulfillment of the
Requirements for the Degree of

MASTER OF SCIENCE

In

MECHANICAL ENGINEERING

April, 1995

UMI Number: 1375330

**UMI Microform 1375330
Copyright 1995, by UMI Company. All rights reserved.**

**This microform edition is protected against unauthorized
copying under Title 17, United States Code.**

UMI

**300 North Zeeb Road
Ann Arbor, MI 48103**

11

KING FAHD UNIVERSITY OF PETROLEUM AND MINERALS
DHAHRAN, SAUDI ARABIA
COLLEGE OF GRADUATE STUDIES

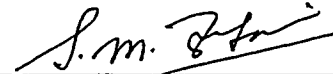
This thesis, written by

Manzoor-ul-Haq

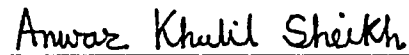
*under the direction of his Thesis Advisor, and approved by his Thesis committee, has
been presented to and accepted by the Dean, College of Graduate Studies, in partial
fulfillment of the requirements for the degree of*

**MASTER OF SCIENCE IN MECHANICAL
ENGINEERING**

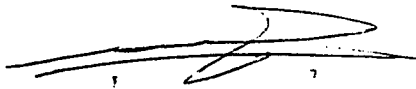
Thesis Committee :



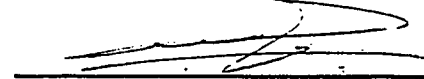
Dr. Syed M. Zubair (Chairman)



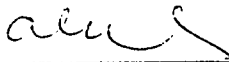
Dr. Anwar K. Sheikh (Co-Chairman)



Dr. Muhammed O. Budair
Department Chairman



Dr. Mohammed O. Budair (Member)



Dr. Ala H. Rabeh
Dean, College of Graduate Studies



Dr. O. A. Ashiru (Member)

Date: 28.6.95



**Reliability-Based-Maintenance Strategies for
Heat Exchangers Subject to Fouling**

Manzoor-ul-Haq

Mechanical Engineering

April 1995

Dedicated to

**My beloved parents, whose sacrifices enabled me
to reach this stage,**

and

My younger brother Imtiaz

Acknowledgments

In the name of Allah, Who is most beneficent and most merciful.

He has made subject to you, the night and the day, the sun and the moon. And the stars are in subjection: Verily in this are signs for men who are wise. It is He who sends down rain from the sky; From it ye drink, And out of it (grows), The vegetation on which Ye feed your cattle.

(The Holy Quran, Surah XVI)

All praise be to Almighty Allah Who gave me the patience and perseverance to carry out this work successfully.

Acknowledgement is due to King Fahd University of Petroleum and Minerals (KFUPM)/Research Institute (RI) for providing support to this work.

I am deeply appreciative of my thesis committee Chairman Dr. S. M. Zubair and Co-Chairman Prof. A. K. Sheikh for their constant help, guidance and the countless hours of attention they devoted throughout the course of this work. My

innumerable interruptions into their offices always generated a cheerful response. Thanks to Dr. Zubair and Dr. Sheikh for introducing me to a new dimension in the world of heat-transfer.

Thanks are due to my thesis committee members Dr. M. O. Budair and Dr. O. A. Ashiru for their interest, co-operation, advice and constructive criticism.

I am also indebted to Dr. M. O. Budair, as department chairman and other faculty members for their support, encouragement during my stay as a graduate student in the department.

I am also grateful to Mr. Abdul Quddus of RI (Div. V), whose continued help, assistance and guidance made the experimental task possible. I greatly appreciate his role in achieving my objectives related to experimental work.

Lastly, but not the least, thanks are due to my family members and friends, specially Mr. Rizwan I. Butt, for their support and understanding, throughout my academic career and special thanks to my wife for her patience and encouragement throughout this work.

Table of Contents

Acknowledgements	i
List of Figures	vii
List of Tables	xii
Abstract (Arabic)	xv
1 Introduction	1
2 Literature Review	4
2.1 Historical Background and Fouling Models	4
2.1.1 Historical background	4
2.1.2 Mathematical models of fouling	5
2.2 A General Review on Present Fouling Research	8
2.2.1 Literature review on different types of fouling	9
2.2.2 Fouling control methods	17

	iv
2.3 Economic Impact of Fouling	19
2.3.1 Capital expenditures	19
2.3.2 Additional energy costs	23
2.3.3 Maintenance costs	25
2.3.4 Costs due to loss in production	26
2.3.5 Safety	28
2.4 Maintenance Strategies of Heat Exchangers Subject to Fouling	28
3 Collection and Physical Characterization of Fouling Data	31
3.1 Introduction	31
3.2 <i>CaCO</i> ₃ Scaling	32
3.2.1 Experimental work regarding <i>CaCO</i> ₃ scaling	32
3.2.2 Fouling characteristics at different sections	41
3.2.3 Microscopic characterization of <i>CaCO</i> ₃ crystals under flow conditions	44
3.2.4 Some observations on initial testing and experimentation	49
3.2.5 Replicate experiments at some test sections for statistical in- vestigation	57
3.3 Corrosion Fouling	58
3.3.1 Experimental details regarding corrosion fouling	58

4 Reliability-Based Statistical Analysis and Interpretation of Fouling

Data 68

4.1 Stochastic Nature of Fouling Phenomena 68

4.2 Fundamentals of Statistical Analysis 69

 4.2.1 Reliability function (Distribution of time to survive critical
 fouling) 70

 4.2.2 Probability density function 71

4.3 Reliability-Based Statistical Analysis for $CaCO_3$ Scaling 71

 4.3.1 Results and discussion 83

4.4 Corrosion Fouling 83

 4.4.1 Increased fouling resistance 83

5 Mitigating Techniques and Cost-Based Maintenance Strategies 88

5.1 Mitigating Fouling During Plant Operation and Shutdown 91

 5.1.1 On-line chemical treatment 91

 5.1.2 On-line mechanical techniques 92

 5.1.3 Off-line chemical cleaning 95

 5.1.4 Off-line mechanical techniques 95

5.2 Economics of Maintenance Against Fouling Based on Linear Growth

 Law - An Industrial Application 96

 5.2.1 Thermal Analysis 97

5.2.2	Economic Analysis	108
5.2.3	Derivation of dimensionless cost function	110
6	Conclusions and Recommendations	128
	Appendix	131
A	Statistical Characterization of Fouling Data	131
A.1	Empirical Distribution of Random Variable "t"	132
A.2	The Postulated Distribution for $CaCO_3$ Scaling	133
A.2.1	Estimation of Parameters C and α	134
A.3	Corrosion Fouling	135
B	Tabulated Results of Reliability-Based Statistical Data Analysis	137
C	Method for Determination of Enthalpy of Petroleum Fractions	142
	Nomenclature	144
	References	148
	Vita	161

List of Figures

2.1 Typical fouling resistance-time curves.[52] 7

3.1 Pi-chart showing the relative effects of different types of fouling [51] . 33

3.2 Schematic representation of the scale deposition mechanism. [73] . . . 35

3.3 A general photograph of the scale-deposition experiment rig 36

3.4 Schematic of the scale-deposition equipment. 39

3.5 A test specimen details. 40

3.6 An end view of a test specimen. 40

3.7 Fouling resistance-time curves for five test sections. 45

3.8 Teflon holder photograph 46

3.9 Time-1 hr, X1500 ; Negligible crystals and the shape of crystal, if
any, is unidentifiable 52

3.10 The corresponding EDXSA plot 52

3.11 Time-1.25 hr, X150 ; Crystals are nucleating and growing at preferential sites. Rhombic, sand-rose like, needle like and combination of needle & flower shape. 53

3.12 The corresponding EDXSA plot 53

3.13 Time-1.5 hr, X170 ; Irregularly ordered, colonial growth of needle as well as half moon shaped 54

3.14 The corresponding EDXSA plot 54

3.15 Time-2 hr, X ; Thickly populated with rhombic, sand-rose like, needle-like and needle-flower shaped crystals 55

3.16 The corresponding EDXSA plot 55

3.17 Fouling resistance-time curve for section # 1. 62

3.18 Fouling resistance-time curve for section # 2. 63

3.19 Fouling resistance-time curve for section # 3. 64

3.20 The corrosion fouling resistance-time curves [29] 67

4.1 Flow chart of the computer program to determine the distribution functions. 73

4.2 Linear regression lines (Section # 1). 74

4.3 Superimposed curves for reliability (Section # 1). 75

4.4 Superimposed curves for PDF (Section # 1). 76

4.5 Linear regression lines (Section # 2). 77

4.6 Superimposed curves for reliability (Section # 2). 78

4.7 Superimposed curves for PDF (Section # 2). 79

4.8 Linear regression lines (Section # 3). 80

4.9 Superimposed curves for reliability (Section # 3). 81

4.10 Superimposed curves for PDF (Section # 3). 82

4.11 Regression lines for corrosion fouling curves. 85

4.12 Reliability curves for corrosion fouling 86

4.13 PDF curves for corrosion fouling 87

5.1 heat exchanger cost versus fouling factor and construction material [2] 90

5.2 A Simplified crude oil preheat train [71] 98

5.3 Sample functions of linear random fouling growth law 100

5.4 The effect of $\sqrt{\alpha}$ with increasing risk level p , on dimensionless planned
maintenance interval, t_p/\hat{C} . See Fig.(5.3) 101

5.5 A flow diagram of a computer program to determine the effectiveness
of heat exchanger at one particular time step. [Modified version of
the flow chart proposed by Casado [71], incorporating random linear
fouling growth law.] 106

5.6 Decrease in effectiveness of heat exchanger, with an increase in oper-
ating time, undergoing linear deterministic fouling (based on data in
Table 5.1 [71]). 107

5.7 Total daily cost for data by Casado [71] (plot of Eq.(5.31) for $\alpha=0$, or for $p = 0.5$ for any $\sqrt{\alpha}$.) 112

5.8 Total daily costs at varying risk level p and scatter parameter $\sqrt{\alpha}$. . 113

5.9 Total daily costs at varying risk level p and and scatter parameter $\sqrt{\alpha}$.114

5.10 Total daily costs at varying risk level p and and scatter parameter $\sqrt{\alpha}$ 115

5.11 Cost optimizing function. 118

5.12 Dimensionless cost as a function of dimensionless time, for different risk level p and scatter parameter $\sqrt{\alpha}=0.2$. The cost parameters γ_1 , γ_2 and γ_3 are 0.32914, 0.13042 and 1.0 respectively 119

5.13 Dimensionless cost as a function of dimensionless time, for different risk level p and scatter parameter $\sqrt{\alpha} =0.3$. The cost parameters γ_1 , γ_2 and γ_3 are 0.32914, 0.13042 and 1.0 respectively 120

5.14 Dimensionless cost as a function of dimensionless time, for different risk level p and scatter parameter $\sqrt{\alpha} =0.4$. The cost parameters γ_1 , γ_2 and γ_3 are 0.32914, 0.13042 and 1.0 respectively 121

5.15 The effect of cost parameter γ_1 on the dimensionless cost. These curves represent either a deterministic case $\sqrt{\alpha} =0$, or cost corresponding to $p = 0.5$ for any value of $\sqrt{\alpha}$ The case by Casado [71] is represented by curve with $\gamma_1 = 0.32914$ 122

- 5.16 The effect of cost parameter γ_2 on the dimensionless cost. These curves represent either a deterministic case $\sqrt{\alpha}=0$, or cost corresponding to $p = 0.5$ for any value of $\sqrt{\alpha}$. The case by Casado[71] is represented by curve with $\gamma_2 = 0.13042$ 123
- 5.17 The effect of cost parameter γ_3 on the dimensionless cost. These curves represent either a deterministic case $\sqrt{\alpha}=0$, or cost corresponding to $p = 0.5$ for any value of $\sqrt{\alpha}$. The case by Casado [71] is represented by curve with $\gamma_3 = 1.0$ 124
- 5.18 The sensitivity of dimensionless cost fuction w.r.t γ_1 . This curve represent either a deterministic case $\sqrt{\alpha}=0$, or cost corresponding to $p = 0.5$ for any value of $\sqrt{\alpha}$ 125
- 5.19 The sensitivity of dimensionless cost fuction w.r.t γ_2 . This curve represent either a deterministic case $\sqrt{\alpha}=0$, or cost corresponding to $p = 0.5$ for any value of $\sqrt{\alpha}$ 126
- 5.20 The sensitivity of dimensionless cost fuction w.r.t γ_3 . This curve represent either a deterministic case $\sqrt{\alpha}=0$, or cost corresponding to $p = 0.5$ for any value of $\sqrt{\alpha}$ 127

List of Tables

3.1	Fouling related data from a local refinery unit. [72]	34
3.2	Trial run results.	42
3.3	Experimental data regarding $CaCO_3$ scaling for section # 1.	59
3.4	Experimental data regarding $CaCO_3$ scaling for section # 2.	60
3.5	Experimental data regarding $CaCO_3$ scaling for section # 3.	61
3.6	Corrosion related experimental data. [29]	66
5.1	The relevant properties and cost parameters for the fluid streams in the heat exchanger. [71]	102
B.1	Parameters and non-parametric results for $CaCO_3$ scaling - Section #1.	138
B.2	Parameters and non-parametric results for $CaCO_3$ scaling - Section #2.	139
B.3	Parameters and non-parametric results for $CaCO_3$ scaling - Section #3.	140

B.4 Parameters and non-parametric results for corrosion fouling. 141

Abstract

Name: Manzoor-ul-Haq
Title: Reliability-Based Maintenance Strategies for
Heat Exchangers Subject to Fouling
Major Field: Mechanical Engineering
Date of Degree: April, 1995

The present research includes fouling related experimental work and the reliability-based statistical analysis of the fouling data. In this regard, several replicate experiments related to CaCO_3 scaling under identical operating conditions are conducted. In addition, data is obtained from literature regarding corrosion fouling. The fouling curves are drawn as a function of time and corresponding to a critical fouling resistance $R_{f,c}$, the probability distribution of time 't' to reach this critical level of fouling and some of its associated functions are determined. The distribution for time to foul 't' for CaCO_3 is found to be inverted normal or α -distribution, whereas for the case of corrosion it is a modified version of α -distribution. Thermo-economic analysis is carried out for a heat-exchanger used in the preheat train of crude oil refining process. In this regard, a dimensionless cost function is derived and the influence of various parameters on the optimum costs and maintenance period have been studied by incorporating a risk factor p .

Master of Science Degree
Department of Mechanical Engineering
King Fahd University of Petroleum and Minerals
Dhahran, Saudi Arabia
April, 1995

ملخص الرسالة

إسم الباحث : منظور الحق
 عنوان الرسالة : استراتيجيات الصيانة القائمة على الإعتمادية للمبادلات
 الحرارية المعرضة للترسب
 التخصص الرئيسي : الهندسة الميكانيكية .
 تاريخ الدرجة : إبريل ١٩٩٥ م .

إن البحث العالي يحتوي على تجارب عملية وتحليل إحصائي لنتائج متعلقة بمشكلة الترسب على الأسطح الداخلية لمعدات نقل الحرارة . وفي هذا المجال تم إجراء العديد من التجارب المعادة والمتعلقة بترسب قشور من كربونات الكالسيوم تحت ظروف تشغيل متطابقة . بالإضافة إلى ذلك تم الحصول على نتائج من الأبحاث السابقة خاصة بالترسب الناتج عن التآكل . منحنيات الترسب تم رسمها كدالة في الزمن (t) وتقابل مقاومة حرجة ($R_{f.c.}$) كما تم تحديد توزيع الإحتمالات للزمن (t) المطلوب للوصول إلى هذا المستوى الحرج من الترسب مع بعض الدوال ذات الصلة . إن توزيع زمن الترسب (t) لكربونات الكالسيوم وجد أنه توزيع طبيعي مقلوب أو مايسمى توزيع (α) بينما وجد أنه نسخة معدلة من توزيع (α) في حالة الترسب الناتج من التآكل . وقد أجريت دراسة حرارية - إقتصادية لمبادل حراري مستخدم في خط التسخين السابق لعملية تكرير الزيت الخام . وفي هذا المجال تم اشتقاق دالة تكلفة لابعدية كما تم دراسة تأثير العوامل المختلفة على التكلفة المثلى وعلى فترات الصيانة مع إدخال معامل المخاطرة (p) .

درجة الماجستير في العلوم

جامعة الملك فهد للبترول والمعادن

الظهران / المملكة العربية السعودية

أبريل ١٩٩٥ م

Chapter 1

Introduction

The heat exchangers are used extensively in several industrial applications, e.g., power generation, petroleum refining, petrochemical plants, etc., to recover heat from hot fluid streams. Its size and numbers varies from application to application. Being an important plant item in maintaining process conditions (e.g., temperature), its performance is monitored regularly to ensure the required efficiency. The major factor responsible for its decreased efficiency is the deposition of unwanted material on the heat-transfer surface, also called "fouling". The deposition of an unwanted layer represents an additional resistance to heat transfer in addition to those present in a typical design of the exchanger. In addition, the reduction of the flow area due to presence of deposits increases the pressure drop through the heat exchanger. Both these consequences represent an additional energy requirements.

In general any extensive fouling will mean that the heat exchanger will have to be cleaned on a regular basis to restore the lost efficiency. The frequency of cleaning will depend upon the severity of the fouling and its associated costs.

The costs associated with fouling of heat exchangers are very high and this is one of the main reasons for an increased research in this area. For instance, during the design stage, providing extra heat-transfer surface for a fixed duty exchanger is a frequently adopted measure. But this increases costs of manufacturing, transportation and installation. The capital costs of antifouling measures represent an additional cost component for an exchanger in operation.

Many strategies are possible for reducing, controlling or eliminating fouling problems in heat exchangers. These strategies ranges from careful design and construction of the exchangers to techniques applied during installation and operation of the exchangers. Although many of these strategies can reduce or control fouling, their benefits are difficult to quantify. The present research is aimed at devising reliability-based, cost-effective maintenance strategies for heat exchangers subject to fouling. For this purpose, experiments were performed regarding $CaCO_3$ scaling (precipitation fouling) in the Research Institute (RI) on a scaling loop test facility, simulating a single tube heat exchanger. Furthermore, data was extracted directly from the literature regarding corrosion fouling. The stochastic analysis of the avail-

able fouling data was carried out. In addition, economic aspects were quantified by incorporating a risk factor p in the cost model for a specific heat exchanger in an industrial application.

To effectively meet the desired objectives, a relevant state-of-the-art literature review was carried out as discussed in chapter 2. The details of experiments to generate fouling data and resulting fouling resistance versus time (R_f vs t) curves are presented in chapter 3. The reliability-based statistical analysis of time to reach a critical level of fouling resistance, $R_{f,c}$, for a particular set of R_f vs t curves is discussed in chapter 4.

Chapter 5 includes a discussion on mitigating techniques and a probabilistic model of cost-based-maintenance for heat exchangers subject to fouling. For this purpose thermoeconomic analysis is carried out for a specific heat exchanger used in a crude oil refining process. The results are presented in the form of a dimensionless cost function and the effect of incorporating scatter parameter ' α ' and risk factor ' p ' in the model has been studied. Finally, the outcome of the present research and related future work is outlined in chapter 6.

Chapter 2

Literature Review

2.1 Historical Background and Fouling Models

2.1.1 Historical background

The fouling of heat-transfer equipment has been one of the major unresolved problems in the design and maintenance of heat exchangers. It is becoming clear that fouling is a factor of increasing importance in the design and operation of heat exchangers [1]. Increasing energy and raw material costs, declining availability of high quality cooling water, and environmental restrictions limiting the use of certain additives that could be used to mitigate fouling, have combined to increase the importance of understanding fouling phenomena in the design and operation of heat exchangers. This increased interest in fouling is evidenced by the growth in the

volume of published literature and in the number of conferences held on the subject in recent years [2].

Fouling literature has been classified in several bibliographies. The first of these, published in 1970 by Battelle Laboratories under the sponsorship of American Society of Mechanical Engineers (ASME) Ash Deposits and Corrosion Committee, provides an extensive bibliography on corrosion and deposits from combustion gases [2]. In 1979, AERE Harwell in cooperation with Hemisphere publishing corporation, began publication of a quarterly awareness journal, "Fouling Prevention Research Digest". The journal provides an annotated bibliography of recent literature pertaining to fouling. Several review articles have documented the state of the art of fouling knowledge. In 1974, Taborek et al. [3] provided a systematic treatment of fouling that has been recognized as a major contribution to the subject of fouling. Epstein presented an overview of fouling as discussed in [2], in which he proposed six basic types of fouling which has since been widely accepted. A general review of cooling water fouling was presented in 1977 [2]. The most recent overall reviews on cooling water fouling are presented by Knudsen [4, 5]

2.1.2 Mathematical models of fouling

The process of heat-exchanger fouling involves the deposition of unwanted material on the heat-transfer surface. Such deposition causes an increase in the resistance to

heat transfer and often causes a significant increase in friction loss as well. As the deposit becomes thicker, and depending on its physical strength, a certain amount of material may be removed from the surface and re-entrained in the flowing stream. The following material balance equation expresses the rate of change of the fouling resistance as a function of the deposition rate (ϕ_d) and the removal rate (ϕ_r) as [6],

$$dR_f/dt = \phi_d - \phi_r \quad (2.1)$$

It should be noted that fouling is a dynamic process. Therefore, the fouling resistance changes with time in a manner dictated by the deposition and removal rates. The above equation can be represented by a fouling resistance-time curve which is shown in Fig. 2.1. The shape of the curve is indicative of the phenomena occurring during the fouling process. A linear relationship (curve A) is generally characteristic of tough, hard, adherent deposits, and indicates that the deposition rate minus the removal rate is constant. A falling rate or asymptotic curve (curve B) may be obtained even though there is no removal, due to retardation forces that increase as the deposits builds up. An asymptotic relationship (curve C) is generally characteristic of "soft" or fragile deposits, which flake off easily due to the shearing force of the fluid flowing past them. This behavior can be obtained if the deposition rate is constant and removal rate is proportional to the thickness of the deposit. This assumption leads to a simple exponential equation as shown in the figure. Occasionally a delay time t_D is observed before deposition occurs. During this time

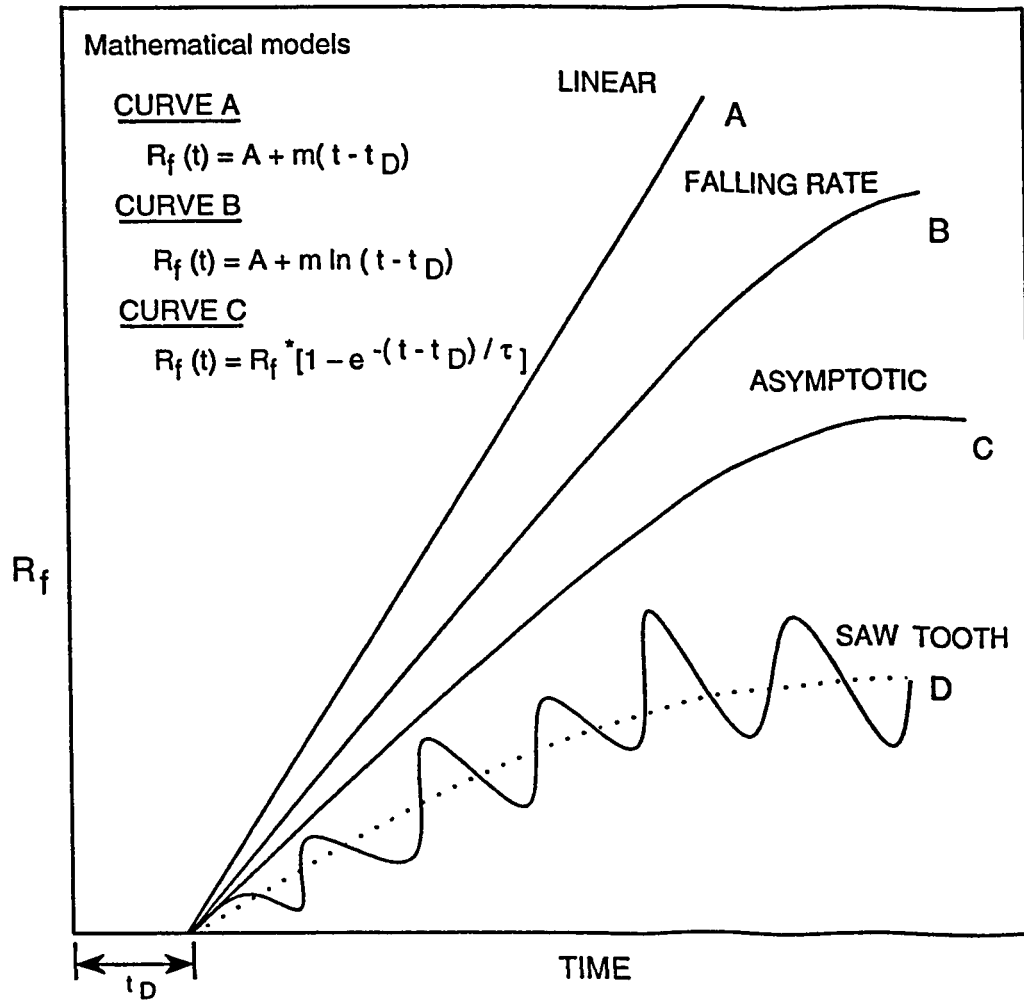


Figure 2.1: Typical fouling resistance-time curves. [52]

nuclei are forming on the surface; as their population grows, gross deposition occurs and create resistance to heat-transfer.

2.2 A General Review on Present Fouling Research

Fouling of heat-transfer equipment received attention of many engineers and scientists, as the time passed. A lot of experimental and analytical work has been carried out and published to date. An increased knowledge and research in this area made it necessary to review the existing fouling section of widely used Tubular Exchanger Manufacturer Association (TEMA) standards. In this regard, a joint committee of Heat Transfer Research Institute (HTRI) and TEMA was set up to review the fouling section of TEMA standards and their recommendations were included in the final report compiled by Chenoweth [7]. The changes of 1988 TEMA standards and their effect on mechanical and thermo-hydraulic design have been critically reviewed by Taborek and Aurioles [8].

Pilavachi and Isdale [9] presented information on research activities aimed at controlling the fouling behavior of heat exchangers in industry. Hesselgreaves [10] devised a simple analysis to examine the relationship between the pump or fan characteristics and the performance of basic heat-exchanger surfaces with a given fouling deposit (or resistance). Konings [11] presented guide values for the fouling

resistances of cooling water on the basis of field and laboratory experiments as well as the published data. Recommendations were given by Watkinson [12] to assign fouling resistances for augmented tubes in terms of corresponding plain-tube fouling resistances. A technique to measure the local fouling resistance was devised by Thompson and Bridgewater [13] and its plant demonstration was carried out. Crittenden and Khater [14] have given a more general analysis of the selection of fouling resistances, taking into account the costs of plant cleaning and loss of revenue during shut-down, with particular reference to the petroleum and petrochemical industries.

2.2.1 Literature review on different types of fouling

There is more than one way to classify the types of fouling, the very fundamental classification that was proposed by Epstein at the 1979 International Conference on the Fouling of Heat Transfer Equipment [1] has been widely adopted. This scheme classifies fouling according to the principal process that gives rise to the phenomenon.

Particulate fouling

Suspended particulate matter is encountered in many industrial fluid streams and the accumulation of particles from a fluid stream on heat-exchanger surfaces is a common fouling phenomenon [15]. For example, river water is used as a cooling medium, particles of clay and mineral matter are carried into the river by run-off and the subsequent concentration can be high or low depending on local rainfall

conditions.

Steinhagen and Blochl [16] carried out experiments to determine the effects of particle size, particle concentration, and particle/fluid combination on fouling. The influence of the above parameters on the fouling resistance was measured. The model to predict the particulate fouling behavior of repeated rib tubes was presented by Kim and Webb [17]. The influence of flow velocity, wall temperature, heat flux, particle concentration and particle size on the fouling behavior was compared to the prediction of several fouling models from the literature by Steihagen et al. [18]. Chan et al. [19] presented fouling data for geothermal brines with different pH values, chemical compositions, and thermal-hydraulic conditions. The effects of supersaturation, pH, Reynold number and concentration of ion in the brine solution on the formation of silica scale in the heat-exchanger tubes were discussed and silica deposition model was proposed. Neusen et al. [20] presented a semi-analytic model for silica fouling.

Biological fouling

Biological growth on heat-exchangers surfaces can be roughly divided into two groups depending on the size of the organisms. For example, microfouling is usually associated with larger animals such as mussels, barnacles, hydroids and serpulid worms and vegetation such as seaweed. These are particularly associated with sea

water or estuarine cooling water systems. On the other hand, micro-organisms such as bacteria, fungi and algae may be the sources of surface contamination. Because such fouling involves living matter, the temperature over which it can exist is limited between 0 and 90°C. The highest concentration occurs roughly in the range 20 to 50°C. Excessively thick layers of biological material are possible under certain conditions. In cooling water systems particularly, the presence of a biofilm may promote other fouling processes such as corrosion. For instance, under the slime layer it is quite common to find pitting corrosion [15].

Chemical reaction fouling

Oufer and Knudsen [21] developed a model to predict the fouling on a heat transfer surface under local boiling conditions, due to the deposition of unwanted materials, which were products of a given chemical reaction. Panchal and Watkinson [22] also developed a fouling model on the premise that the chemical reaction for generation of precursor can take place in the bulk, in the thermal-boundary layer, or at the fluid wall interface depending upon the interactive effects of fluid dynamics, heat and mass transfer, and the control parameters influencing the chemical reaction. Fryer et al. [23] obtained an optimum combination of exchanger size and tube-side temperature for asymptotic reaction fouling.

Freezing fouling

The deposition of a layer of a solid material derived from the process fluid itself through cooling down to its freezing point reduces the heat-transfer rate. Examples of freezing would be the formation of ice in a heat exchanger during the production of chilled water or deposits formed in margarine coolers or phenol coolers [15]. The nature of the deposits will depend on the fluid being processed. As a rule, freezing fouling is associated with temperatures well below 100°C and may require temperatures much closer to, or below, ambient [15].

Corrosion fouling

When any metallic heat-transfer surface is exposed to a corrosive liquid medium the products of corrosion can foul the surface, provided the pH of that medium is not such as to dissolve the corrosion products as they are formed. Corrosion commences immediately if a surface is brought into contact with the corrodant. Furthermore, the corrosion products are such a potent foulant that an effect on the heat transfer is observed immediately. Not only are the effects of corrosion fouling probably quicker to appear than those of other categories of fouling, but their ultimate effect on heat transfer is as great as that of other categories of fouling. It is a very important phenomenon because loss of material due to corrosion of heat-transfer surface could lead to the failure of the surface in a given operation. Somerscales classified corrosion fouling into two types [24]: ex-situ and in-situ. As a result of corrosion

in heat-transfer systems, the corrosion products may be released into the flowing stream either in particulate form or as dissolved species. The material may then be deposited on heat-transfer surfaces and fouling thus resulted is ex-situ. Likewise, the corrosion fouling due to corrosion products formed on the heat-transfer surface is known as in-situ corrosion.

Corrosion mechanisms damage tube materials in service water system heat exchangers which eventually result in leakage across the tube wall. Witt [25] has indicated that the primary cause of service water degradation is corrosion and erosion. An extensive research is going on to combat the problem of corrosion fouling properly in industrial applications. Panchal and Saccceer [26] presented short-and long-term biofouling and corrosion fouling results for a rectangular-flow channel and for the spirally fluted tubes made of aluminum. Lister [27] reviewed the mechanism of corrosion and corrosion product movement and fouling in heat-transport systems of thermal electric generating stations. Oil and coal fired boilers were considered along with nuclear power systems. A model to predict the particle size distribution in a fluid and at the surface due to corrosion fouling is discussed by Beal and Armstrong [28].

Somerscales and Kassemi [29] carried out extensive experiments on in-situ corrosion related fouling and obtained replicate data of fouling resistance as a function

of time. It should be noted that they only presented the data and no specific data analysis was carried out. Considering the stochastic nature of this data, a reliability-based statistical analysis is carried out as discussed in chapter 4.

Precipitation fouling

Precipitation fouling may be defined as the phenomenon of a solid-layer deposition on a heat-transfer surface arising primarily from the presence of dissolved inorganic salts in the flowing solution which exhibit supersaturation under the process conditions. For example, a solution which is evaporated beyond the solubility limits can cause supersaturation. Another process condition causing the supersaturation to occur is due to a solution containing a dissolved salt of normal solubility is cooled below its solubility temperature or a solution containing a dissolved salt of inverse solubility is heated above its solubility temperature. Finally, it may also be due to mixing of different streams leading to creation of supersaturated conditions [30].

The industrial systems and operations in which the problem of precipitation fouling is of major significance are cooling water system, steam generation system, saline water desalination system, geothermal brine system and potable water supply system.

Calcium carbonate scaling

The term "scaling" is generally used to describe a dense crystalline deposit, well bounded to the metal surface. It is often associated with the crystallization of salts (e.g., $CaCO_3$) of inverse solubilities under heat-transfer conditions. Taborek et al. [3] described two mechanisms of scaling as

- Crystallization of relatively pure $CaCO_3$ in which the scale is well bounded and removal processes are ineffective.
- Crystallization of $CaCO_3$ contaminated by precipitating impurities and depositing particulate matter, in this case the scale layer is weaker and removal processes are effective.

Many efforts have been devoted to the study of $CaCO_3$ batch precipitation kinetics in controlled systems under conditions of both spontaneous precipitation [31] and seeded precipitation [32].

Many industrial applications e.g., cooling tower or applications involving sea water for cooling purpose face the problem of $CaCO_3$ scaling in the heat-transfer equipment and, therefore, received a particular attention of many researchers. Fryer [33] conducted the research to investigate the similarities between two types of temperature dependent fouling from geothermal fluids and food. A systematic study of scaling characteristics of cooling tower water was conducted by Morse and Knudsen

[34], Story and Knudsen [35], Lee and Knudsen [36] and Coates and Knudsen [37]. This is a somewhat extensive investigation to determine the effect of the various parameters that offer the fouling (or scaling) characteristics of cooling tower water; that includes the flow velocity, surface temperature, and water quality parameters. Practical and fundamental aspects of precipitation fouling ($CaCO_3$ scaling) were reviewed by Hasson [30] by considering the background of known physico-chemical principles. The problem of defining the precipitation fouling tendency was considered by reviewing principles of solution equilibria and of precipitation kinetics for salt systems frequently encountered in heat-exchanger applications. A model for improved prediction of $CaCO_3$ scale deposition in heat exchangers of secondary loops, typically used in thermal and nuclear power plants was presented by Tretyakov [38]. Branch and Steinhagen [39] modeled fouling in shell-and-tube heat exchangers by combining Hasson's ionic-diffusion model for $CaCO_3$ scaling with a model for predicting the temperature distribution by Gaddis and Schlunder [40].

It should be noted that the data presented and analysed by Knudsen and coworkers [34, 35, 36, 37] is based on deterministic approach as illustrated in Fig.2.1, however, due to randomness of the fouling process, the fouling growth models [e.g., $R_f(t) = m(t - t_o)$] can be properly explained by taking the repeated data at a specific sections of the heat exchanger tubes under the same thermal-hydraulic conditions, this will demonstrate the nature of randomness of parameters of the fouling

model. For this purpose, several replicate experiments under nominally identical operating conditions are conducted in the laboratory to observe the time dependent growth of $CaCO_3$ scale in a heat exchanger tube. The relevant details are presented in chapter 3.

Mixed fouling

Frequently two or more mechanisms may be present. Heat-exchangers through which cooling water passes may be subject to biofouling, corrosion and particulate deposition. Chemical reaction fouling may be accompanied by particulate deposition and corrosion whilst changes in operating conditions, either of the heat exchanger itself or in the process plant of which it forms a part, may change the nature of the fouling [15].

2.2.2 Fouling control methods

Yang et al. [41] used a spiral wire to augment the heat transfer inside the tubes of surface condensers or shell-and-tube heat exchangers. Experimental investigations on the cleaner-augmenter and the comprehensive evaluation criterion for the device as a fouling cleaner were presented. A spiral tubulator was used by Kim [42] to enhance the rate of the heat-transfer inside the tubes in shell and tube heat exchangers. Based on the experimental investigations, the relations among the heat transfer, drag, effectiveness of cleaning the foul, and the geometric variables of the

cleaner/augmenter were found.

A variable antifoulant treatment was made by Dickakian [43] according to the daily fouling analysis by a fouling analyzer. It provided economical, optimal and alert of dramatic changes in crude oil fouling characteristics. Fouling experiments were carried out by Crittenden et al. [44] with light Arabian crude oil (containing 10 % waxy residue from a crude oil tank) flowing inside 3/4 inch OD, 14 BWG heat exchanger grade tubes of a pilot scale recycle flow test rig. A greater reduction in fouling appears to occur with inserts of higher loop density and they concluded that the presence of an insert can alter the hydrodynamics in a beneficial manner.

Miyuki et al. [45] observed that pitting and crevice corrosion resistance of stainless steel was improved with an increase in the amount of $Cr + 3Mo(+10N)(\%)$. Schwarz et al. [46] carried out various chemical treatment programs to minimize fouling of surface condensers and service water heat exchangers, as well as to meet carbon steel and 90-10 Cu-Ni corrosion rate goals.

Knudsen [47] showed that with appropriate chemical treatment, most cooling water will foul only minimally so that continuous operation of heat exchangers was possible. He further concluded that the fouling characteristics of most cooling water was such that fouling may be decreased by low temperatures and high velocities.

An extensive summary of the fouling control methods which are currently used in industrial applications are presented in chapter 5.

2.3 Economic Impact of Fouling

An understanding of the economic penalties associated with fouling is one of the primary reasons for greater interest in the fouling research. Pritchard [48] presented cost estimates associated with fouling in Britain. Thackery [49] estimated the overall annual cost of surface fouling in U.K is about 0.3 % of GNP (approximately \$1 billion). The order of magnitudes of these estimates is confirmed by Van Nostrand et al. [50] while investigating the fouling related costs for the U.S specific refinery units. Steinhagen et al. [51] indicated the fouling-related costs for New Zealand at about \$30 to \$46 million which is about 0.1 % to 0.17 % of the annual GNP. It should be emphasized that the costs associated with fouling can be classified under four main headings: Capital Expenditures, Fuel Costs, Maintenance Costs and Loss of Production [52].

2.3.1 Capital expenditures

This section covers increased cost of heat exchangers due to fouling. The costs can be subdivided into a number of components. For example, costs associated with the provision of extra heat-transfer surface to allow for fouling, and the costs of extra

civil engineering works associated with the installation of larger heat exchangers. However, a substantial amount is to be allowed for adding the plant items connected with antifouling measures such as clarifiers, filters, settlers, etc. in water treatment plant. A detailed discussion on the effects of fouling on the condenser design for power plants, including heat exchanger size, flow velocity (and thus pumping power) and pressure and temperature drop was presented by Curlett and Impagliazzo [53], they concluded that an increase of 50% could be expected in the capital cost of a \$ 10M condenser for a hypothetical 600 MW coal fired power plant depending upon the fouling resistance chosen.

Provision of extra heat transfer surface

Heat exchangers are usually designed for a fixed heat-transfer duty that can be described in terms of the overall heat-transfer coefficient U and the surface area A

$$1/UA = [1/hA + R_f]_{outside} + [1/hA + R_f]_{inside} + R_w. \quad (2.2)$$

It is obvious from this relation that fouling resistance, R_f , can result in providing more surface area 'A'. The designer of a heat exchanger should therefore be able to decide what values of R_f to use before he can decide on the surface area. The increased cost of the heat exchanger due to fouling thus arises from [52]:

- (a) the extra surface area to compensate for the fouling that actually happens in practice, and

- (b) the extra surface area that is provided by the designer as an allowance against any R_f value that he may have been able to find being too low.

A value of 30-40% excess was found in a survey of heat exchanger manufacturers in the United States in 1982, leading to an extra cost of \$320M [2]. Cases are known in which the excess area has been up to an order of magnitude larger than was subsequently found to be necessary, and this suggests that about half of the extra surface area currently being built into heat exchangers may be unnecessary [52].

The cost of installation

Provision of more heat-transfer surface results in larger and heavier heat exchangers. The cost of extra-surface area must therefore be added to the cost of the civil engineering work required, involving the provision of extra space, stronger foundations, and increased transport and installation charges. On readily accessible sites, this may do little more than double the cost of heat exchanger itself, but in remote sites (e.g., on offshore oil platforms) a factor of ten may be reasonable as recommended by [52].

Capital costs of antifouling equipment

These include a range of items [52]:

- (a) systems installed on heat exchangers such as those that distribute and recirculate abrasive rubber balls or brushes through the tubes of shell-and-tube heat

- exchangers during operation to keep the tubeside clean,
- (b) the extra cost of providing non-fouling heat exchangers such as scraped surface devices or fluidized bed heat exchangers,
 - (c) pretreatment plants that reduce the fouling tendency of fluids, such as water clarifiers, filters, settlers, ion exchange etc.,
 - (d) cleaning-in-place equipment such as that installed for food processing plant, and
 - (e) dosing pumps and tanks etc. for antifouling chemicals.

The division between capital and running costs varies with the system; ball or brush cleaning systems are expensive to install, but relatively cheap to run, whereas the reverse is true for chemical dosing systems. Penner et al. [54] estimated that the capital cost in 1981 of gas clean-up systems was about 10 % of the capital cost of \$1000/kW(e) for a coal-fired power-station. The percentage of the cost might rise as much as 45% for a station designed to meet 1985 standards. The provision of anti-biofouling equipment for a proposed 300MW(e) Ocean Thermal Energy Conversion plant, the capital costs (reported in 1977) ranged from \$1-2M to \$ 10M depending upon the choice of chemical treatment or balls/brushes [55]. One of the major techniques for controlling biofouling in cooling waters is dosing with chlorine gas or hypochlorite solution. This is widely used in power industry, it was estimated that

the total capital cost of chlorination facilities in the U.S.A., calculated on a fixed charge rate of 20% related to the value of chlorine consumed, was \$267M [56].

2.3.2 Additional energy costs

The prime function of a heat exchanger is to recover expensive energy by transferring heat from one fluid stream to another. If, through reduced efficiency of a heat exchanger, energy that should have been recovered ultimately finds its way into the cooling water utility, the overall recovery efficiency of the network is reduced and two consequences follow [52]:

- (a) the shortfall in energy has to be made up from the hot utility (say steam) usually by additional burning of primary fuels such as fuel oil or coal.
- (b) the heat rejected to the cold utility has to be dissipated, usually to the atmosphere via a cooling tower.

Although these two effects represent the obvious result of heat-exchanger inefficiency on energy costs, other secondary costs may be occurred which may not always be apparent. It should be noted that if substantial increases in pressure drop across heat exchanger occur as a result of fouling, a significant increase in energy requirements for pumping is apparent. Generally, doubling the pressure drop will double the energy dissipated in the exchanger [52].

In one of the most detailed assessments made to date Van Nostrand et al. [50] calculated the fouling related expenses attributable to extra fuel burnt, lost output and maintenance and cleaning in various refinery units in the U.S.A., giving a total cost due to extra fuel burnt of \$427.7M per year, based on a process fuel cost of \$2.80/MBtu. The largest part of this was due to fouling in hydrotreaters, vis-breakers and reformers, where coking occurs. Extension of these calculations to the non-communist world suggested a cost of over \$1,500M per year, though of course the individual costs will depend upon the local cost of process fuel. The calculations for the U.S.A. is reasonably consistent with the estimate of Garrett-Price et al. [2], that is; \$700-3500M fuel burnt to overcome fouling problems, though this estimate included natural gas and coal as well as petroleum products.

The loss of heat transfer due to scale formation on boilers has been calculated [57] to lead to losses of output of 2-7% for a scale thickness of 0.8 mm, the loss depending upon the methodology and composition of the scale. Significant fuel savings could be made if some or all of the dissolved salts were removed from the feedwater beforehand, thus allowing a higher concentration factor without scaling, and a smaller loss of heat through the reduced rate of blowdown. A figure of 0.8-1.0% of fuel costs for 2% blowdown has been suggested [58], together with costs of water treatment ranging from 15% of the raw water cost for sodium zeolite ion exchange treatment to 100-400% for complete demineralization. Examples of increased pumping costs due

to fouling are hard to mention, but Terrel [59] stated that in a 250 m³ reciprocating system with a 10-inch (254 mm) main, a 10% decrease in diameter would double the pressure drop and thus the pumping power.

2.3.3 Maintenance costs

The annual sales in 1982 of companies supplying heat exchanger on-line and off-line cleaning equipment, chemicals and cleaning services in the U.S.A. were quoted as \$2,000M [2]. Substantial use is made of antifoulant chemicals in oil refineries, and Van Nostrand et al. [50] suggested that antifoulant costs of \$155,000/year for a crude unit processing 100,000 bpd, and \$40,000/year on a hydrotreater processing 25,000 bpd. Steinhagen et al. [51] have indicated that maintenance costs constitute 72.4% of the total heat-exchangers fouling costs for NewZealand.

It should be emphasized that maintenance costs can be divided into two main classes, i.e., the costs of removing fouling deposits during planned or unplanned maintenance, and the costs of chemicals or other operating costs of antifouling devices.

Costs of fouling deposit removal

The cost of cleaning an exchanger obviously depends upon the type of deposit and the size of the exchanger [52]. The deposit removal of a heat exchanger can be

carried out in two ways; either by in situ cleaning or a heat exchanger shut down and partial or complete dismantling of the equipment. Apart from the labour costs involved, the need for special cleaning chemicals may be an additional cost burden. If hazardous chemicals are employed in the cleaning process elaborate and costly safety precautions may be required.

Costs of antifouling measures

The major part of on-line cleaning is the cost associated with, e.g., water treatment. Since water is provided as a service commodity that may be used for a variety of purposes. Some of the treatment may have been unnecessary, since fouling would not have been a problem even with untreated water. However, the main uses of chemicals, for pH control and softening, clarification, and disinfection can all be considered as processes that have the effect of reducing different types of fouling (scaling, particulate fouling, biofouling, etc.) to a greater or lesser extent [52].

2.3.4 Costs due to loss in production

This is often considered to be the main cost penalty of fouling, arising from unwanted plant shut-downs or possibly contamination of the product as a result of fouling. Therefore, if a plant has to be shut-down for a heat-exchanger cleaning, the production is lost. With experience, scheduled shut-downs can be arranged to return the exchanger to normal operation before problem gets out of hand, thereby

minimizing costs in terms of lost production [52]. There are occasions, however, when fouling can cause rapid deterioration in operating efficiency, requiring immediate shut-down for cleaning. In either case, but particularly in the latter, the lost production may represent substantial sums of money. Furthermore, the likely production of off-grade material during the interval between the problem being noticed and the final decision made to stop production represents a further expense. Van Nostrand et al. [50] estimated an annual cost of \$872M due to loss of throughput caused by fouling in United States refineries, the largest part is found to be associated with crude-distillation units.

A survey of 27 ammonia plants in the U.S.A. in 1973 showed that a waste heat boiler failure could be expected every three years, leading to 5 days loss of output [60]. It does not seem unreasonable to expect that these failures were mainly associated with deposit formation, giving an annual loss of 100,000 pounds of product in 1973. Longer shutdowns were not uncommon. More reliable data are available for the power generation industry. Collier [61] stated that the loss of electricity generation attributable to steam generator unreliability in pressurized water reactors (mainly caused by corrosion associated with deposit formation) averaged 10-11 days/year. He stated that the mean duration of an outage for repairs was 20 days, and for a 1000 MW(e) plant this caused an economic loss of 4M pounds.

2.3.5 Safety

Fouling is not normally associated with safety problems, and this is probably one reason why it has not received as much attention as corrosion etc. But it can contribute to equipment failure like a boiler explosion. It has been observed that many of the explosions were caused by waterside scaling of the boiler, reducing the heat-transfer coefficient and thus allowing the metal to become overheated, increasing the creep rate and leading to cracking or creep rupture [52]. In addition, boiling beneath scale deposits can also allow salts in the boiler water to concentrate and form corrosive solutions that lead to failure of tubes through corrosion during operation.

2.4 Maintenance Strategies of Heat Exchangers Subject to Fouling

It is apparent from our earlier discussion that the cost of fouling is significant and some analytical guidelines will help to make maintenance-management decisions. Crittenden and Khater [14] showed that, if the fouling resistance-time curve can be predicted, the optimum number of plant shutdowns per year may be determined by balancing investment costs against plant cleaning costs and loss of revenue during the shut down period. Epstein [62] derived an analytical expression for maximum production, minimum cost evaporation cycles based on the Hasson-Retizer scale for-

mation model. Curlett and Impagliazzo [53] made an analysis of a power plant to predict the effect of condenser tube fouling on the performance of the plant. An inspection and repair data management through software was devised by Singh and Tweddell [63]. Zubair et al. [64] presented a probabilistic approach to characterize various fouling processes and their influence on maintenance strategies of heat exchangers subject to fouling. Some common fouling models were discussed and a strategy for planned maintenance schedules in the case of a linear fouling growth model was described. The effect of this strategy on overall costs of these repairable systems was outlined. Trade-offs were examined in terms of cost parameters.

Axson [65] discussed semi on-line cleaning procedure for the crude side of the crude-preheat exchangers using proprietary solvent that offered cleaning methods to cut costs and increase the throughput. An economic analysis of three hydrogen liquification systems with associated cost comparisons was presented by Syed et al. [66]. Walker and Cockerill [67] presented a systematic maintenance planning with respect to production reliability and product costs by use of Reliability, Availability and Maintainability (RAM) techniques which produced tangible benefits.

Barton [68] derived cost-objective function for optimizing the duration of an operating cycle of the transfer line heat exchanger, or waste-heat boiler, on ethylene furnaces for generation of high pressure steam. Wang and Gee [69] proposed a math-

emtical model for the optimum cleaning period of a power condenser. Graphical procedures were derived by Ma and Epstein [70] for predicting both the maximum production and minimum cost cycles for falling rate fouling. In an excellent article, Casado [71] carried out rigorous analysis to indicate the trend of fouling costs. He used an asymptotic fouling growth law and found that the optimum schedules are obtained by minimizing the total cost per unit time over the life of heat-exchanger equipment.

It should be noted that in the above studies, the analytical relations are essentially based on deterministic characterization of various quantities involved in the fouling model. Based on the literature review [64, 69, 71], it can be emphasized that certain elements of cost increase with respect to time whereas some other elements decrease and the overall-cost function is often a concave function with an optimum value of cleaning cycle. In chapter 5, an attempt has been made to incorporate the stochastic characterization of various quantities involved in the linear fouling model and interpreting the various cost elements in a stochastic manner in the cost-objective function.

Chapter 3

Collection and Physical

Characterization of Fouling Data

3.1 Introduction

An understanding of the economic penalties associated with fouling is, no doubt, the primary reason for increased research in this area. Power plants (thermal and/or nuclear) and chemical industries (including oil refineries) are vulnerable to fouling from time to time during their life cycle. Based on the literature review as discussed in chapter 2 and data from the local industry [72] indicated that precipitate and corrosion fouling are the major mechanisms affecting the industrial plants and their facilities.

Steinhagen et al. [51] have shown that corrosion and precipitate fouling are the major mechanisms usually found in industry, as depicted in Fig. 3.1. These results have been confirmed by the data collected from the local refinery unit [72], which is presented in Table 3.1. It was therefore decided to focus our research on the two fouling types of major concern:

- (a) Precipitation fouling - $CaCO_3$ Scaling, and
- (b) Corrosion Fouling

3.2 $CaCO_3$ Scaling

The term scaling is generally used to describe a dense crystalline deposit, well bounded to the metal surface. It is often associated with the crystallization of salts, e.g., inverse solubility characteristics of $CaCO_3$. That is, the $CaCO_3$ deposition increases with an increase in the surface temperature. The mechanism of scale deposition [73] is illustrated in Fig. 3.2.

3.2.1 Experimental work regarding $CaCO_3$ scaling

The experimental work was accomplished in the Research Institute (RI) of King Fahd University of Petroleum and Minerals (KFUPM) to generate our own data for $CaCO_3$ scaling. From a laboratory point of view, it is impractical to handle large volumes of water for making numerous tests. So the accelerated tests were

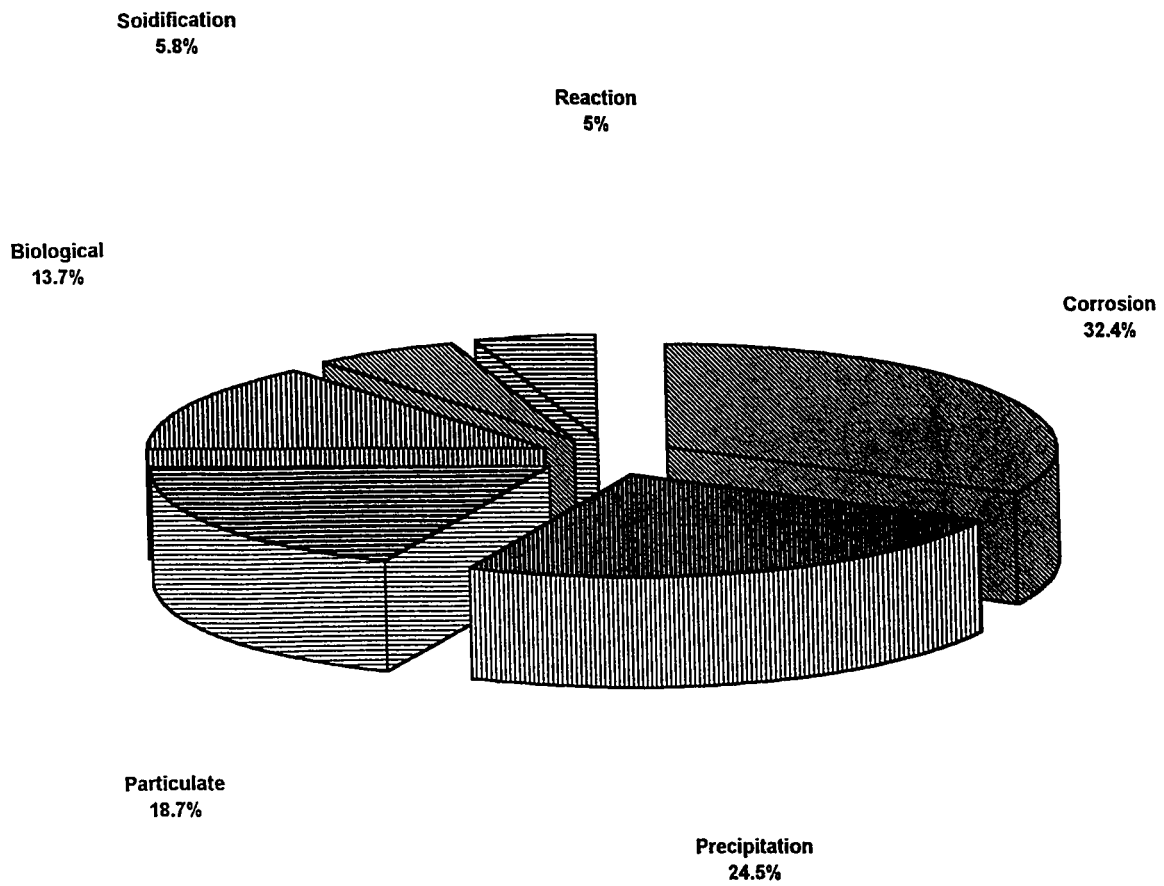


Figure 3.1: Pi-chart showing the relative effects of different types of fouling [51]

Table 3.1: Fouling related data from a local refinery unit. [72]

<i>The nature and source of scale/material deposits</i>				
Scale/Deposit from Heat Exchanger #	Color	Service	Shell Side	Tube side
19-E-201 A	Dark	Stabilizer column reboiler	Sour cude	Diesel oil
26-E-4	Brick red	Debutanizer reboiler	Hydrocarbons	Steam
488-E-205	Off white	Desulfurizer OH trimclr.	HC, H ₂ H ₂ S	Sea water
<i>Relative approximate weight % by X-ray powder diffraction</i>				
Component Minrl./Chmcl. name	Formula	Ht. Exch. # 19-E-201 A Wt. %	Ht. Exch. # 26-E-4 Wt. %	Ht. Ex. # 488-E-205 Wt. %
Magnetite	Fe ₃ O ₄	80	29	-
Hematite	Fe ₂ O ₃	-	53	-
Aragonite	CaCO ₃	-	-	89
<i>X-ray fluorescence analysis</i>				
Elements	Ht. Exch. # 26-E-4 Wt. %	Ht. Exch. # 19-E-201 A Wt. %	Ht. Ex. # 488-E-205 Wt. %	
Fe	62	65.5	0.2	
Ca	0.2	0.3	32.9	

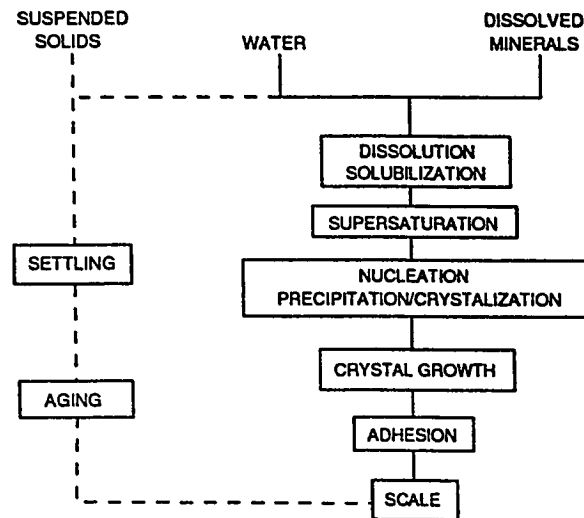


Figure 3.2: Schematic representation of the scale deposition mechanism. [73]

conducted, using a higher degree of supersaturation (concentration) than is found normally in the field applications. A general photograph showing the equipment setup is shown in Fig. 3.3.

The objective of the experimental research study program is to demonstrate that the fouling resistance varies from point to point along a horizontal tube and also for the same point it varies from replicate to replicate i.e., the fouling resistance can be considered as random variable and the scale formation is a random process. The data thus generated would be useful to form the basis for the design and maintenance considerations of heat exchangers subject to fouling.

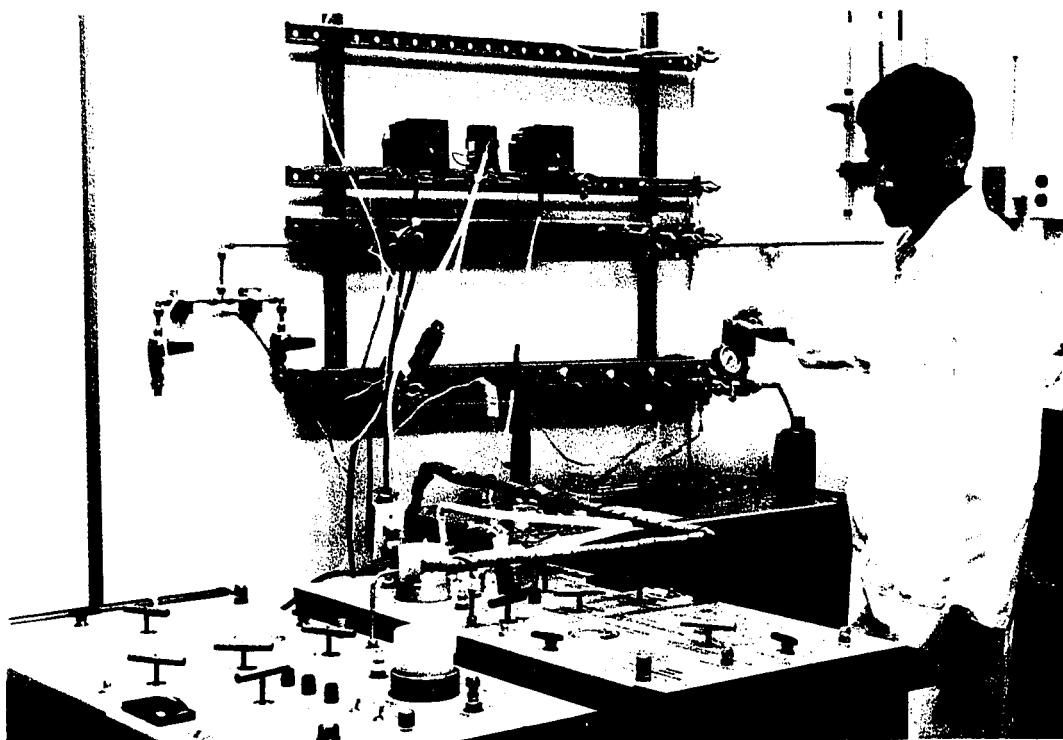
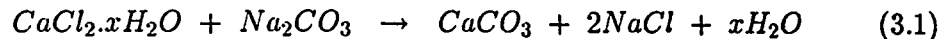


Figure 3.3: A general photograph of the scale-deposition experiment rig

Scaling loop

A schematic diagram of the scaling loop is shown in Fig.3.4. The main components of the equipment are storage tanks for solutions of $CaCl_2$ and Na_2CO_3 , high pressure metering pumps (HPP), pre-heaters, mixing chamber, test sections and Back Pressure Regulator (BPR). The loop was of once-through type, i.e., the solution was circulated through the loop only once, and then drained out. The pressure of the system was controlled by the BPR and the flow was controlled by adjusting the stroke length of the two high pressure diaphragm pumps. The solutions were heated by pre-heaters and by heating tapes wrapped around the pre-mixing sections. The temperature was controlled by thermocouples, and temperature controllers. The demineralized (distilled) water was used for the preparation of the solutions for the experiment. The concentration of the product solution was fixed at 0.0006 moles/liter i.e., 40 liters of the product solution required 3.5285 and 2.5438 gm of $CaCl_2$ and Na_2CO_3 respectively. The two equivolume reactant solutions meet in the mixing chamber to produce $CaCO_3$ precipitates according to the following chemical reaction



The product solution is then passed through the vertical, bend and the horizontal sections where the deposition of $CaCO_3$ precipitates takes place. The rate of flow is determined by using a graduated cylinder at the outlet, which is partially filled

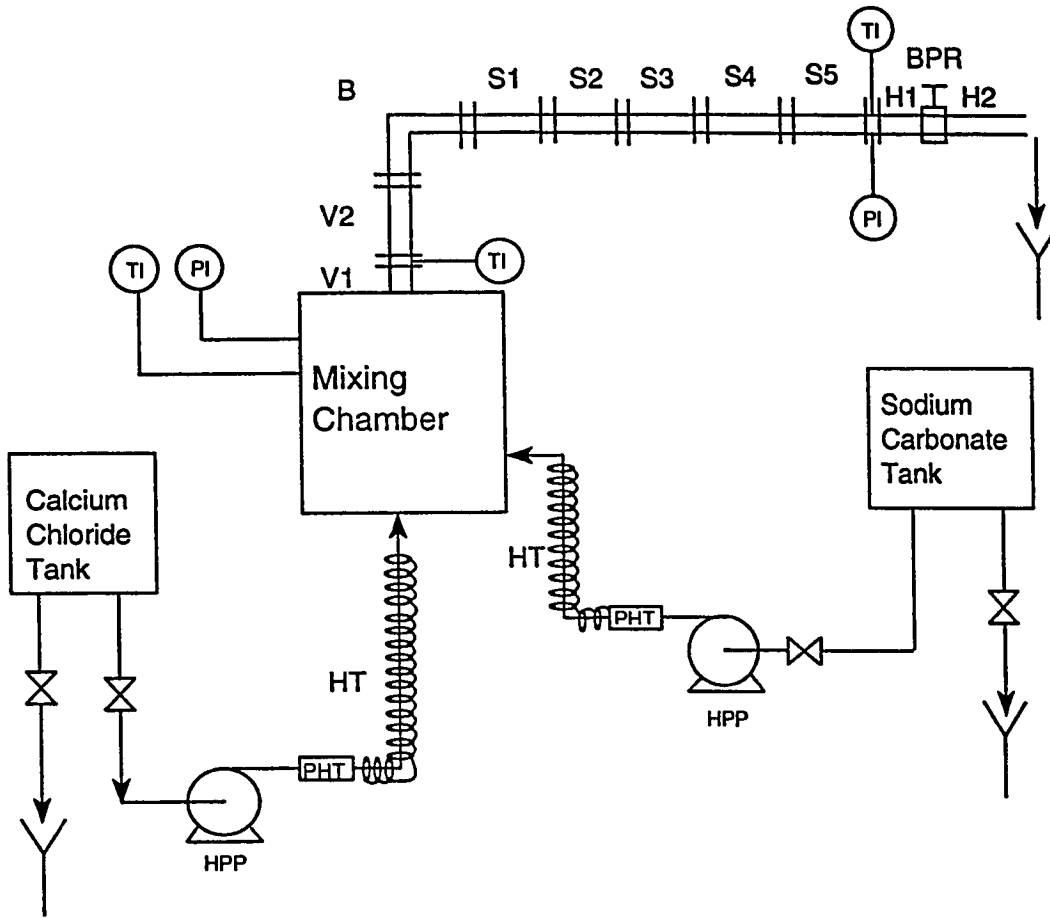
for some specific period of time.

The test specimen

The test sections were cut from commercial grade AISI-316 (stainless steel) tubing having 6.4 mm (0.25 inch) OD and 4.6 mm (0.18 inch) ID. The length of each section was set to approximately 76 mm (3 inch). Each of the test sections was provided with ferrules and nuts and washed thoroughly with distilled water and acetone to remove dirt and oil traces. These were then put in an oven at moderate temperature to let them completely dry. A detailed view of a test specimen is shown in Fig. 3.5. All the test sections were carefully weighed on a highly precise electronic balance (± 0.1 mg) after drying. Five such test sections were then coupled in line with the help of unions and used for a single experiment as shown in Fig. 3.4.

Calculation of fouling resistance, R_f

The procedure for calculating the fouling resistance involved dismantling, mild washing with distilled water of each section at the end of an experimental run. The fouling resistance in tubes due to $CaCO_3$ scale deposition results when the experiment is allowed to run for some specific period of time. These were then put in an oven for completely drying so as to yield the true weight gain due to deposition of $CaCO_3$ crystals, i.e., vaporizing water contents in and around the tests sections. An exaggerated end view of a test section which is showing scale deposition inside the tube is



B.H.S.V	TEST SECTIONS
BPR	BACK PRESSURE REGULATOR
PHT	PRE HEATER
HPP	HIGH PRESSURE PUMP (VARIABLE SPEED)
TI	TEMPERATURE INDICATOR
PI	PRESSURE INDICATOR
HT	HEATING TAPE
Y	DRAIN

Figure 3.4: Schematic of the scale-deposition equipment.

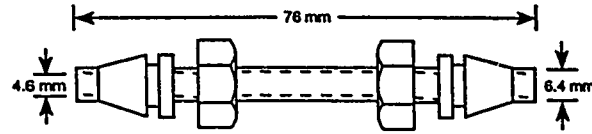


Figure 3.5: A test specimen details.

shown in Fig.3.6. The weight gain due to $CaCO_3$ scale is calculated by subtracting

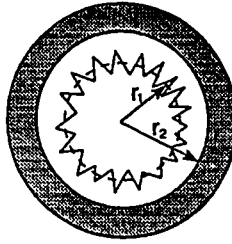


Figure 3.6: An end view of a test specimen.

the initial weight from the final weight. We can find the fouling resistance $R_f(t)$ due to the scale from this weight gain by using the following procedure [74].

The fouling resistance (in $m^2 K/W$) is expressed as

$$R_f = \frac{r_2^2}{2kl} \ln\left(\frac{r_2}{r_1}\right) \quad (3.2)$$

where r_2 is the inside radius of the tube while r_1 is the average value of radius due to scale deposit for a particular section. This can be calculated by using the relation

$$r_1 = \sqrt{r_2^2 - \frac{\text{weight gain}}{\pi \gamma l}} \quad (3.3)$$

It should be noted that thermal conductivity of scale (k) and weight density (γ) can easily be obtained from chemical engineering handbook [75].

3.2.2 Fouling characteristics at different sections

The initial experiments were performed to see the general trend of the fouling resistance vs time curves for different sections, and the effect of changing various parameters like pressure, temperature, etc. on the fouling resistance. These initial tests were very helpful and formed the basis for the subsequent replicate experiments for reliability-based statistical analysis.

Initial experiments

The initial set of experiment were performed with a 2 hour duration for recording data ,i.e., each time the experiment was stopped after two hours, the whole procedure was repeated to measure the fouling resistance as described in the previous sections and again run the experiment for two hours. It should be noted that each time the test sections were assembled at their previous locations and with the same sides, i.e., the upstream side of section remained upstream for every run. The operating parameters of the apparatus were temperature, pressure, solution concentration and velocity and these were kept constant during the experiment. The experiment was continued until blockage of the flow path (tubes) occurred due to the scale deposition.

The recorded data and the fouling resistance vs time curves are shown in Table 3.2

Table 3.2: Trial run results.

	t (hrs)	Wt. gn. (gm)	In. Rad., r_1 (m)	R_f ($m^2 K/W$)
S E C T I O N # 1	0	0	0.00229	0
	1.5	0.003	0.00228	9.5E-07
	3.5	0.0192	0.00228	6.1E-06
	5.5	0.0472	0.00227	1.5E-05
	7.5	0.082	0.00225	2.6E-05
	9.5	0.1177	0.00223	3.7E-05
	11.5	0.1544	0.00222	4.9E-05
	13.5	0.195	0.0022	6.2E-05
	15.5	0.2363	0.00218	7.5E-05
S E C T I O N # 2	0	0	0.00229	0
	1.5	0.0011	0.00229	3.5E-07
	3.5	0.0169	0.00228	5.3E-06
	5.5	0.043	0.00227	1.4E-05
	7.5	0.0762	0.00225	2.4E-05
	9.5	0.1084	0.00224	3.4E-05
	11.5	0.1359	0.00223	4.3E-05
	13.5	0.1693	0.00221	5.3E-05
	15.5	0.201	0.0022	6.3E-05
S E C # 3	0	0	0.00229	0
	1.5	0.0031	0.00228	9.8E-07
	3.5	0.0193	0.00228	6.1E-06
	5.5	0.0468	0.00227	1.5E-05
	7.5	0.0805	0.00225	2.5E-05

Table 3.2 continued.

	<i>t</i> (hrs)	<i>Wt. gain</i> (gm)	<i>In. Rad.,</i> <i>r₁</i> (m)	<i>R_f</i> (m ² K/W)
S C # 3	9.5	0.1145	0.00224	3.6E-05
	11.5	0.1415	0.00222	4.5E-05
	13.5	0.1713	0.00221	5.4E-05
	15.5	0.1995	0.0022	6.3E-05
S E C T I O N # 4	0	0	0.00229	0
	1.5	0.0016	0.00229	5.1E-07
	3.5	0.0166	0.00228	5.2E-06
	5.5	0.0395	0.00227	1.2E-05
	7.5	0.0685	0.00226	2.2E-05
	9.5	0.0969	0.00224	3.1E-05
	11.5	0.1207	0.00223	3.8E-05
	13.5	0.1463	0.00222	4.6E-05
	15.5	0.1689	0.00221	5.3E-05
S E C T I O N # 5	0	0	0.00229	0
	1.5	0.0014	0.00229	4.4E-07
	3.5	0.0139	0.00228	4.4E-06
	5.5	0.0323	0.00227	1E-05
	7.5	0.057	0.00226	1.8E-05
	9.5	0.0827	0.00225	2.6E-05
	11.5	0.1005	0.00224	3.2E-05
	13.5	0.1217	0.00223	3.8E-05
	15.5	0.1383	0.00222	4.4E-05

and Fig. 3.7, respectively. It can be observed from Fig. 3.7 that the characteristic fouling resistance - time curves for $CaCO_3$ scaling are essentially linear in nature. It can further be seen that there is an induction time because a relatively new surface (tube) was exposed to $CaCO_3$ precipitates, as discussed in chapter 1.

3.2.3 Microscopic characterization of $CaCO_3$ crystals under flow conditions

An important consideration while analyzing the fouling data for different sections is the induction time and the growth structure of $CaCO_3$ crystals. The morphology and the characterization of $CaCO_3$ crystals was achieved by Scanning Electron Microscopy (SEM) and augmented by Energy Dispersive X-Ray Spectroscopy Analysis (EDXSA).

Test specimen

Metallographic test coupons of $18 \times 8 \times 1.5$ mm size were cut from AISI 316 stainless steel sheet. The ends of the coupons were grounded to fit in the special Teflon holder while the flat surfaces were progressively wet-polished down to 600 grit with silicon carbide (SiC) paper. After polishing, the samples were washed with distilled water and degreased with acetone on a metallographic paper. Two samples were mounted in the holder at a time as shown in Fig. 3.8. The holder was then placed in the mixing chamber of the scaling loop for $CaCO_3$ scale deposition. The experiment

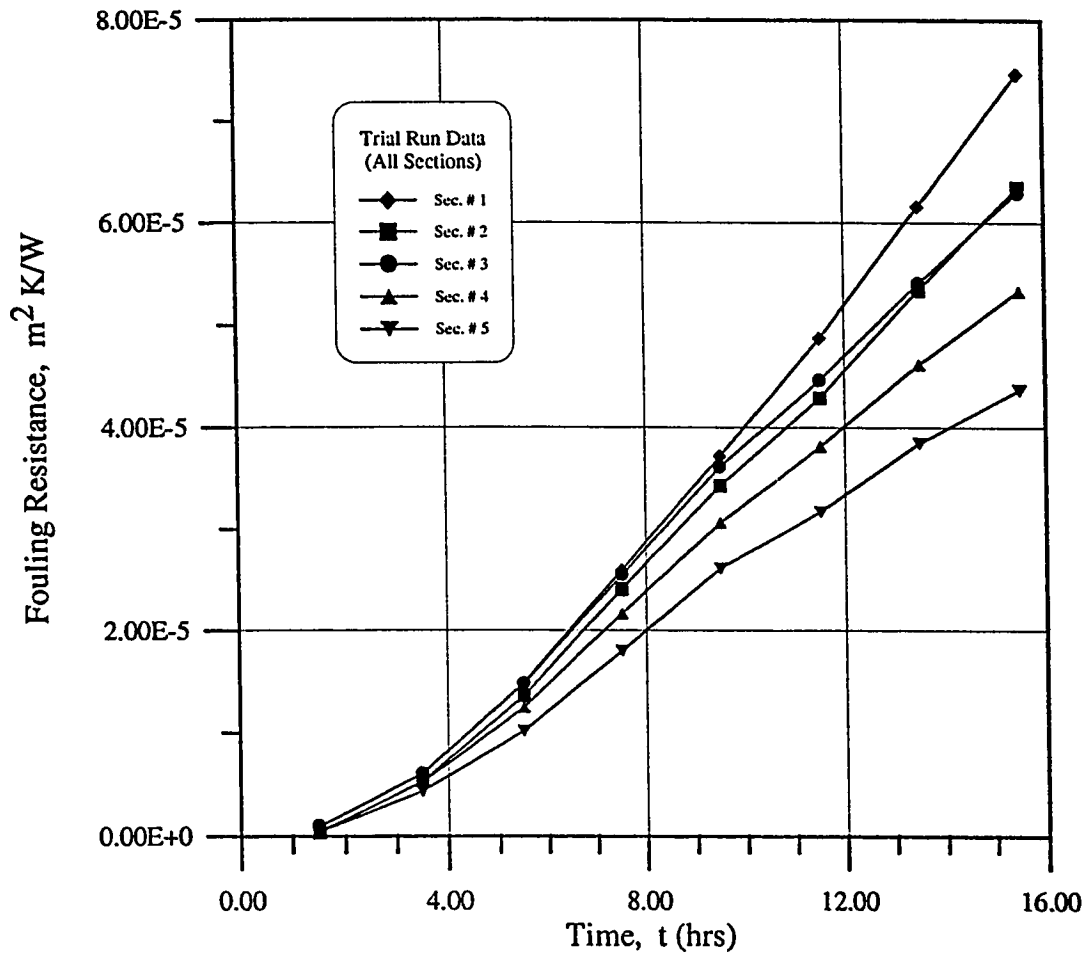


Figure 3.7: Fouling resistance-time curves for five test sections.

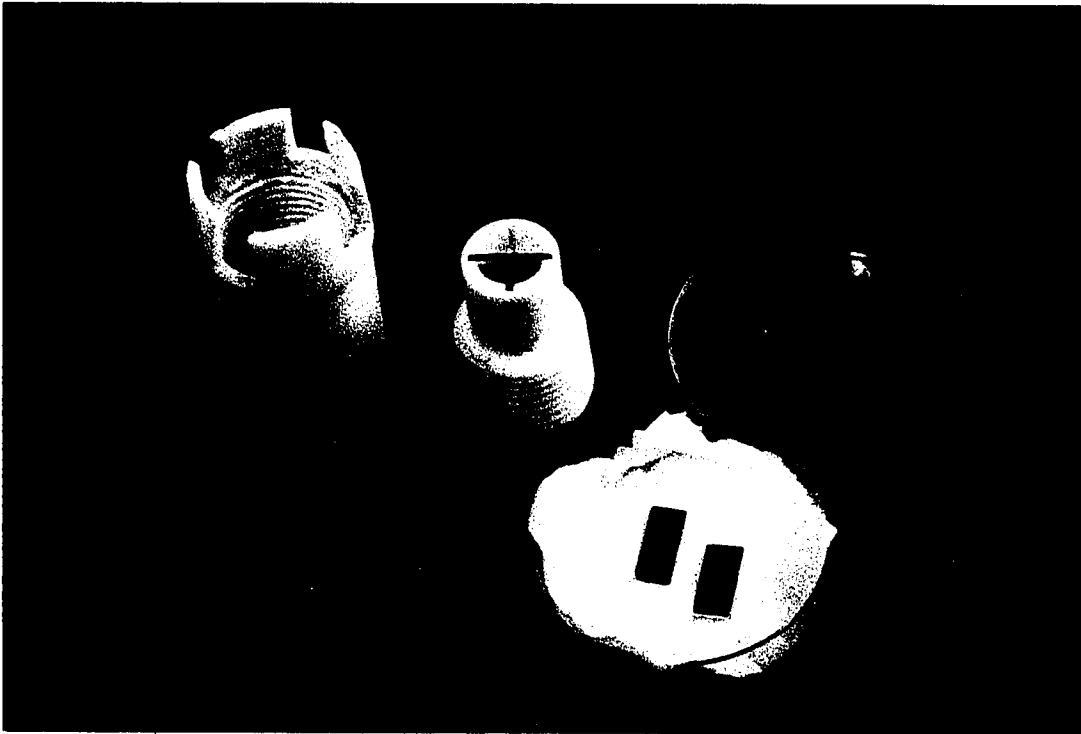


Figure 3.8: Teflon holder photograph

was run for a specific period of time. After the test, the coupons were retrieved from the chamber, mildly rinsed with distilled water and acetone and preserved for further analysis.

SEM and EDXSA procedure

The AISI 316 stainless steel coupons exposed to $CaCO_3$ precipitate/scale forming solution for different durations in the flow loop were sputter coated with gold for about 1 min.; (a) to prevent charging, (b) to make the scale conductive and (c) to help improve the focusing for the photomicrographs of the substrate.

The morphological and microscopic studies were conducted on Jeol JSM 840 Scanning Electron Microscope provided with Polaroid camera and interfaced with a Personal Computer. This model can detect and resolve the particles as distant as 40\AA (i.e., Angstrom) with maximum magnification factor of 10^6 . The coupons were mounted in the SEM chamber and energized by an accelerating voltage source of 20 kV_{ac} to reveal the morphology of $CaCO_3$ crystals. The qualitative micro compositional analysis for the confirmation of $CaCO_3$ crystals at particular spots on the substrate were accomplished by EDXSA. This analysis technique, although qualitative in nature, becomes semi quantitative when spot scan is conducted.

Morphology and characterization of $CaCO_3$ crystals: SEM and EDXSA analysis

The SEM micrographs of the deposited crystals exhibited, in general, various structural shapes of $CaCO_3$ crystals comprising typically rhombic, hexagonal, needle, half moon, combination of needle and flower-like shape, i.e., dendritic structure, etc. The growth generally started at preferential nucleating sites consisting of surface heterogeneities such as roughness, scratch/polishing marks and other adherent impurities which provided the necessary anchorage or crystal traps on the coupons surface for the inception and subsequent crystal growth. For higher exposure time (>1 hr), $CaCO_3$ crystals formation was dense as opposed to scattered colonial or patchy growth for lower exposure times. The SEM photographs for different exposure durations are shown in Figs. 3.9 to 3.15 and their respective EDXSA charts are shown in Figs. 3.10 to 3.16.

SEM and EDXSA analysis in general, revealed that the crystals formation was obvious on coupons exposed to the scalant for relatively longer periods of time while it was thin and sparse on the substrate for short exposure periods. The EDXSA performed at different locations/spots on the coupons that were exposed to scale forming solution for more than 1 hr showed high Ca contents, confirming the presence of $CaCO_3$ crystals. Any appreciable presence of $CaCO_3$ crystals can help

to predict the induction time for a particular heat-transfer under specific prevailing conditions. Furthermore, the spot analysis of coupons exposed for shorter time duration (e.g., 15, 30 min.) did not reveal existence of any $CaCO_3$ crystals. This shows that initially the process of crystals attachment and detachment to the coupon surface continues at preferential sites. In order, for the crystals to stick at scratches and other surface irregularities, deposition occur in a multistep reaction: charge transfer, surface diffusion and transfer from plane sites to step sites, followed by diffusion along the step to to a kink site, and finally surface incorporation [76]. Once the crystals are stuck to the surface then their subsequent outward growth commences. This ultimately results in an increased fouling resistance which is the most undesirable state in a heat-exchange equipment. Thus, rough surfaces are more susceptible to fouling than smooth surfaces.

3.2.4 Some observations on initial testing and experimentation

A brief discussion on the initial set of experiments for various test sections and SEM analysis is presented in this section.

Loop experiments

There is a negligible weight gain for each test section during the initial runs. Any appreciable deposition of crystals (or the fouling resistance), depends upon the in-

duction time of the heat-transfer surface and the prevailing test conditions.

The primary scale deposits are very fine, homogeneous and tightly held to the inside surface of the tube. But the subsequent deposits are loose and non homogeneous and grow at a faster rate. The loose scale particles are likely to change their position with time and move along the tube. There is a chance of accumulation of these particles at some point along the tube to cause the blockage of the flow path. Sometimes, these accumulated scale particles form small lumps which are hard to break and move from point to point along the tube and have every chance of accumulation into bigger lumps at any point to cause the line blockage. In addition, these can cause the blockage of the BPR. Once the line blockage occurs, it causes the back pressure to increase. A tremendous increase in the back pressure can break the blockage causing a sudden relief in the line pressure. This sudden impact have the capacity to damage the whole system depending upon the amount of pressure build up and is a very undesirable state in a given process. Therefore to avoid such an incident and have an effective heat-transfer, it is necessary to clean the tubes (e.g., of a heat exchanger) regularly in an industrial application.

The effects of various parameters like pressure, temperature, etc., by changing one keeping the rest constant, on the scale deposit is briefly described hereunder:

Effect of pressure

It has been observed through this experimental study that a decrease in the system pressure (e.g., from 1000 psi to atmospheric) causes an increase in the rate of $CaCO_3$ deposition. The observed increase in the deposition rate by decreasing the system pressure may be attributed to turbulence caused by pressure changes.

Effect of temperature

Results of the weight gain experiments showed that an increase in the solution temperature increased the rate of scale deposition. This can be explained from the fact that $CaCO_3$ salt has inverse solubility characteristics, i.e., the deposition rate of these salts increases with temperature.

Effect of supersaturation

A supersaturated solution is defined as the one which contains a higher concentration of dissolved solute than its equilibrium concentration. One of the most common expressions of supersaturation is the percentage supersaturation, which may be defined as:

$$\text{Percentage Supersaturation} = 100\left[\frac{G - G^*}{G^*}\right] \quad (3.4)$$

where "G" is the solute concentration of supersaturated solution, and G^* is the solute concentration at equilibrium saturation.

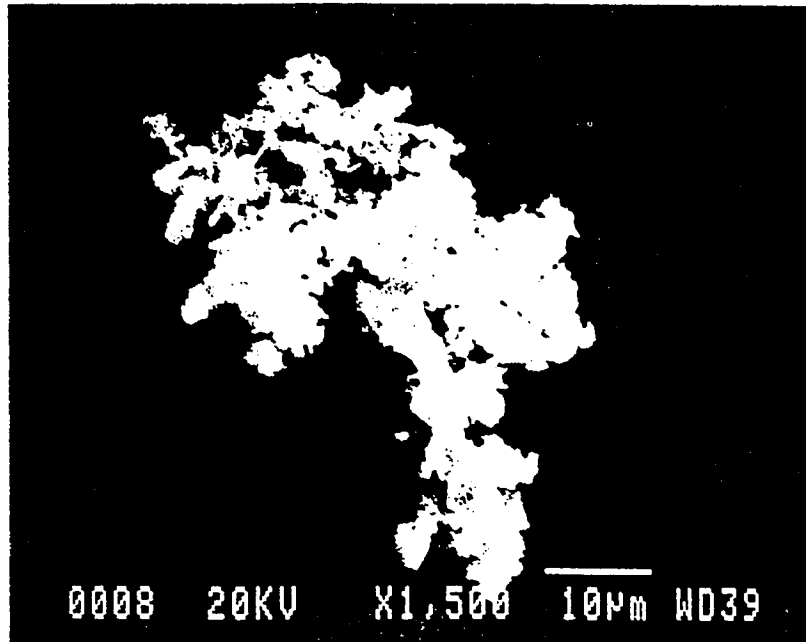


Figure 3.9: Time-1 hr, X1500 ; Negligible crystals and the shape of crystal, if any, is unidentifiable

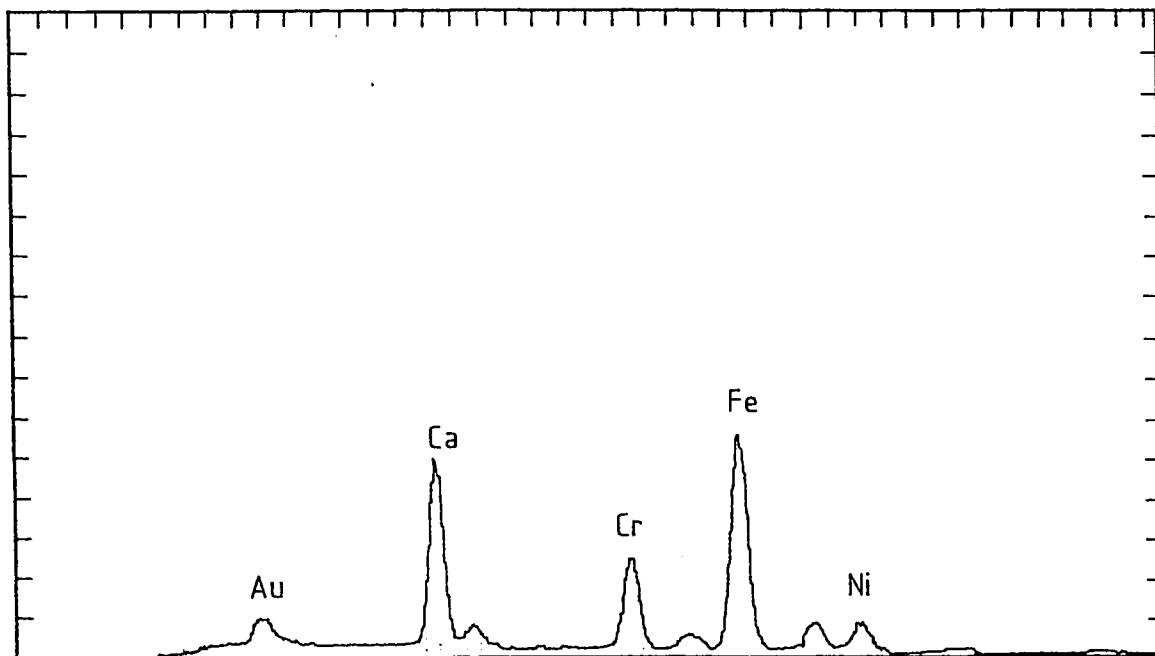


Figure 3.10: The corresponding EDXSA plot



Figure 3.11: Time-1.25 hr, X150 ; Crystals are nucleating and growing at preferential sites. Rhombic, sand-rose like, needle like and combination of needle & flower shape.

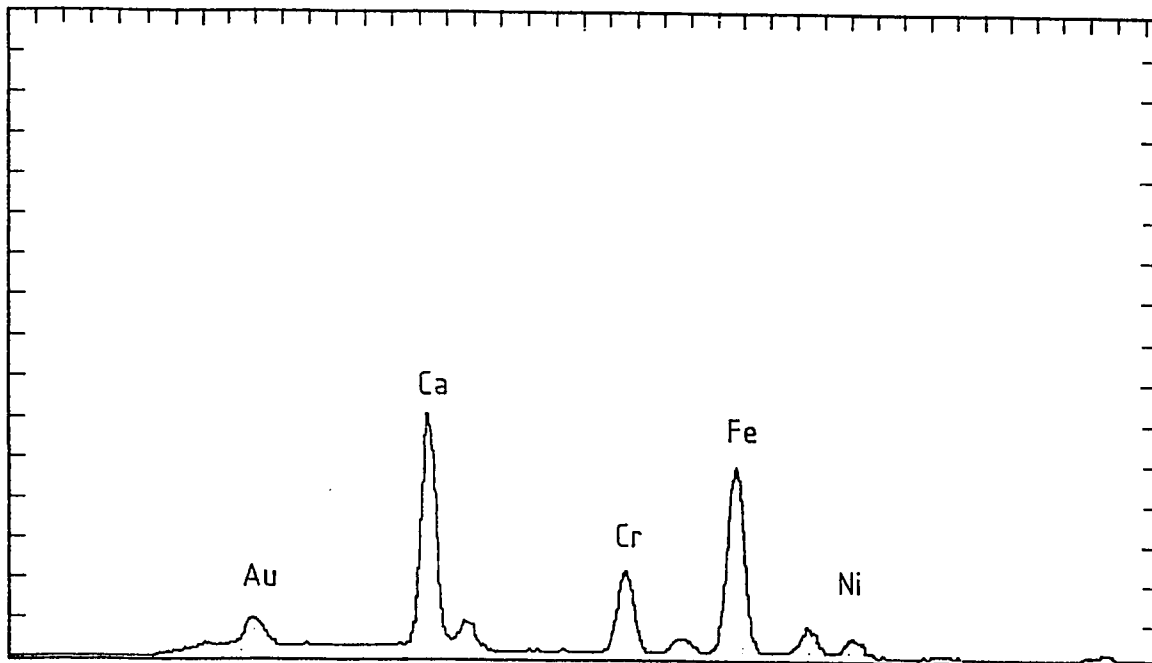


Figure 3.12: The corresponding EDXSA plot



Figure 3.13: Time-1.5 hr, X170 ; Irregularly ordered, colonial growth of needle as well as half moon shaped

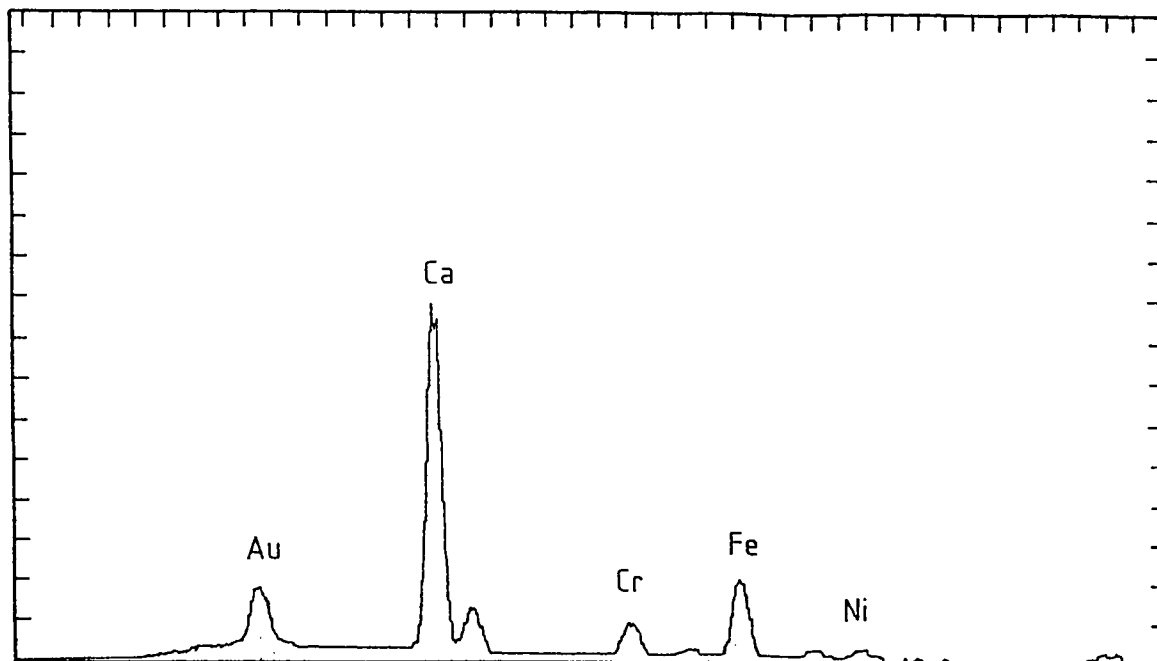


Figure 3.14: The corresponding EDXSA plot



Figure 3.15: Time-2 hr, X ; Thickly populated with rhombic, sand-rose like, needle-like and needle-flower shaped crystals

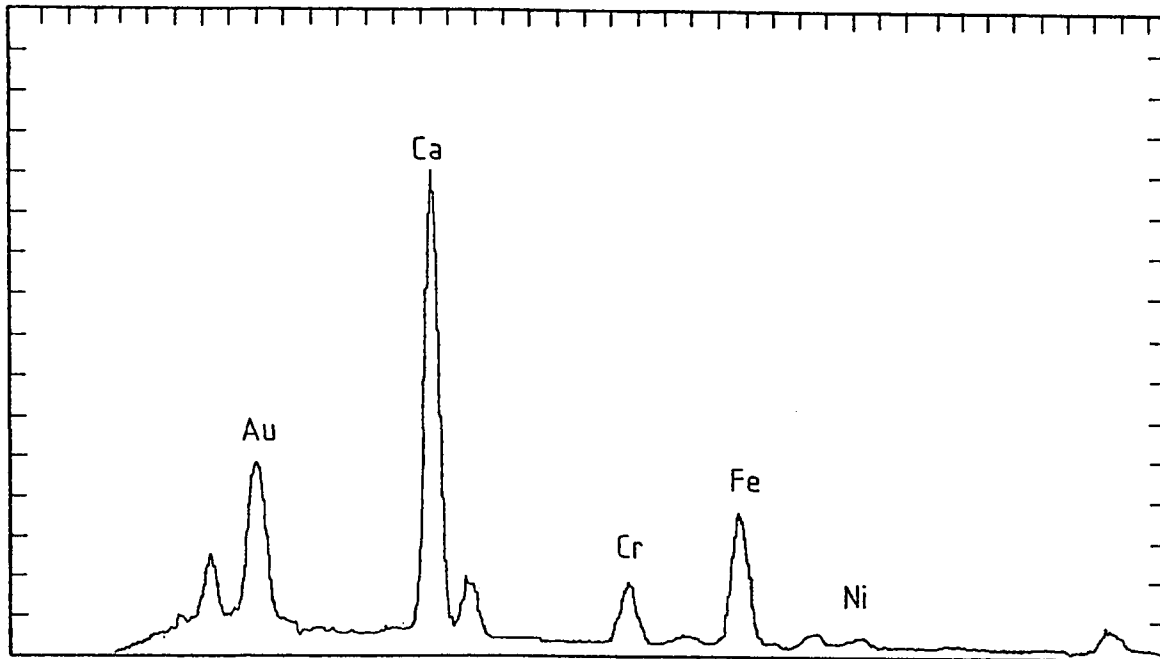


Figure 3.16: The corresponding EDXSA plot

It was observed that at lower supersaturation the induction time is longer, and this delays the initial onset of deposition.

Experimental limitations

Following were the experimental limitations encountered during the present study on $CaCO_3$ scaling:

1. It was observed that about 15-20 minutes were required to attain steady-state conditions.
2. It was difficult to run the experiment for longer time durations (e.g., 4-6 hrs) due to control-valve blockage. Therefore, sometimes, a particular run had to be stopped for valve cleaning.
3. The variations in conditions during an experimental run were:
 - Temperature : $60 \pm 2^\circ C$
 - Pressure : $100 \pm 10 \text{ psi}$
 - Flow rate : $10 \pm 0.5 \text{ liter/hr}$
4. Adjustments in the stroke lengths of the two diaphragm pumps were made to ensure mixing of equal volumes of reactant solutions in the mixing chamber.

3.2.5 Replicate experiments at some test sections for statistical investigation

In view of the general trends of the fouling resistance-time curves, it was decided that the final experiments be run in six replicates under nominally identical operating conditions. And for each replicate the data to be recorded every 2,6 and 14 hrs or at times in between whenever necessary. The temperature, pressure, solution concentration and velocity were kept constant at 60° C, 100 psi, 0.0006 moles/liter and 0.17 *m/sec* (10 liter/hr), respectively, during an experimental run. It should be noted that the vertical sections and the 90° bend were kept in the clean condition from the inside for as long as possible under the prevailing test conditions. This was achieved by washing them in diluted acid at the end of each experimental run and rinsing them with distilled water to neutralize the effect of any of the acidic contents in these sections. The rest of the procedure for recording the data remained the same as described in the previous section. The data thus obtained is presented in Tables 3.3 to 3.5 for section 1, 2 and 3, respectively. As can be seen from these tables that duration of the experimental runs in different replicates is not constant. This was due to the experiment limitations, i.e., sometimes the experiment had to be stopped because of the blockage of BPR due to $CaCO_3$ scale deposits. Therefore, few of the readings were obtained by linear interpolation because of some experimental problems.

The results given in Tables 3.3 to 3.5 are plotted in Figs. 3.17 to 3.19, respectively; in the form of fouling resistance-time curves. These curves also indicate that the deposition rate is slow in the beginning with an induction time but gradually increases with time, and is relatively constant until the blockage of the flow path. The general behavior of the fouling resistance vs time curves is obviously linear.

3.3 Corrosion Fouling

As mentioned in the beginning of this chapter that corrosion fouling is the other most important mechanisms of concern in the industrial applications. Analysis shall be carried out regarding corrosion fouling. A brief description regarding them is presented hereunder.

3.3.1 Experimental details regarding corrosion fouling

Somerscales and Kassemi [29] conducted some experiments to investigate the significance and nature of corrosion fouling without the presence of other categories of fouling. This provides a simple, low-cost technique for assessing the significance and characterization of corrosion fouling.

The test specimens are in the form of small diameter (about 1 mm) wire arranged

Table 3.3: Experimental data regarding $CaCO_3$ scaling for section # 1.

	Time t (hr)	Orig. Wt. (gm)	New Wt. (gm)	Wt.Gain (gm)	In. Rad(r_1) (m)	Fling. Res. R_f m^2 K/W
R	0	30.9183	30.9183	0	0.002286	0
E	2	30.9183	30.9191	0.0008	0.00228565	2.5277E-07
P	6	30.9183	30.9774	0.0591	0.00225992	1.8673E-05
# 1	14	30.9183	31.1586	0.2403	0.00217802	7.5896E-05
R	0	30.9461	30.9461	0	0.002286	0
E	2	30.9461	30.9528	0.0067	0.00228306	2.1169E-06
P	6	30.9461	31.0109	0.0648	0.00225739	2.0474E-05
# 2	14	30.9461	30.9766	0.0305	0.00227258	0.0001029 *
R	0	30.956	30.956	0	0.002286	0
E	2	30.956	30.9698	0.0138	0.00227994	4.3603E-06
P	6	30.956	31.0433	0.0873	0.00224737	0.02570152
#	10	30.956	31.1673	0.2113	0.00219133	6.6743E-05
2A	14	30.956	31.3341	0.3781	0.00211361	0.00011934
R	0	30.7402	30.7402	0	0.002286	0
E	2	30.7402	30.7444	0.0042	0.00228416	1.327E-06
P	6	30.7402	30.8058	0.0656	0.00225703	2.0726E-05
# 3	14	30.7402	31.0887	0.3485	0.00212761	0.00011002
R	0	30.7516	30.7516	0	0.002286	0
E	2	30.7516	30.7551	0.0035	0.00228446	1.1059E-06
P	6	30.7516	30.8405	0.0889	0.00224666	0.02618084
#	9.5	30.7516	30.8689	0.1173	0.00223394	6.463E-05 *
4	14	30.7516	30.8903	0.1387	0.00222431	0.0001185 *
R	0	30.6008	30.6008	0	0.002286	0
E	2	30.6008	30.6122	0.0114	0.00228099	3.602E-06
P	6	30.6008	30.6918	0.091	0.00224572	2.8751E-05
#	9.75	30.6008	30.8049	0.2041	0.00219462	6.447E-05
5	14	30.6008	31.0014	0.4006	0.0021029	0.00012643

*Adjusted Data

Table 3.4: Experimental data regarding $CaCO_3$ scaling for section # 2.

	Time t (hr)	Orig. Wt. (gm)	New Wt. (gm)	Wt.Gain (gm)	In. Rad(r_1) (m)	Fling. Res. R_f m^2 K/W
R E P # 1	0	30.7366	30.7366	0	0.002286	0
	2	30.7366	30.7397	0.0031	0.00228464	9.7948E-07
	6	30.7366	30.7911	0.0545	0.00226196	1.6733E-05
	14	30.7366	30.9333	0.1967	0.002198	6.2134E-05
R E P # 2	0	30.7515	30.7515	0	0.002286	0
	2	30.7515	30.7537	0.0022	0.00228503	6.9511E-07
	6	30.7515	30.809	0.0575	0.00226063	1.8167E-05
	14	30.7515	30.7519	0.0004	0.00228582	7.411E-05 *
R E P # 2A	0	30.8122	30.8122	0	0.002286	0
	2	30.8122	30.8218	0.0096	0.00228178	3.0332E-06
	6	30.8122	30.8851	0.0729	0.00225379	2.3033E-05
	10	30.8122	30.9743	0.1621	0.00221374	5.1208E-05
	14	30.8122	31.0646	0.2524	0.00217244	7.9714E-05
R E P # 3	0	30.9269	30.9269	0	0.002286	0
	2	30.9269	30.9304	0.0035	0.00228446	1.1059E-06
	6	30.9269	30.992	0.0651	0.00225726	2.0569E-05
	14	30.9269	31.1744	0.2475	0.0021747	7.8168E-05
R E P # 4	0	30.6559	30.6559	0	0.002286	0
	2	30.6559	30.6603	0.0044	0.00228407	1.3902E-06
	6	30.6559	30.7186	0.0627	0.00225832	1.981E-05
	9.5	30.6559	30.779	0.1231	0.00223134	3.8891E-05
	14	30.6559	30.7485	0.0926	0.002245	6.677E-05 *
R E P # 5	0	30.6188	30.6188	0	0.002286	0
	2	30.6188	30.6208	0.002	0.00228512	6.3192E-07
	6	30.6188	30.681	0.0622	0.00225854	1.9652E-05
	9.75	30.6188	30.7574	0.1386	0.00222436	4.3787E-05
	14	30.6188	30.8642	0.2454	0.00217567	7.7505E-05

*Adjusted Data

Table 3.5: Experimental data regarding $CaCO_3$ scaling for section # 3.

	Time t (hr)	Orig. Wt. (gm)	New Wt. (gm)	Wt.Gain (gm)	In. Rad(r_1) (m)	Fling. Res. R_f m^2 K/W
R E P # 1	0	30.8856	30.8856	0	0.002286	0
	2	30.8856	30.8884	0.0028	0.00228477	8.8469E-07
	6	30.8856	30.9238	0.0382	0.00226918	1.207E-05
	14	30.8856	31.0332	0.1476	0.0022203	4.6629E-05
R E P # 2	0	30.6776	30.6776	0	0.002286	0
	2	30.6776	30.6829	0.0053	0.00228367	1.6746E-06
	6	30.6776	30.7305	0.0529	0.00226267	1.6714E-05
	14	30.6776	30.7106	0.033	0.00227147	1.043E-05 *
R E P # 2A	0	30.6906	30.6906	0	0.002286	0
	2	30.6906	30.6981	0.0075	0.00228271	2.3697E-06
	6	30.6906	30.7457	0.0551	0.0022617	1.7409E-05
	10	30.6906	30.8119	0.1213	0.00223214	3.8322E-05
	14	30.6906	30.8727	0.1821	0.00220465	5.7524E-05
R E P # 3	0	30.934	30.934	0	0.002286	0
	2	30.934	30.9368	0.0028	0.00228477	8.8469E-07
	6	30.934	30.9845	0.0505	0.00226373	1.5956E-05
	14	30.934	31.1228	0.1888	0.0022016	5.9639E-05
R E P # 4	0	30.7318	30.7318	0	0.002286	0
	2	30.7318	30.7391	0.0073	0.00228279	2.3065E-06
	6	30.7318	30.7858	0.054	0.00226218	1.7062E-05
	9.5	30.7318	30.8496	0.1178	0.00223372	3.7217E-05
	14	30.7318	30.8323	0.1005	0.00224147	6.635E-05 *
R E P # 5	0	31.0153	31.0153	0	0.002286	0
	2	31.0153	31.0206	0.0053	0.00228367	1.6746E-06
	6	31.0153	31.0823	0.067	0.00225641	2.1169E-05
	9.75	31.0153	31.1469	0.1316	0.0022751	4.1576E-05
	14	31.0153	31.2355	0.2202	0.00218725	6.9552E-05

*Adjusted Data

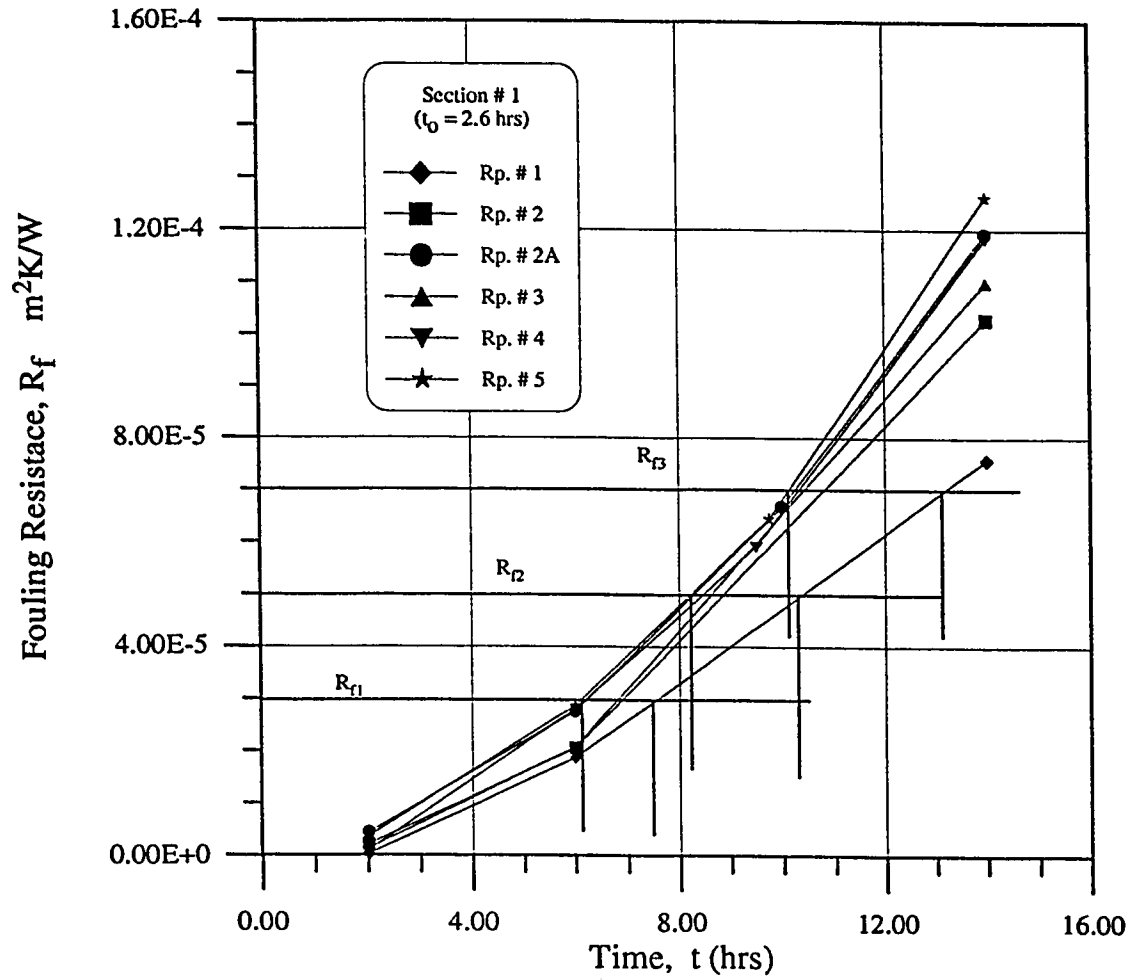


Figure 3.17: Fouling resistance-time curve for section # 1.

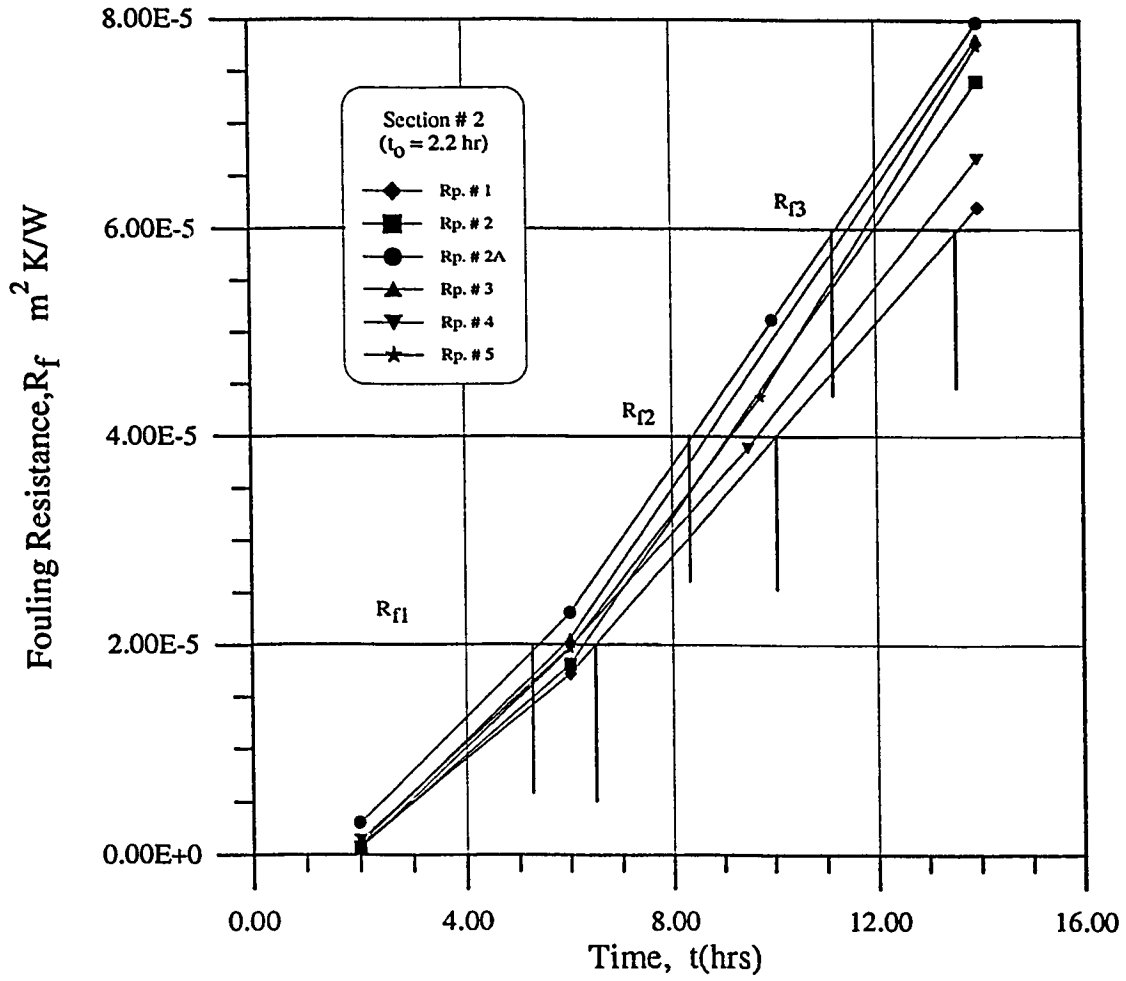


Figure 3.18: Fouling resistance-time curve for section # 2.

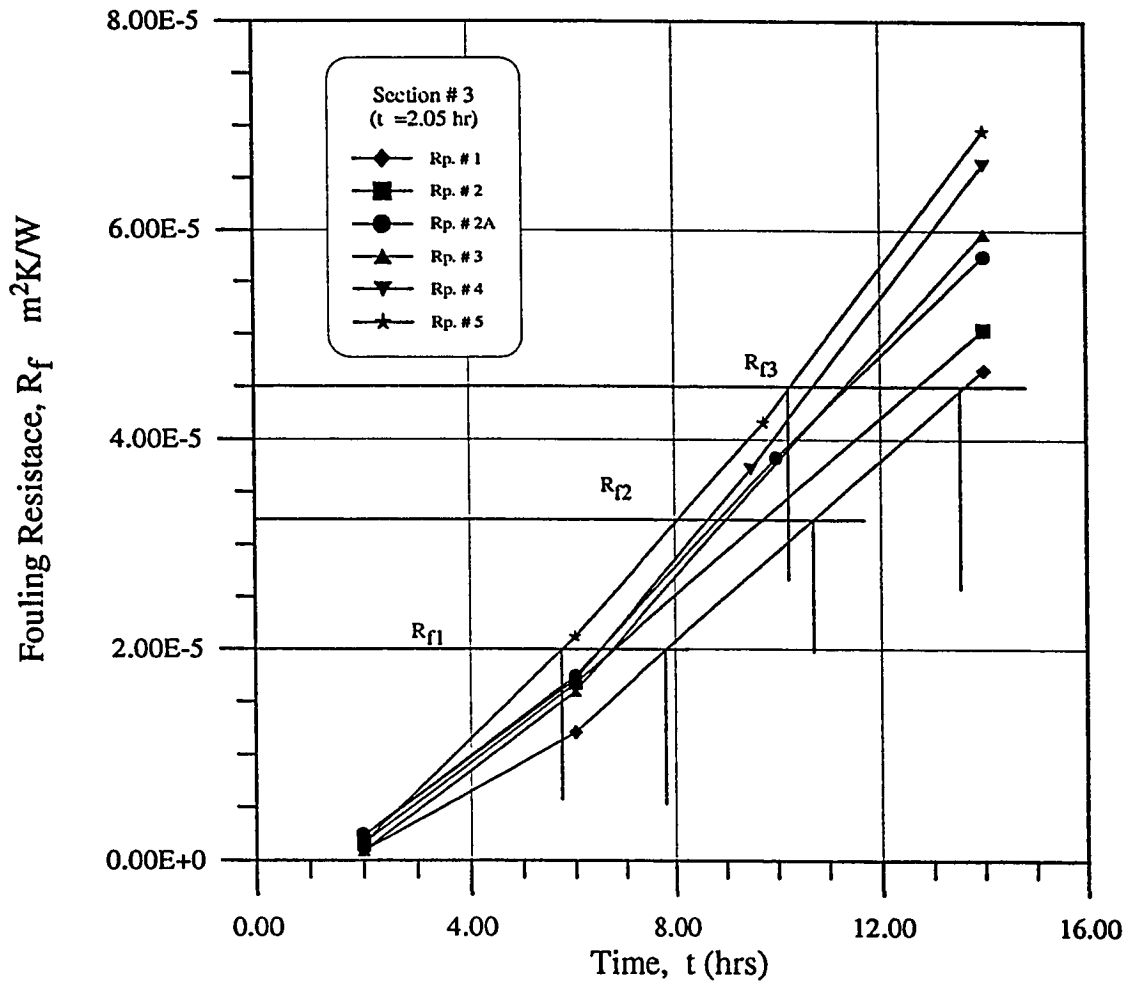


Figure 3.19: Fouling resistance-time curve for section # 3.

in U-form and exposed to a flowing stream of water. The wire is heated electrically and the power ($Q = I^2 R_e$) dissipated to the water and the surface temperature (T_s) of the wire was determined from its electrical resistance. The measurements of the wire temperature (T_s), the electrical power dissipated (Q) by the wire, and the bulk temperature (T_b) of the water are used to determine the resistance (R) to heat transfer between the wire and the water by using the following equation

$$Q = \frac{T_s - T_\infty}{R}. \quad (3.5)$$

The fouling resistance (R_f) is determined from the measured value of R assuming that its magnitude when the wire is first exposed to the flowing water is equal to the convective thermal resistance (R_c). Then R_f can be obtained immediately from the equation

$$R = R_c + R_f. \quad (3.6)$$

The resulting data and the fouling resistance-time curves are shown in Table 3.6 and Fig. 3.20, respectively.

Table 3.6: Corrosion related experimental data. [29]

Specimen # 4		Specimen # 5		Specimen # 6	
Time t (hr)	Fling. Res. R_f $m^2 K/W$	Time t (hr)	Fling. Res. R_f $m^2 K/W$	Time t (hr)	Fling. Res. R_f $m^2 K/W$
0	0	0	0	0	0
9	0.000115	10	0.00012	10	0.000074
24	0.00022	25	0.00022	22	0.000145
33.5	0.000261	51	0.000258	48	0.000142
51	0.00032	68	0.00028	60	0.000134
70	0.000355	81	0.000258	78	0.000225
103	0.00039	100	0.000296	102	0.000215
120	0.000439	118	0.000334	126	0.000272
144	0.00036	148	0.00036	148	0.00017
148	0.00042	164	0.00039	179	0.000148
170	0.000459	192	0.000436	212	0.00023
178	0.00055	222	0.00045	-	-
190	0.000522	249	0.00048	-	-
202	0.00048	260	0.0005	-	-
230	0.000487	-	-	-	-
Specimen # 7		Specimen # 8		Specimen # 9	
Time t (hr)	Fling. Res. R_f $m^2 K/W$	Time t (hr)	Fling. Res. R_f $m^2 K/W$	Time t (hr)	Fling. Res. R_f $m^2 K/W$
0	0	0	0	0	0
10.5	0.000128	10	0.000154	15	0.000038
23	0.000121	22	0.000165	32	0.00002
33	0.000086	48	0.000023	65	0.0001
48	0.00005	80	0.00014	89	0.000114
60	0.00007	101	0.000143	112	0.00027
79	0.000147	126	0.000125	141	0.000283
101	0.0001	150	0.000124	160	0.000264
118	0.000148	173	0.000148	184	0.000308
143	0.00016	204	0.00017	220	0.000282
155	0.00016	220	0.000185	240	0.00038
-	-	246	0.000185	262	0.000365
-	-	-	-	288	0.00032
-	-	-	-	312	0.000468
-	-	-	-	340	0.00044
-	-	-	-	361.5	0.000398
-	-	-	-	378	0.000465
-	-	-	-	400	0.000427

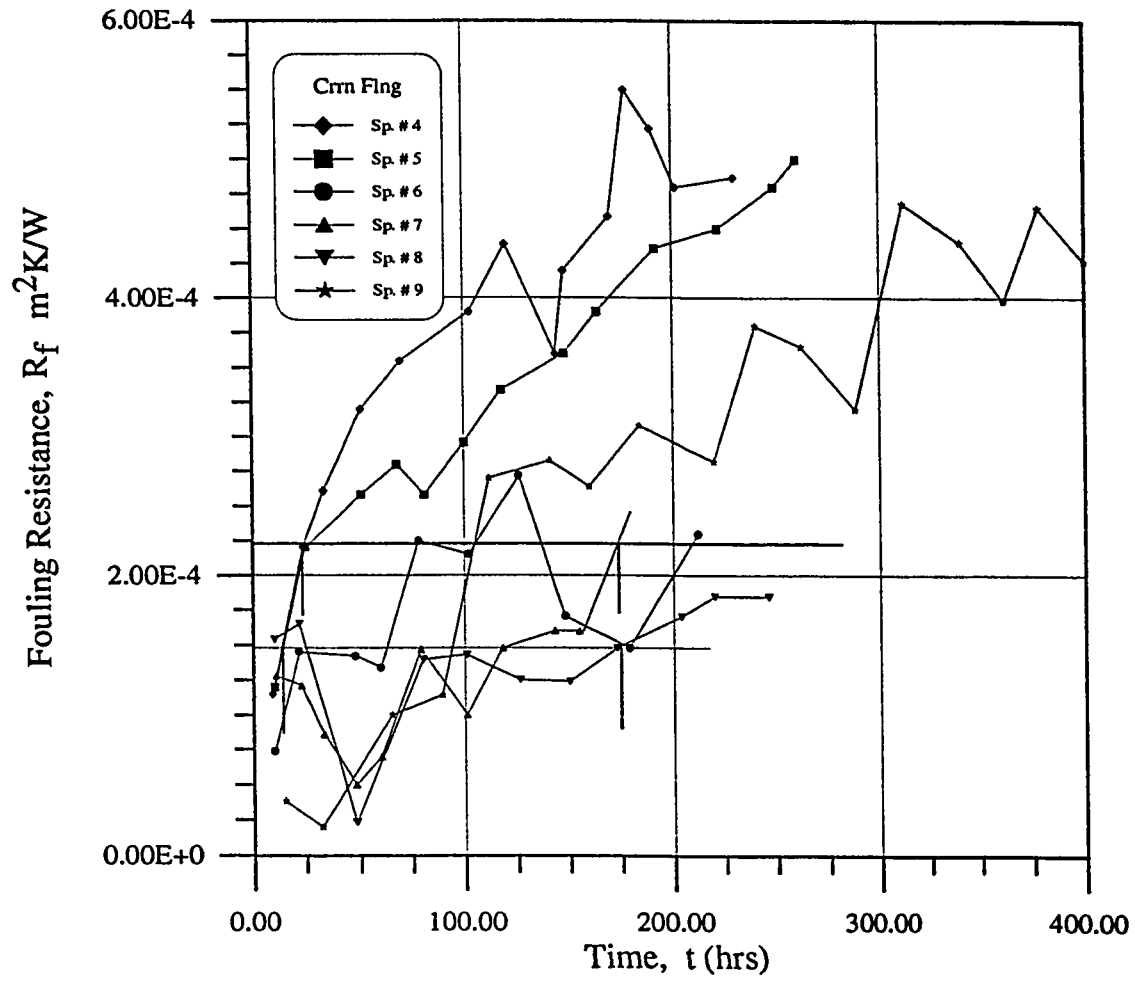


Figure 3.20: The corrosion fouling resistance-time curves. [29]

Chapter 4

Reliability-Based Statistical Analysis and Interpretation of Fouling Data

4.1 Stochastic Nature of Fouling Phenomena

Both replicate laboratory experiments as discussed in chapter 3 and field investigations suggest that there is a considerable scatter in the value of R_f at time t . This randomness is due to various factors such as, variations and fluctuations in velocity and temperature around their nominal values, perturbations in the foulant chemistry, metallurgical features of the tube materials, operating and environmental conditions. The scatter in R_f can be expressed by its probability distribution

$f[R_f(t)]$. The main indicators of the distribution are its mean value $\mu[R_f(t)]$ and standard deviation $\sigma[R_f(t)]$. It is often convenient to discuss the the scatter in terms of non-dimensional parameter [64, 77]

$$K[R_f(t)] = \sigma[R_f(t)]/\mu[R_f(t)] . \quad (4.1)$$

The evolution of distribution of $R_f(t)$ with respect to 't' is represented by random sample functions of the growth model. Each sample function represents a realization of the process. For example, a heat-exchanger which has many tubes, the fouling resistance response of the tubes will have its own growth curve. These curves will follow some type of fouling kinetic models with linear, asymptotic or falling rates.

4.2 Fundamentals of Statistical Analysis

The fouling of heat-exchanger tubes result in increased fouling resistance, R_f and thus reduce the ultimate heat transfer per unit time. As discussed in chapter 2, the fouling process can, in general, be represented by the following random functions of time

$$\text{linear fouling} \quad R_f(t) = mt \quad (4.2)$$

$$\text{non - linear fouling} \quad R_f(t) = mt^n \quad 0 < n < 1 \quad (4.3)$$

Where m is the slope of the fouling curve and is normally distributed with mean μ , and variance σ^2 . It should be noted that the fouling resistance at $t = 0$ is

assumed to be zero (i.e., no initial damage). Corresponding to a critical fouling resistance $R_{f,c}$, distribution of times for tubes to reach a critical level of fouling 't' can be determined as discussed in Appendix A and the life of heat-exchanger tube subject to fouling can be assessed. Some of the basic probability functions which are needed to be determined for the life assessment of heat-exchanger tubes, are briefly discussed below:

4.2.1 Reliability function (Distribution of time to survive critical fouling)

The reliability function, $R(t)$ provides the relationship between the age(subject to a critical level of fouling) of a tube and the probability that the tube survives upto that age while it starts working at zero time. In other words, the reliability is the probability that the time to reach a critical level of fouling, t of the tube is equal to or greater than the duration of the mission, t_1

$$R(t_1) = \int_{t_1}^{\infty} f(t) dt \tag{4.4}$$

which shows that the reliability function defined by the above equation is given by the area under $f(t)$ of time for tubes to reach a critical level of fouling, to the right of t_1

$$\int_{-\infty}^{\infty} f(t) dt = \int_{-\infty}^{t_1} f(t) dt + \int_{t_1}^{\infty} f(t) dt \tag{4.5}$$

$$\Rightarrow F(t_1) + R(t_1) = 1 \tag{4.6}$$

The function $R(t)$ is a probability, therefore it is a dimensionless number.

4.2.2 Probability density function

The probability density function [*pdf* or $f(t)$] is the density of the probability of a random variable (a variable which is distributed and to which a probability of occurrence can be associated). It has the characteristic that the area under the curve, *e.g.*, time for heat-exchanger tubes to reach a critical level of fouling, say from $t_1 = t$ to $t_2 = t + \Delta t$, gives directly the probability that a tube randomly selected from the bundle would reach a critical level of fouling during this life period from $t_1 = t$ to $t_2 = t + \Delta t$.

$$f(t)\Delta t = P[t \leq t \leq t + \Delta t] \quad \Delta t = t_2 - t_1 \quad (4.7)$$

In other words, the probability density is the probability associated with the existence of a particular value of a variable as the width of the interval in which this value falls tends to zero, *i.e.*, $\Delta t \rightarrow 0$, (also called the instantaneous probability).

It should be noted that the function $f(t)$ has 1/time units.

4.3 Reliability-Based Statistical Analysis for $CaCO_3$

Scaling

The linear nature of R_f vs t curves for $CaCO_3$ scaling suggest that a suitable model to represent the times for tubes to reach a critical level of fouling, with re-

spect to a critical-fouling resistance, $R_{f,c}$, would be inverted normal also known as α -distribution [78, 77]. Its suitability can be checked by superimposing the distribution curves drawn following different approaches, as discussed in Appendix A [78, 77, 79] of the thesis.

The first three test sections have been chosen for a thorough reliability-based statistical analysis. The linear fitting of the data for for each section is done by linear regression analysis using a spreadsheet software package. These fitted curves indicate induction times of 2.8, 2.5 and 2.2 hours for sections 1, 2 and 3 as shown in Figs. 4.2, 4.5 and 4.8 respectively. The data regarding time to reach a critical level of fouling (TRCL) is extracted from the R_f vs t curves as shown in Fig. 3.8, 3.9 and 3.10, corresponding to a critical value of fouling resistance, $R_{f,c}$ for each of the three test sections. The non-parametric distribution analysis is performed for the TRCL and its respective results are presented in Tables B.1, B.2 and B.3 of Appendix B. The parametric analysis is carried out by calculating the distribution parameters as discussed in Appendix A. The distribution functions $f(t)$ and $R(t)$ are found by using Eqs. (A.8)-(A.9) respectively and are plotted against t in Figs. 4.4 and 4.3 for section 1, Figs. 4.7 and 4.6 for section 2 and Figs. 4.10 and 4.9 for section 3, respectively.

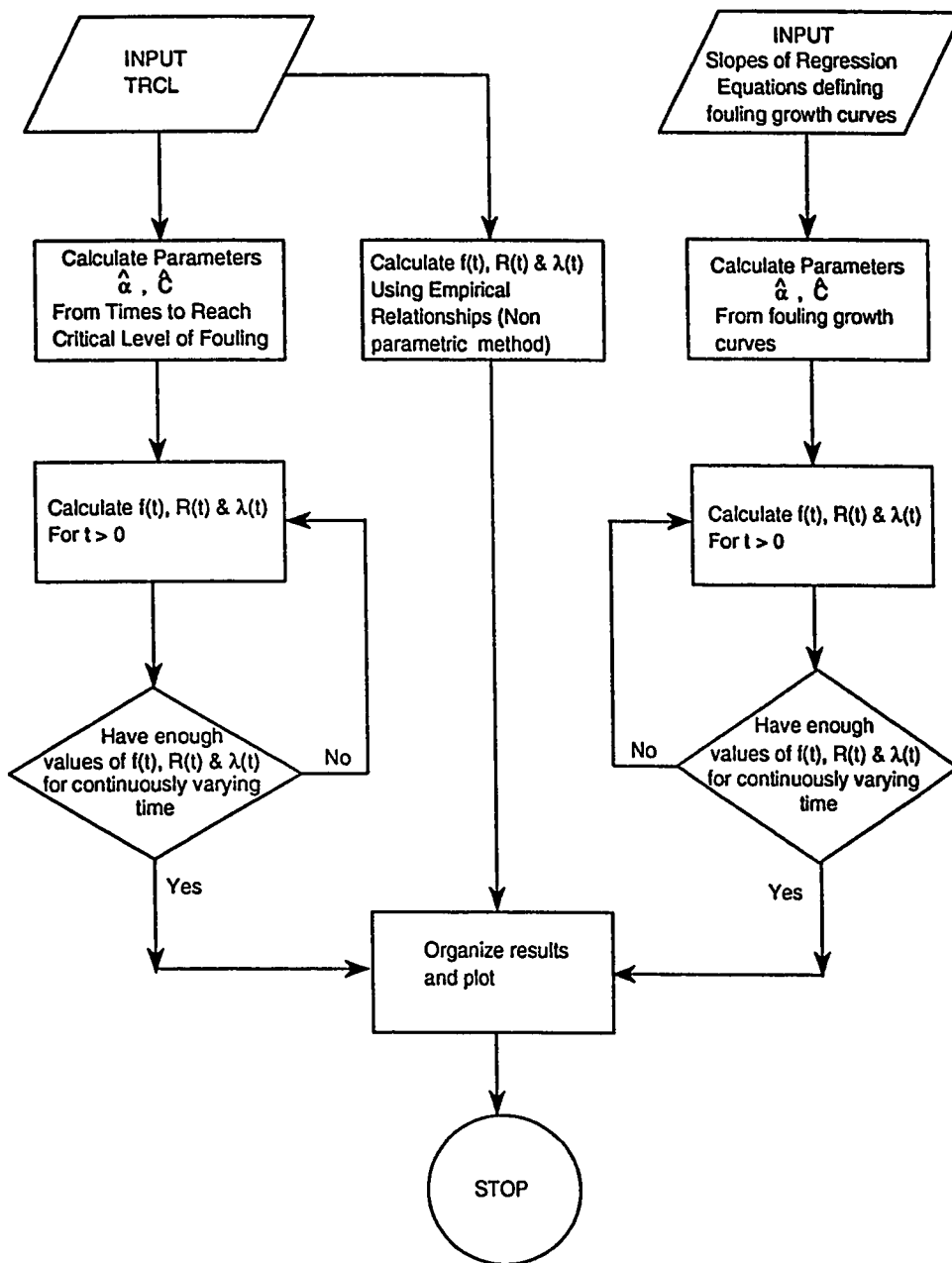


Figure 4.1: Flow chart of the computer program to determine the distribution functions.

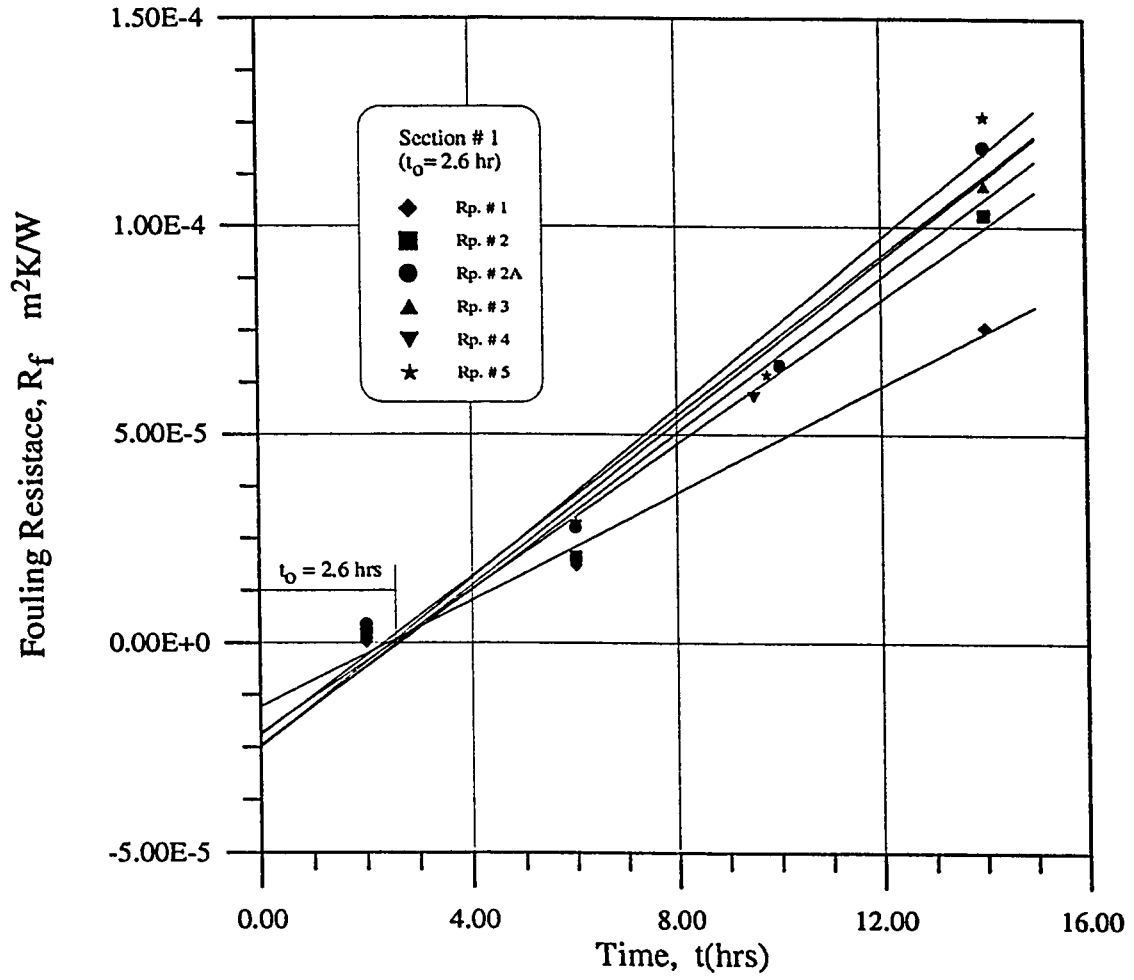


Figure 4.2: Linear regression lines (Section # 1).

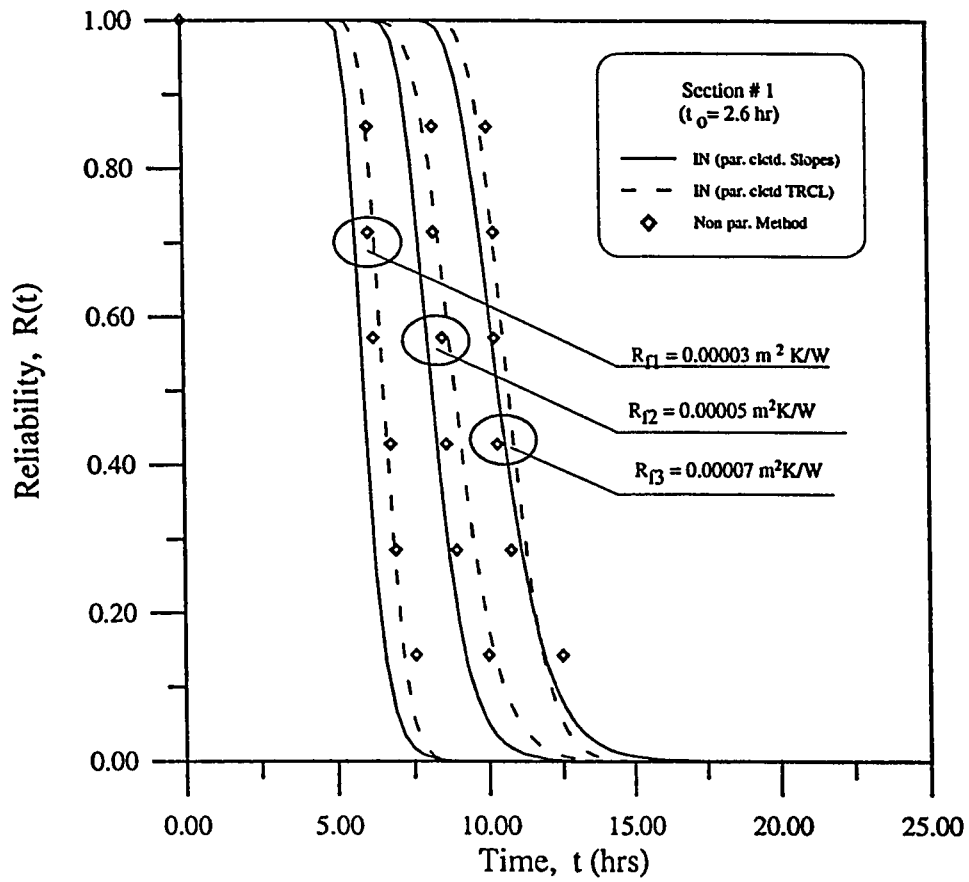


Figure 4.3: Superimposed curves for reliability (Section # 1): details of the curves are given below

	R_{f1}	R_{f2}	R_{f3}
$\sqrt{\alpha}$	0.15	0.15	0.15
C (hrs)	3.33	5.55	7.77
$\sqrt{\alpha}$	0.08	0.12	0.09
C (hrs)	6.58	8.93	10.72

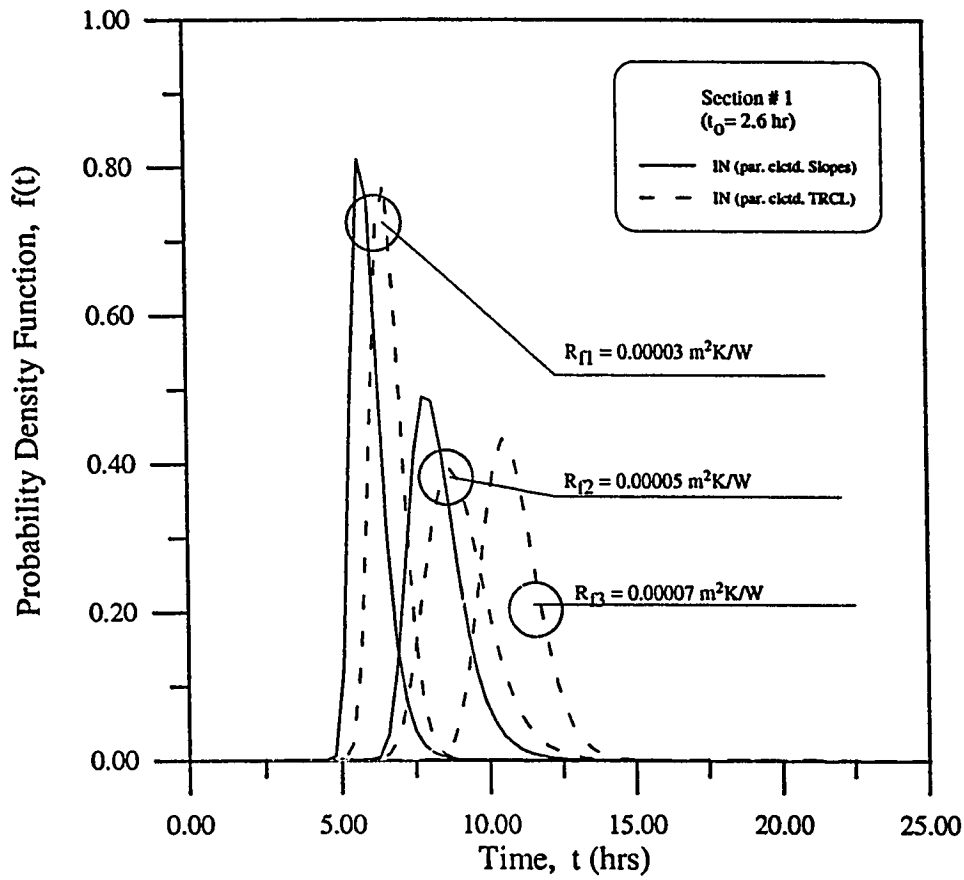


Figure 4.4: Superimposed curves for PDF (Section # 1):
details of the curves are given below

	R_{f1}	R_{f2}	R_{f3}
$\sqrt{\alpha}$	0.15	0.15	0.15
C (hrs)	3.33	5.55	7.77
$\sqrt{\alpha}$	0.08	0.12	0.09
C (hrs)	6.58	8.93	10.72

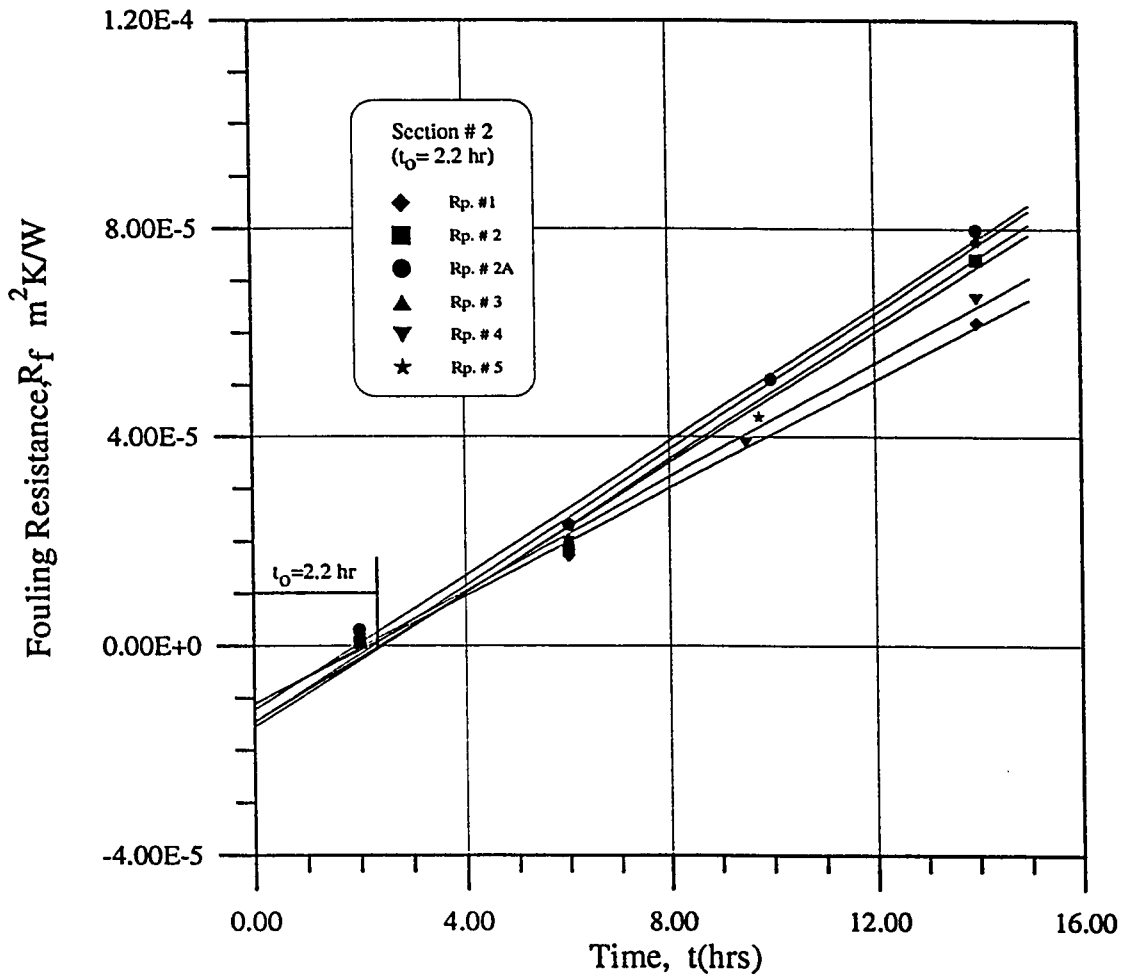


Figure 4.5: Linear regression lines (Section # 2).

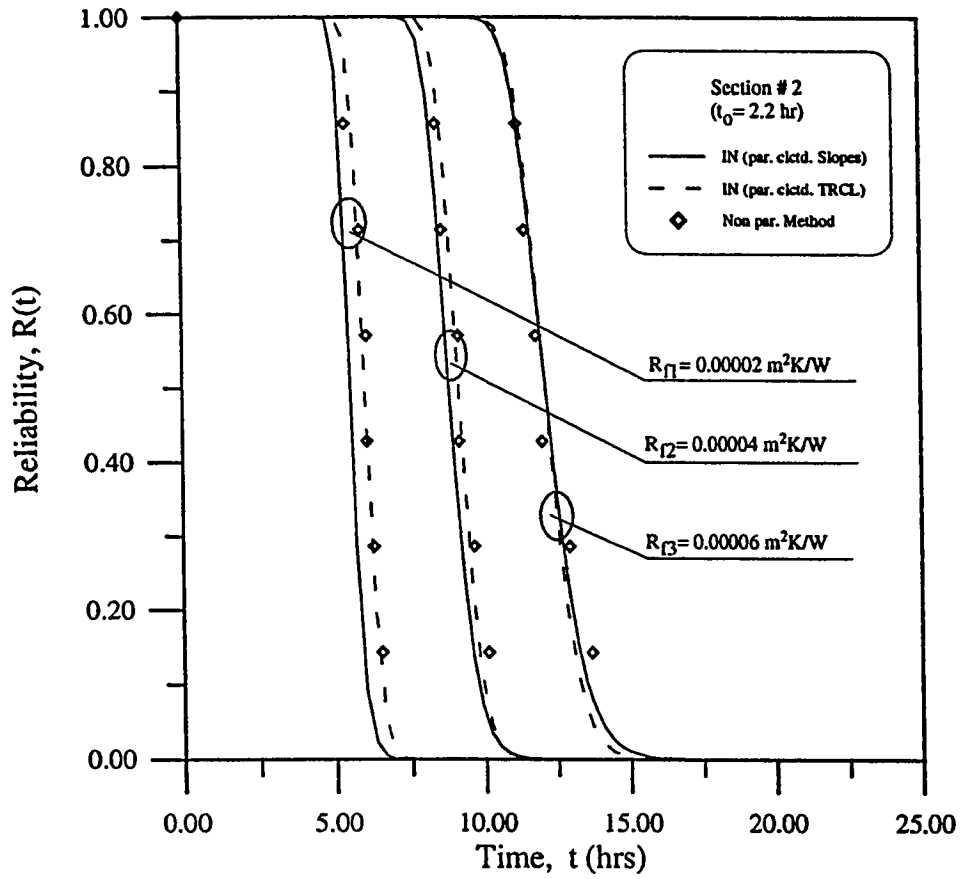


Figure 4.6: Superimposed curves for reliability (Section # 2): details of the curves are given below

	R_{f1}	R_{f2}	R_{f3}
— $\sqrt{\alpha}$	0.09	0.09	0.09
— C (hrs)	3.31	6.62	9.92
- - $\sqrt{\alpha}$	0.06	0.06	0.07
- - C (hrs)	6.00	9.14	12.11

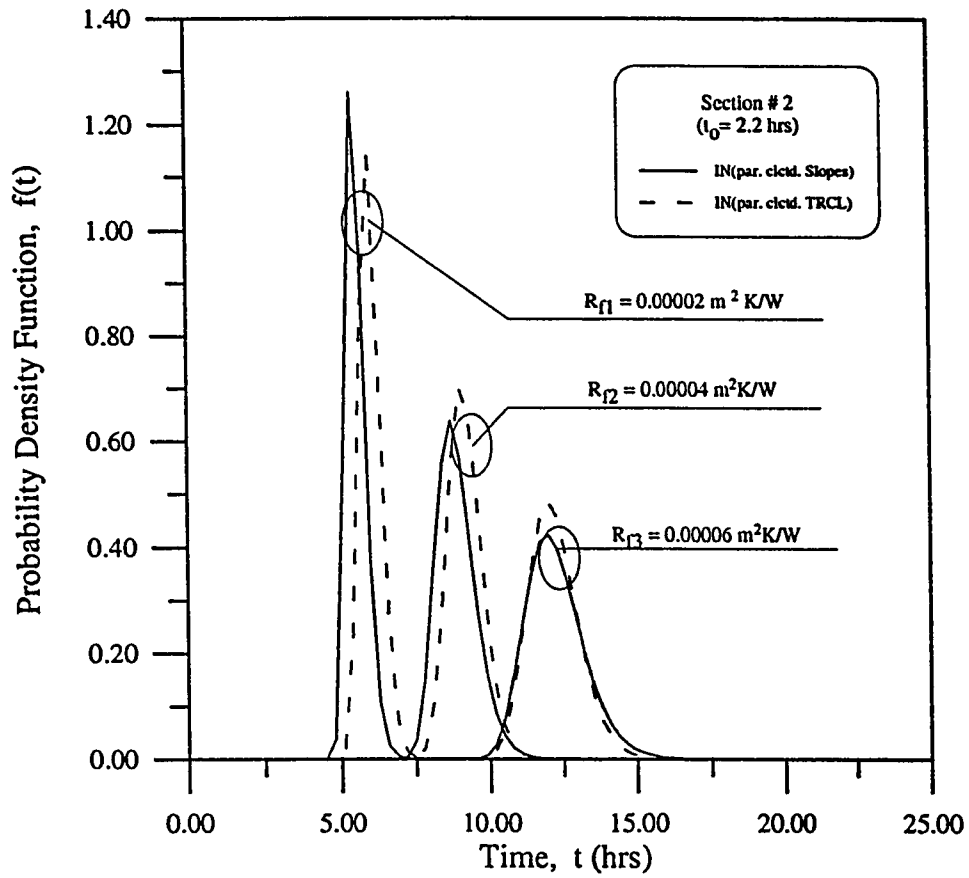


Figure 4.7: Superimposed curves for PDF (Section # 2):
details of the curves are given below

	R_{f1}	R_{f2}	R_{f3}
$\sqrt{\alpha}$	0.09	0.09	0.09
C (hrs)	3.31	6.62	9.92
$\sqrt{\alpha}$	0.06	0.06	0.07
C (hrs)	6.00	9.14	12.11

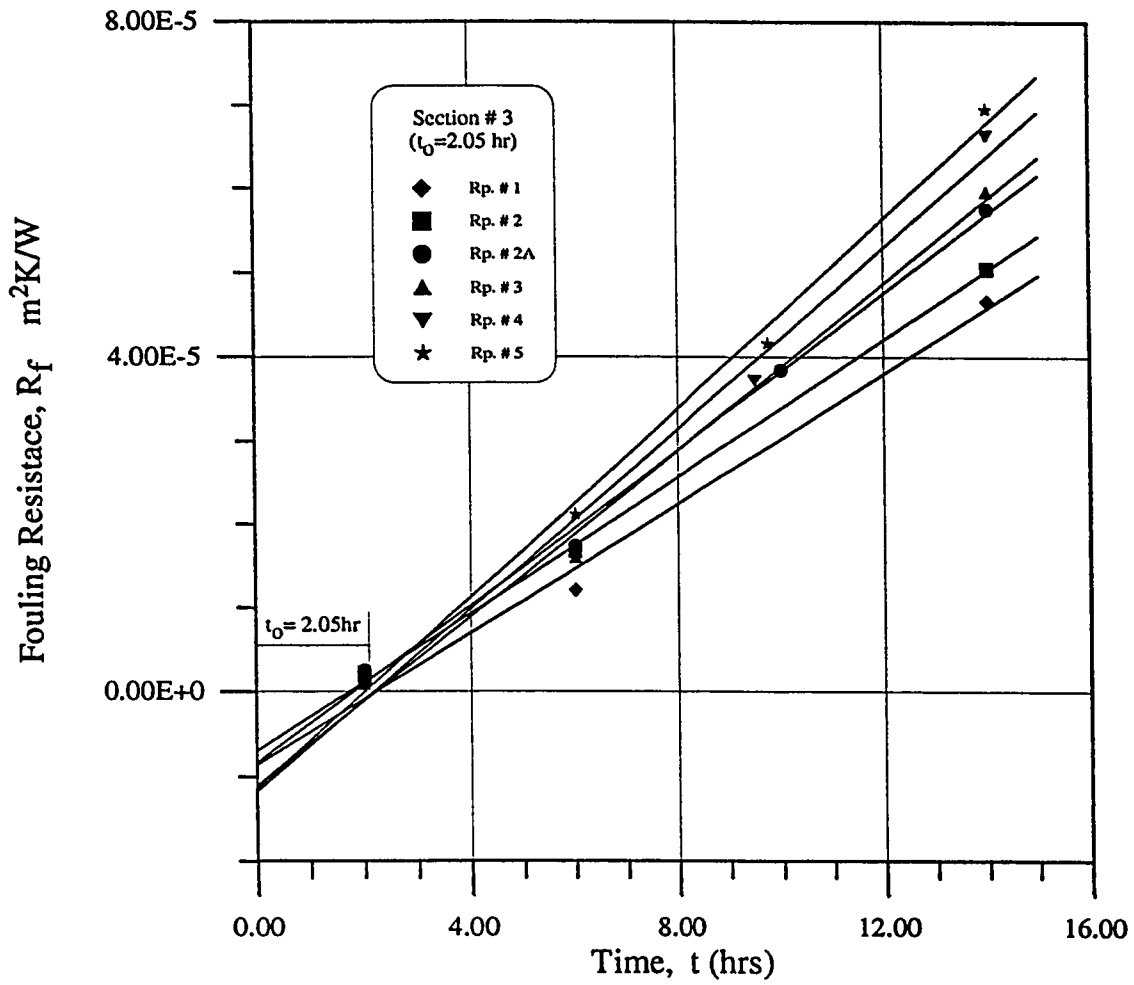


Figure 4.8: Linear regression lines (Section # 3).

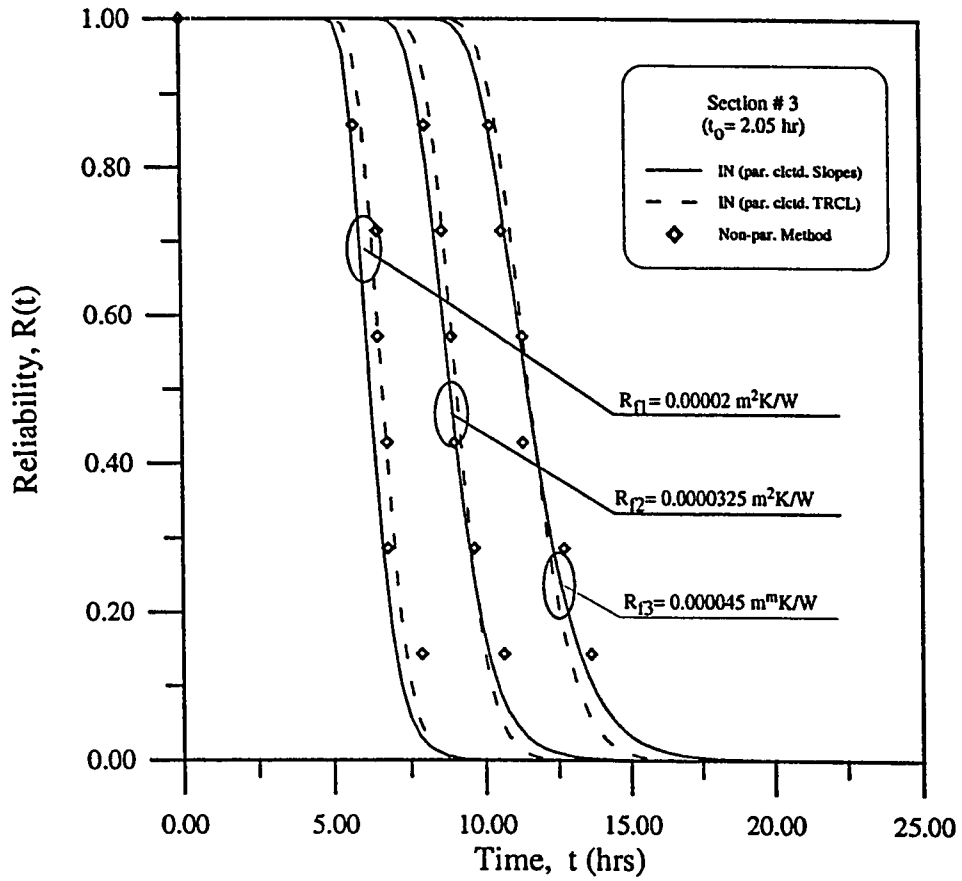


Figure 4.9: Superimposed curves for reliability (Section # 3): details of the curves are given below

		R_{f1}	R_{f2}	R_{f3}
	$\sqrt{\alpha}$	0.15	0.15	0.15
—————	C (hrs)	4.19	6.81	9.43
	$\sqrt{\alpha}$	0.09	0.09	0.09
- - - - -	C (hrs)	6.64	9.07	11.54

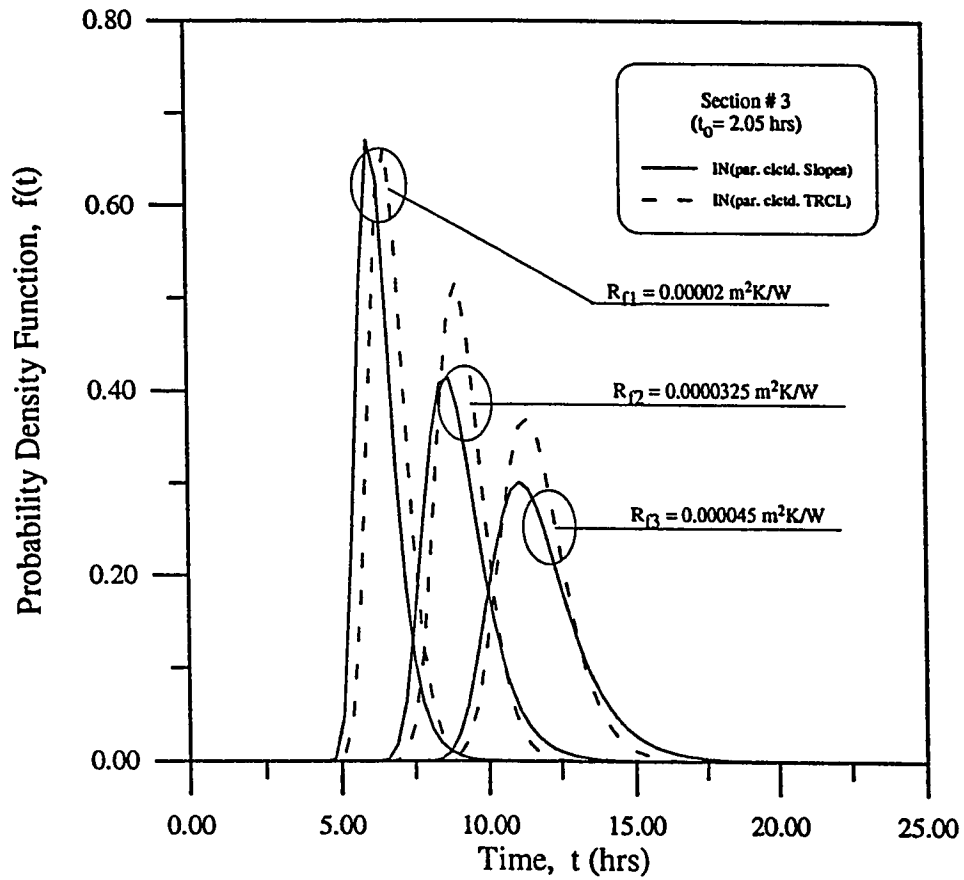


Figure 4.10: Superimposed curves for PDF (Section # 3):
details of the curves are given below

	R_{f1}	R_{f2}	R_{f3}
$\sqrt{\alpha}$	0.15	0.15	0.15
C (hrs)	4.19	6.81	9.43
$\sqrt{\alpha}$	0.09	0.09	0.09
C (hrs)	6.64	9.07	11.54

4.3.1 Results and discussion

A computer program was developed for deriving the distribution functions for each test section. A flowchart showing the general layout of the program is shown in Fig. 4.1. The superimposed curves of distribution functions using different approaches indicate the validity of the inverted normal model for time to reach a critical level of fouling for tubes subject to $CaCO_3$ scaling. These models can further be used for scheduling the maintenance activities, as discussed in chapter 5.

4.4 Corrosion Fouling

The damage due to corrosion of heat-exchanger tubes could result in increased fouling resistance, the effect of which can be minimized by cleaning. Sometimes cleaning has no effect on micro level pits formation due to chemical reaction of the tube material and corrosion products. The depth of pits continue to increase until the leakage of the tubes occur. The statistical analysis of corrosion fouling and distribution of trouble free life against corrosion of heat-exchanger tubes following corrosion damage would be discussed in the subsequent paragraphs.

4.4.1 Increased fouling resistance

Sometimes the corrosion of heat-exchanger tubes reduces the internal effective area resulting in reduced heat-transfer. The R_f vs t curves for such a case are shown earlier

in Fig. 3.20. It is obvious that the fouling resistance never reaches an asymptotic value rather it seems increasing with time, although the rate falls. Therefore the fouling model can best be described by power law as discussed in Appendix-A with a suitable value of n . The linear regression of R_f vs t^n curves help to find value of n to be 0.5 as shown in Fig. 4.11. The distribution function $f(t)$ and $R(t)$ of times corresponding to a critical fouling resistance $R_{f,c}$ is a modified α -distribution and is a special case of generalized distribution discussed by Sheikh [78] and are found using Eqs.(A.16)-(A.17) and are shown in Figs. 4.13 and 4.12, respectively.

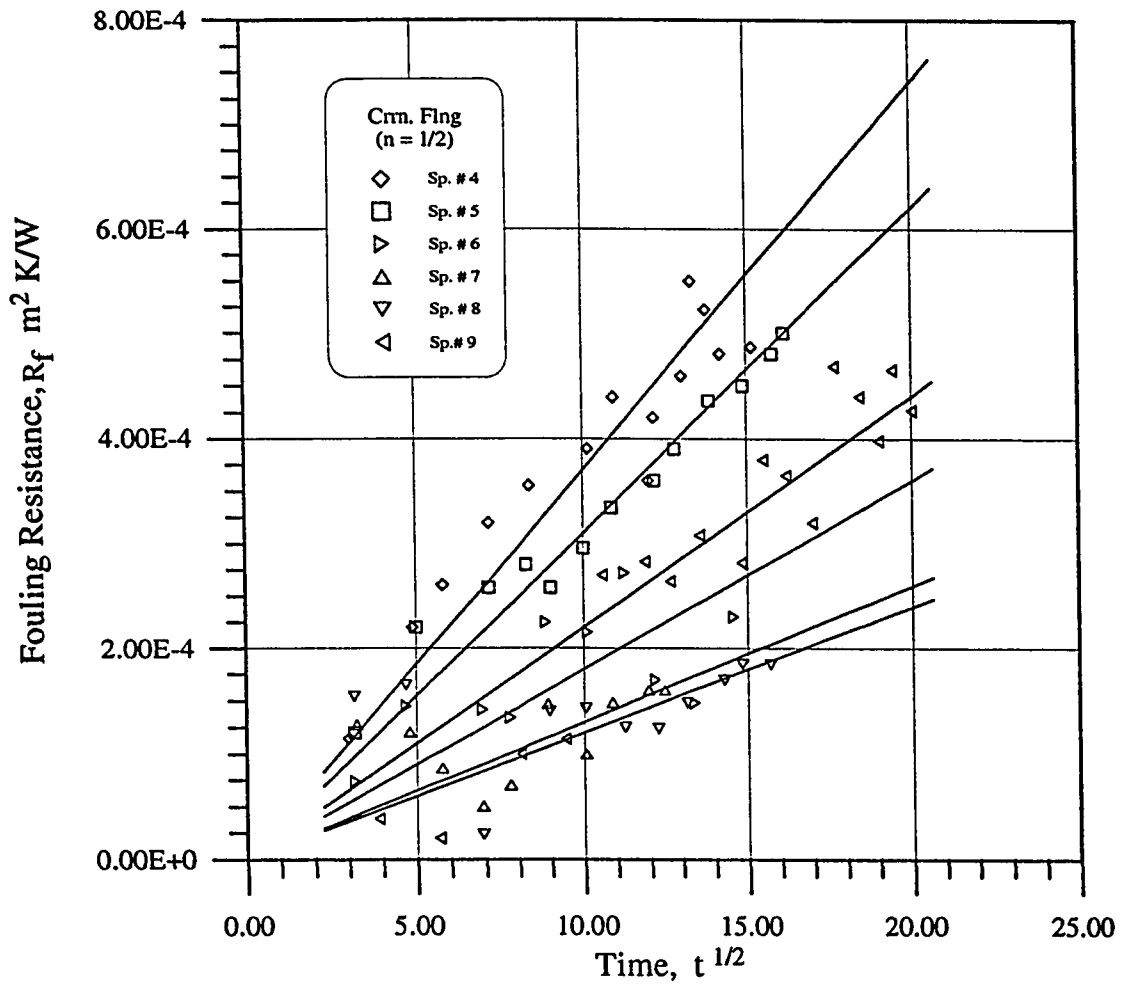


Figure 4.11: Regression lines for corrosion fouling curves.

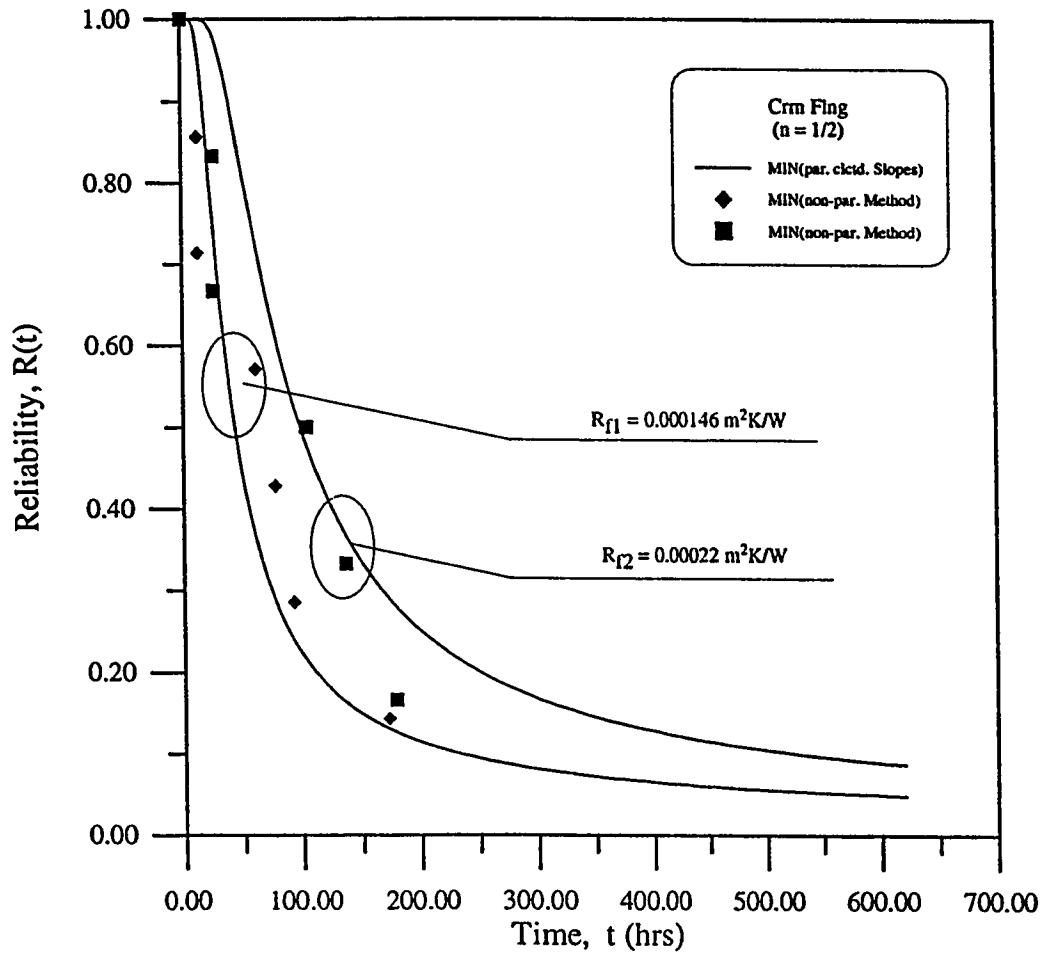


Figure 4.12: Reliability curves for corrosion fouling:
details of the curves are given below

	R_{f1}	R_{f2}
$\sqrt{\alpha}$	0.44	0.44
C (hrs)	6.61	9.94

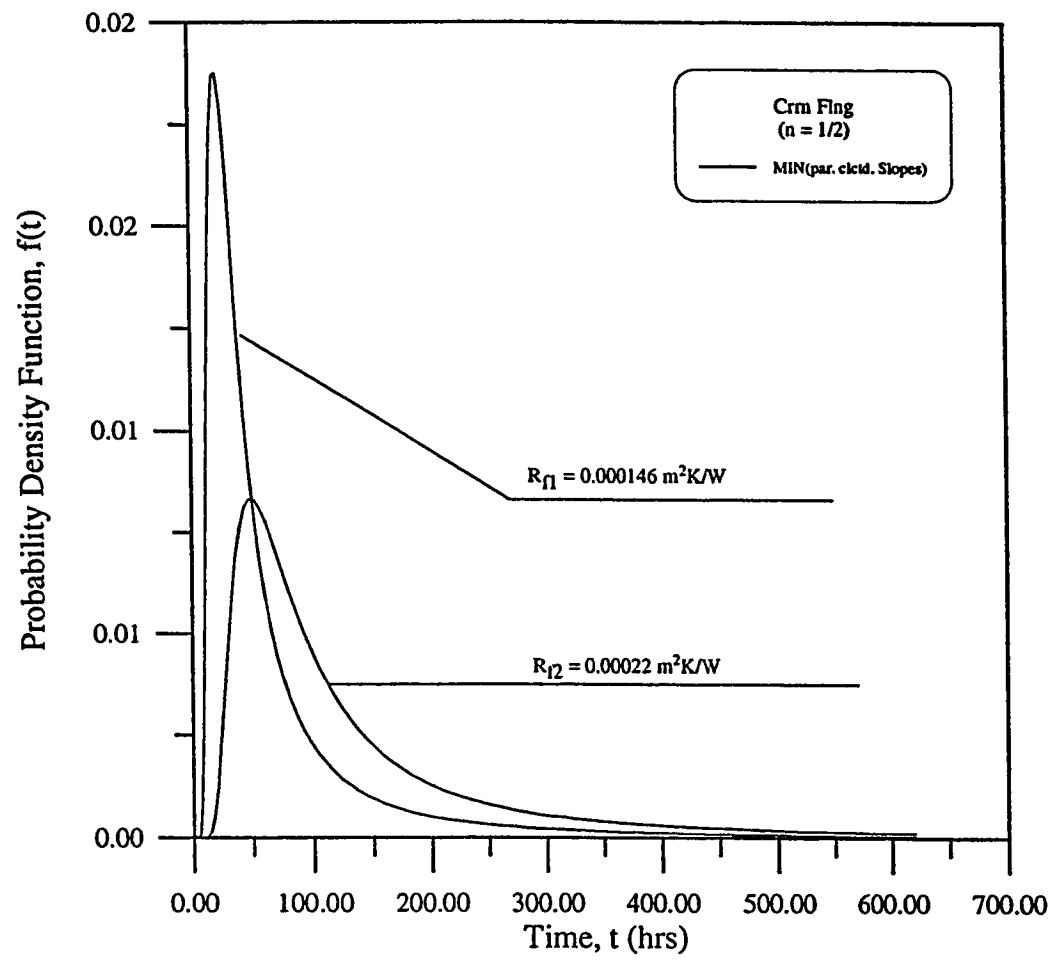


Figure 4.13: PDF curves for corrosion fouling:
 details of the curves are given below

	R_{f1}	R_{f2}
$\sqrt{\alpha}$	0.44	0.44
C (hrs)	6.61	9.94

Chapter 5

Mitigating Techniques and Cost-Based Maintenance Strategies

Many in the industry view fouling as inevitable and deal with it through conservative design, stream treatment and periodic cleaning of the exchangers. Some emphasize providing sufficient heat transfer surface either by having extra exchangers or excess surface in one exchanger to avoid unscheduled plant shutdown from exchanger fouling. Oversizing heat exchangers is probably the most frequently used strategy to mitigate fouling. But it frequently increases fouling. Chemical treatment (on- and off-line) and mechanical cleaning are the most frequent mitigation strategies used other than oversizing. Some people think fouling as a cleaning problem

and believe that efforts should be focused on developing optimum cleaning methods.

At the design stage, fouling factors are difficult to predict. Small increases in the fouling factors cause the designer to make large changes in the heat exchanger size. The heat-exchanger's size and material becomes very important to its cost as shown in Fig. 5.1. Because the heat exchanger user (or the buyer) is the one most concerned with the problems when the heat exchanger fouls, the user usually specifies to the designer the fouling resistances to be used in the design. The user is guided largely by previous experience or on TEMA standards. He wants the heat exchanger to perform at the required duty during the operation period. Unscheduled shutdowns are to be avoided because of the additional cost due to loss in production. As will be discussed, certain steps could be taken during the design process to mitigate fouling.

The ultimate decision to select one or several of the mitigation techniques depend upon the heat-exchanger's application, the type of fouling and various economic parameters of the plant. Currently, most of the major efforts to mitigate or to remove fouling occur during plant operation and shutdown. However, the mitigation of fouling really needs to be addressed during four distinct phases in the life of a heat exchanger [2]:

- design

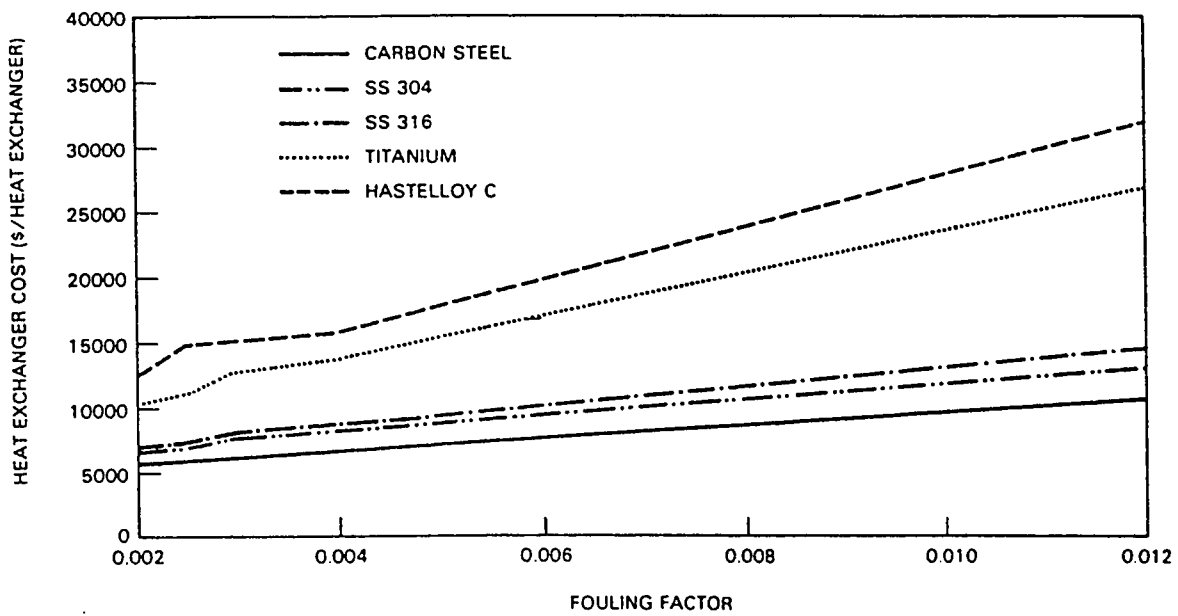


Figure 5.1: heat exchanger cost versus fouling factor and construction material [2]

- construction
- operation (on-line)
- shutdown (scheduled/unscheduled - off-line)

The present discussion will be restricted to the application of the latter two techniques.

5.1 Mitigating Fouling During Plant Operation and Shutdown

The trouble-free operation of well-designed heat exchanger depends on an equally well-designed and controlled treatment program. A large amount of information is available on the effectiveness of various treatment chemicals and mechanical techniques for reducing or preventing fouling.

5.1.1 On-line chemical treatment

Additives to inhibit or to reduce fouling of water streams are used extensively in industry [2, 47, 80, 81]. These include pretreatment chemicals, acid treatment, antiscalants and biocides. Because of environmental regulations and decreased water availability, the amount of water discharged from a cooling system often has to be reduced. Therefore, systems are operating at more concentration cycles and any

liquid discharge from the system is being eliminated if possible, except that which is carried out by entrainment in the effluent plume for the cooling tower.

Several alternatives are available to mitigate or to prevent scale deposition due to high concentrations of scale forming ions. These alternatives include removal of scaling species, pH control, use of scale inhibitor, biofouling control, corrosion control and boiler water treatment.

5.1.2 On-line mechanical techniques

To prevent fouling in liquid systems, two on-line mechanical methods are gaining considerable acceptance. These are [2, 82, 83];

Circulation of sponge rubber balls

The Amertap recirculating ball system uses sponge rubber balls, which are constantly circulated throughout the heat exchanger. The balls are sized slightly larger than the inside diameter of the heat exchanger tube and are slightly compressed as they are moved through the tube by the pressure differential. Each tube "sees" a ball about once every 5 minutes, and the rubbing action of the ball cleans the inner walls by wiping away the deposits, scale, and biological fouling, which are then mixed in with the heat-exchanger's fluid.

An added advantage of this cleaning system is that the balls interrupt the stagnant layer of fluid in the tube, thereby improving heat transfer. The exiting balls are screened, transported, and reinjected upstream to create continuous operation. An automatic ball-counting-and-sorting system pulls out undersized balls (worn down from wear) and keeps a count for replacement. These balls are used almost exclusively in water systems for cleaning heat exchanger and condenser tubes. There are over 500 U.S applications with heaviest representation in utilities, petrochemical, and refinery operations [2, 82].

Backflushing brushes

The Water Service of America (WSA) Superscrubber system uses special brushes made to fit the specific tubes of the heat exchanger [2]. The brushes are sent through the tubes by the fluid flow. A four-way valve returns the brushes for another trip through the tubes by temporarily reversing the flow of fluid in the heat exchanger tubes. Two innovations make this whole process practical, first to get enough force to propel the brush through the tube while it is in contact with the tube wall, a close fitting disc only slightly smaller than the heat exchanger tube is fitted to each end of the traveling brush, and second to have a special retaining basket fitted to each end of heat exchanger tube to retain the brush until the fluid flow is reversed. This basket retains the brush just far enough from the fluid stream so that normal flow is not seriously impeded, but it retains it close enough to the tube end so that

when the flow is reversed, the brush will be inducted into the tube.

Both the Amertap and the WSA systems have advantages and disadvantages. Both require a substantial investment and routine replacement or renewal of the sponges or brushes/retainers. The Amertap system requires special plumbing to install the ball insertion and downstream recovery equipment and special plumbing to avoid unwanted ball diversion or bunching. However, no flow reversal is required with the Amertap system. The WSA system requires no special upstream brush insertion or downstream recovery equipment because of the retainer basket placed on each end of the heat exchanger tubes. The WSA system, however, does require flow reversal of the entire stream of cooling liquid, and valves, plumbing and controls to accomplish this flow reversal. One disadvantage of the WSA brush approach is that in some applications the brushes become fouled. Considerable savings are possible using these two on-line mechanical cleaning systems for fluids. Better heat-transfer coefficients are maintained and, in cooling tower applications, considerable savings can be realized in makeup water because the tubes can be kept clean with higher concentrations of impurities in the water. Manufacturer of these devices claim they can reduce fouling factors to "nearly zero" allowing for savings in initial heat-exchanger costs/reduced operating costs so that the initial investment can be regained in 6 to 24 months, depending on the severity of the operating conditions and the required operating costs. Both systems are limited to modest temperature

operation because of the temperature limitations of the construction materials [2, 83].

5.1.3 Off-line chemical cleaning

Chemical cleaning operations generally use a circulation technique to ensure that the chemicals are always well-mixed and that fresh chemical contacts the heat-transfer surfaces [2, 83]. With this technique, the deposits are dissolved as well as removed by mechanical scouring. Chemical cleaning of heat exchangers is an off-line technique in that the heat exchanger must be taken out of service. The cleaning, however, can usually be accomplished in-situ, so that the exchanger does not have to be removed or opened. An important factor in using acids as cleaning chemicals is the use of an inhibitor so the acid will remove the deposit and not dissolve the heat -transfer surface. Modern inhibitors can be used under extreme temperature and flow rate condition. The metal losses are less than 0.0025 in. for a six hour contact time [2]. It should be noted that purchase of cleaning equipment and/or expensive chemicals may not be cost effective.

5.1.4 Off-line mechanical techniques

Eventually, heat exchangers require cleaning or replacement either during scheduled or unscheduled shutdowns of the plant. If the shutdown is required because the heat exchanger fails, drastic measures may be used to return the equipment to service.

The solution is to fix it quickly or to remove it.

The type of equipment for off-line mechanical cleaning of heat exchangers most frequently used appears to be high pressure jets [2, 83]. These devices use water under pressure as great as 20,000 psi to "blast" away deposits in heat exchanger tubes or on other heat-transfer surfaces. Another technique uses steam injected into the tubes or shell of a heat-transfer device. It has broad industrial application, but their greatest use in industry is for general plant cleanup. The other commonly offered technique is using a lance. This device may be equipped with various cleaning and cutting heads that rotate on the end of the lance. Depending on the tube materials and the deposit, the heads may vary from a soft brush to a drill bit. The source can be air, water, steam, and electric drive and can be mounted either internal or external to the lance [84].

5.2 Economics of Maintenance Against Fouling Based on Linear Growth Law - An Industrial Application

The decisions regarding periodic maintenance/cleaning of heat exchangers subject to fouling in industrial applications is based on thermal and economic behavior. A

detailed deterministic analysis was carried out by Casado [71] for a heat exchanger used in crude oil refining process and results were presented in the form of an optimum exchanger cleaning cycle [71]. The analysis applies to shell-and-tube heat exchangers and an asymptotic deterministic fouling growth law was assumed. A simplified schematic of the preheat train is shown in Fig.5.2 and the relevant properties along with different cost parameters for the fluid streams in the heat exchanger are given in Table 5.1.

5.2.1 Thermal Analysis

In this section the analysis by Casado [71] is generalized by incorporating the stochastic nature of fouling growth law discussed in chapter 4. The linear random fouling growth law is used as a basis of the generalized development, and the modified deterministic case by Casado [71] is also discussed as a special case of the probabilistic analysis.

Planned maintenance interval for a risk level p

The fouling of heat exchanger causes the effectiveness to be dropped with time. The effectiveness of heat exchangers can be calculated at any time 't', if the temperatures of the two fluid streams at the outlet are known. It should be noted that the temperatures at outlet of an exchanger are function of governing fouling model. In the deterministic analysis, for heat exchangers subject to linear fouling, the fouling

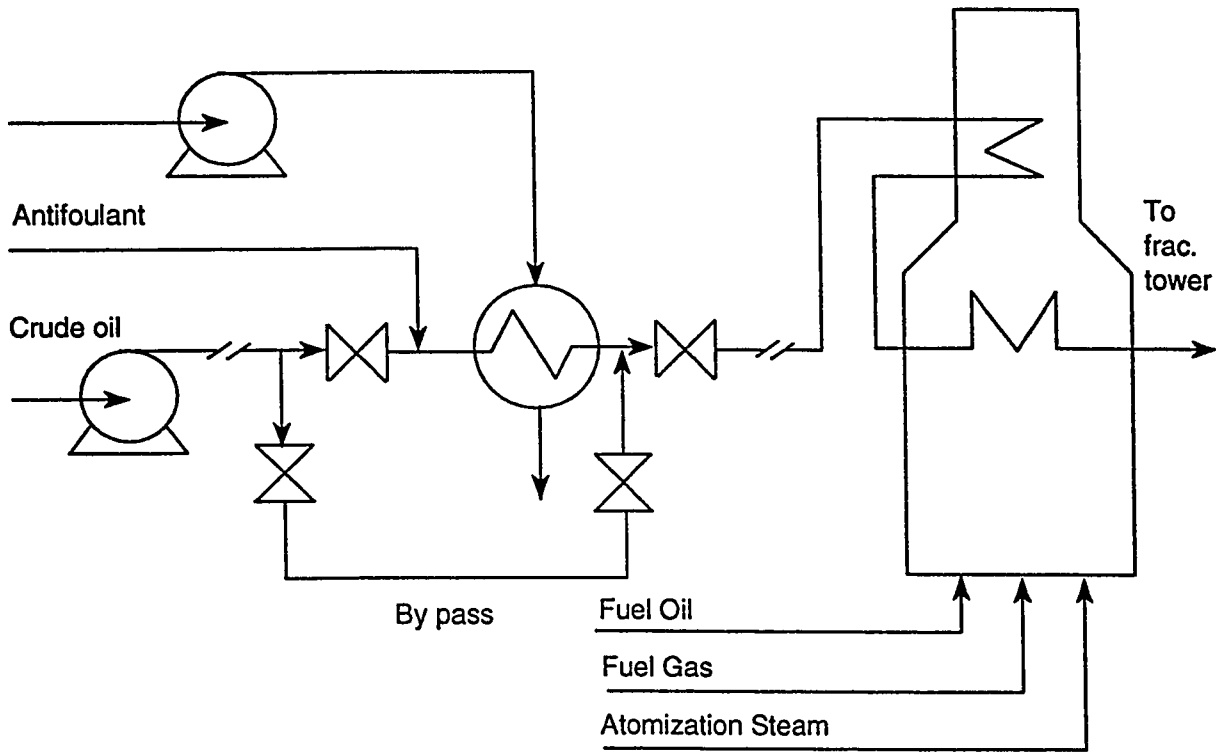


Figure 5.2: A Simplified crude oil preheat train [71].

resistance at any time t is based on a single (mean) value of t_c (time corresponding to a critical level of fouling resistance, $R_{f,c}$), whereas in the probabilistic analysis, the linear fouling growth law incorporates the effect of scatter and risk in the fouling data (see Fig. 5.3). The governing linear fouling law can be expressed in the form

$$[R_f(t)]_p = R_f^\circ + \frac{t}{(t_{p,c})} R_{f,c} , \quad (5.1)$$

however, in the following analysis an abbreviated notation t_p will be used instead of $t_{p,c}$ and $[R_f(t)]_p$ will be abbreviated as $R_f(t)$ with an understanding that it correspond to a risk level p . It should be noted that the the distribution for time to reach critical level of fouling in the linear fouling is α -distribution, for which the risk factor, p defined as $P[t < t_p]$ is given by

$$p = \Phi \left[\frac{t_p - \hat{C}}{\sqrt{\hat{\alpha}} t_p} \right] \quad (5.2)$$

Rearranging the above equation t_p can be expressed as

$$t_p = \frac{\hat{C}}{[1 - \sqrt{\hat{\alpha}} \Phi^{-1}(p)]} \quad (5.3)$$

The governing fouling growth law corresponding to a risk level p expressed in Eq.(5.1) now takes the form

$$R_f(t) = R_f^\circ + \frac{R_{f,c}}{\hat{C}} [1 - \sqrt{\hat{\alpha}} \Phi^{-1}(p)] t. \quad (5.4)$$

Note that Eq.(5.4) defines a straight line passing through a pair of points $(R_f^\circ, 0)$ and $(R_{f,c}, t_p)$; where t_p is reflecting the probabilistic nature of fouling (by Eq.(5.3)) and is plotted in Fig. 5.4.

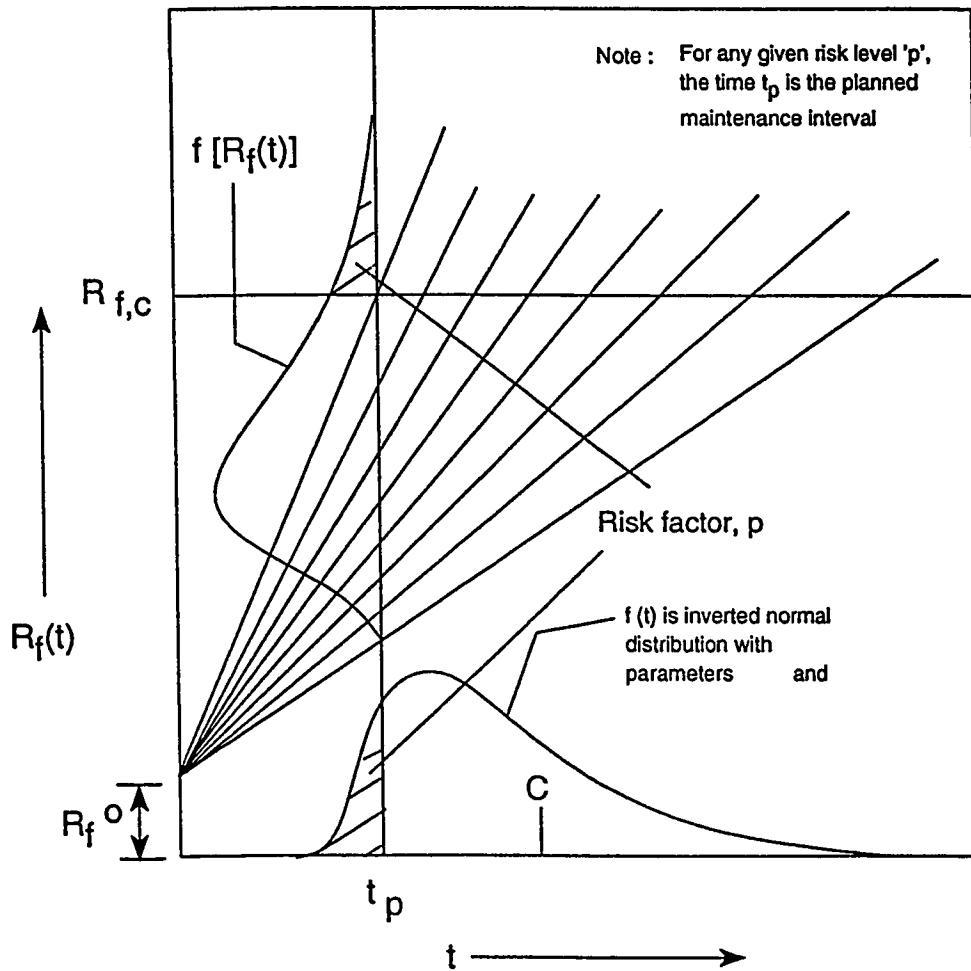


Figure 5.3: Sample functions of linear random fouling growth law

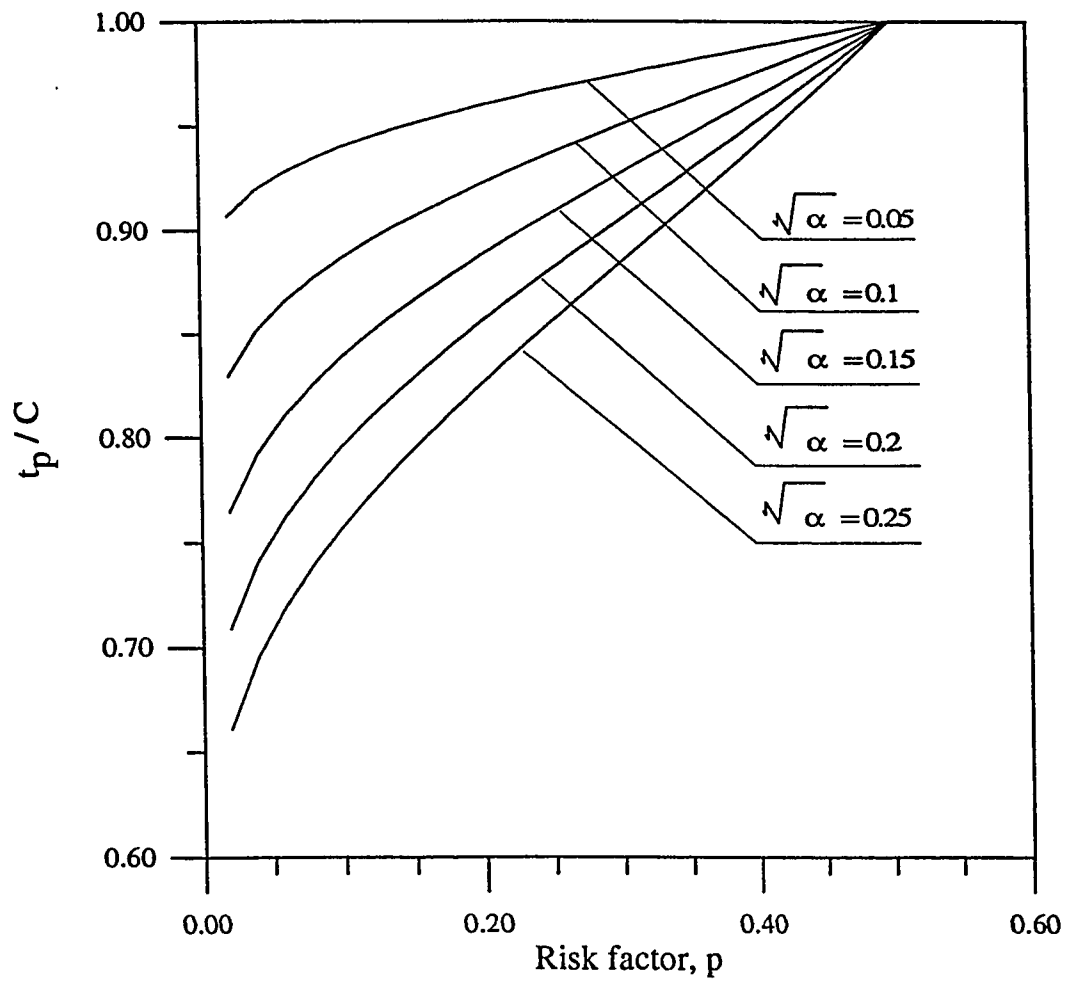


Figure 5.4: The effect of $\sqrt{\alpha}$ with increasing risk level p , on dimensionless planned maintenance interval, t_p/\hat{C} . See Fig.(5.3)

Table 5.1: The relevant properties and cost parameters for the fluid streams in the heat exchanger. [71]

1	Price of 1 FOEB, C_{FOEB}	U.S \$ 16.63
2	Production cost of 15 Kg/cm ² steam, C_s	U.S \$ 3.2/1000 lb
3	API gravity of fuel oil	15 °API
4	Rate: (fuel oil)/(fuel oil+fuel gas), F_{ort}	61.29 %
5	Rate: (steam)/(fuel oil), $F_{s/o}$	20.00 %
6	Fired heater efficiency, e	75 %
7	Total area of heat transfer, A_o	11517 ft ²
8	Number of tube passes, $2n, 4n$, etc.	2
9	Number of shell passes, n	3
10	Antifoulant cost, U.S \$(/1000 lbx1000 ft ²), C_{ad}	7.3
11	Antifoulant concentration, ppm	5 ppm
12	Cleaning cost, C_c'	U.S \$ 677/day
13	Time for cleaning, t_{down}	6
14	Additional heat released by the fired heater during exchanger cleaning, Q_o	23.82 X 10 ⁶ Btu/h
15	Rf^*	0.0145
16	R_f^o	0.000
Tube side - Cold fluid (Crude oil)		
17	Flow rate, W_c	70000 bpd
18	Inlet temperature, T_{ci}	53 °C
19	Outlet temperature, T_{co}	100 °C
20	API gravity	22.7
Shell side - Hot fluid (Atmospheric residue)		
21	Flow rate, W_h	35500 bpd
22	Inlet temperature, T_{hi}	205 °C
23	Outlet temperature, T_{ho}	132 °C
24	API gravity	12.6
For clean exchanger		
25	Outlet temperature (Cold stream), T_{co}	101.7 °C
26	Outlet temperature (Hot stream), T_{ho}	126.3 °C
27	Overall coefficient of heat transfer, U_c	25.65 Btu/h ft ² °F

Determination of Effectiveness

The effectiveness of a heat exchangers is a function of the temperature difference of the hot and cold streams. It normally decreases with time due to increased fouling resistance. At any time 't', corresponding to a targeted risk level p and known \hat{C} and $\sqrt{\alpha}$, which is located on a line characterized by Eq.(5.4), the effectiveness of an exchanger is given by

$$\epsilon_n(t) = \frac{\text{Actual heat transfer}}{\text{Maximum possible heat transfer}} = \frac{Q(t)}{Q_{max}} \quad (5.5)$$

where $\epsilon_n(t)$ is the effectiveness of an exchanger with 'n' shell passes and $2n, 4n, 6n,$ etc. tube passes, and can be expressed as

$$\epsilon_n(t) = \frac{\left[\frac{1-\epsilon_1(t)C}{1-\epsilon_1(t)}\right]^n - 1}{\left[\frac{1-\epsilon_1(t)C}{1-\epsilon_1(t)}\right]^n - C}, \quad (5.6)$$

where $\epsilon_1(t)$ is the effectiveness of an exchanger with one shell pass and 2,4,6 etc. tube passes and is given by [71]

$$\epsilon_1(t) = \frac{2}{1 + C + \frac{1+\exp(-NTU(t)(1+C^2)^{1/2})}{1-\exp(-NTU(t)(1+C^2)^{1/2})} (1 + C^2)^{1/2}}, \quad (5.7)$$

where $NTU(t)$ are the Number of Transfer Units and C is the fluid-capacitance ratio given by

$$C = \frac{C_{min}}{C_{max}} = \frac{(WC_p)_{min}}{(WC_p)_{max}}. \quad (5.8)$$

Here C_{min} is related to the stream that defines the maximum heat-transfer rate that will occur in a counter flow exchanger with infinite area

$$Q_{max} = C_{min} (T_{hi} - T_{ci}), \quad (5.9)$$

T_{hi} and T_{ci} are the temperatures of the hot and cold fluid streams respectively at the inlet to the exchanger. For the present analysis, C is calculated from the equation:

$$Q(t) = (WC_p)_x (\Delta T)_x , \quad (5.10)$$

where x is either "min" or "max". Then solving for $(WC_p)_x$ and replacing in Eq.(5.9) , we get

$$C = \frac{\frac{Q(t)}{(\Delta T)_{min}}}{\frac{Q(t)}{(\Delta T)_{max}}} = \frac{(\Delta T)_{max}}{(\Delta T)_{min}} . \quad (5.11)$$

For the case when "max" belongs to the hot stream and "min" to the cold stream, results in

$$C = \frac{T_{hi} - T_{ho}(t)}{T_{co}(t) - T_{ci}} \quad (5.12)$$

The NTU at any time 't' in Eq.(5.7) is given by relation

$$NTU(t) = \frac{U(t)A_o}{C_{min}} \quad (5.13)$$

where

$$U(t) = \frac{1}{\frac{1}{U_c} + R_f(t)} \quad (5.14)$$

$U(t)$, $R_f(t)$ are the overall heat transfer coefficient and the fouling resistance at any time 't', respectively and U_c is the overall heat-transfer coefficient under clean conditions. It should be noted that the outlet temperatures of hot and cold fluid streams are function of time and can be obtained by calculating their respective enthalpy from the expression

$$Q(t) = W\Delta H(t) \quad (5.15)$$

and making substitution in the following Lee-kessler [71] equations for the hot and cold fluid streams in the exchanger used in crude oil preheat train

$$\Delta H_h(t) = A_1(T_{hi} - T_{ho}(t)) + A_2(T_{hi}^2 - T_{ho}^2(t)) + A_3(T_{hi}^3 - T_{ho}^3(t)) \quad (5.16)$$

$$\Delta H_c(t) = A_1(T_{co}(t) - T_{ci}) + A_2(T_{co}^2(t) - T_{ci}^2) + A_3(T_{co}^3(t) - T_{ci}^3), \quad (5.17)$$

where A_1, A_2 and A_3 are the constants for a fluid stream which can be determined by using the procedure discussed in Appendix C. Using Eqs.(5.6) and (5.16) in Eq.(5.17) for the hot fluid and rearranging, we get

$$\frac{Q_{max}\epsilon_n(t)}{W_h} = (A_1T_{hi} + A_2T_{hi}^2 + A_3T_{hi}^3) - (A_1T_{ho}(t) + A_2T_{ho}^2(t) + A_3T_{ho}^3(t)) \quad (5.18)$$

A computer program was developed as a part of general algorithm shown in Fig. 5.5 and using the data given in Table 5.1 to determine the effectiveness of the heat exchanger for the case considered, undergoing a linear fouling growth model which can be characterized by α -distribution and associated risk level p . The special case discussed by Casado [71] is represented by $\sqrt{\alpha} = 0$ (or it could be representing $p = 0.5$ for any $\sqrt{\alpha}$). The resulting effectiveness curve is shown in Fig. 5.6 for the heat exchanger described in Table 5.1. It should be noted that, this curve is represented for the case of deterministic fouling (i.e., $\sqrt{\alpha} = 0$), or for the probabilistic case it may be interpreted as corresponding to $p = 0.5$ for any $\sqrt{\alpha}$.

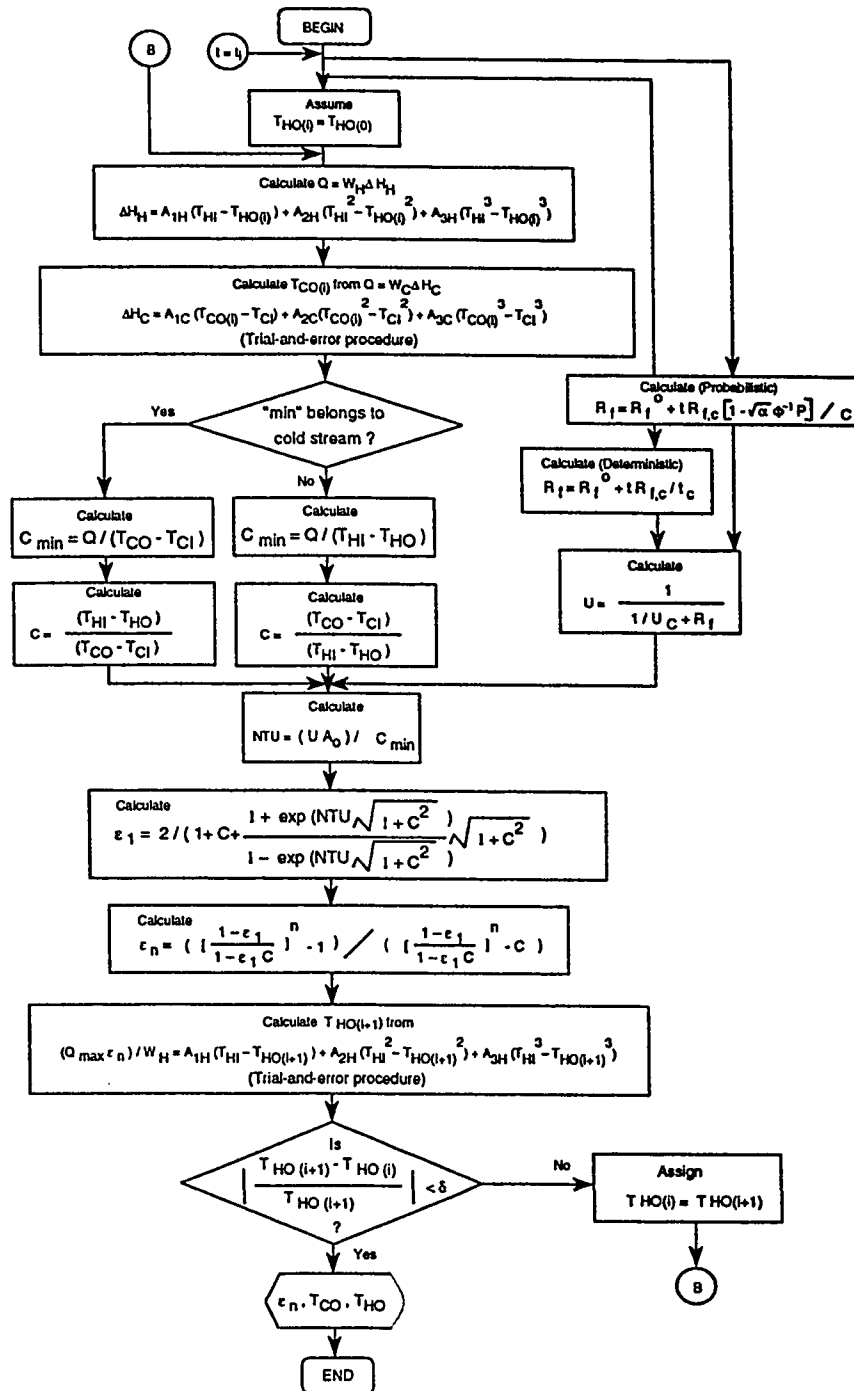


Figure 5.5: A flow diagram of a computer program to determine the effectiveness of heat exchanger at one particular time step. [Modified version of the flow chart proposed by Casado [71], incorporating random linear fouling growth law.]

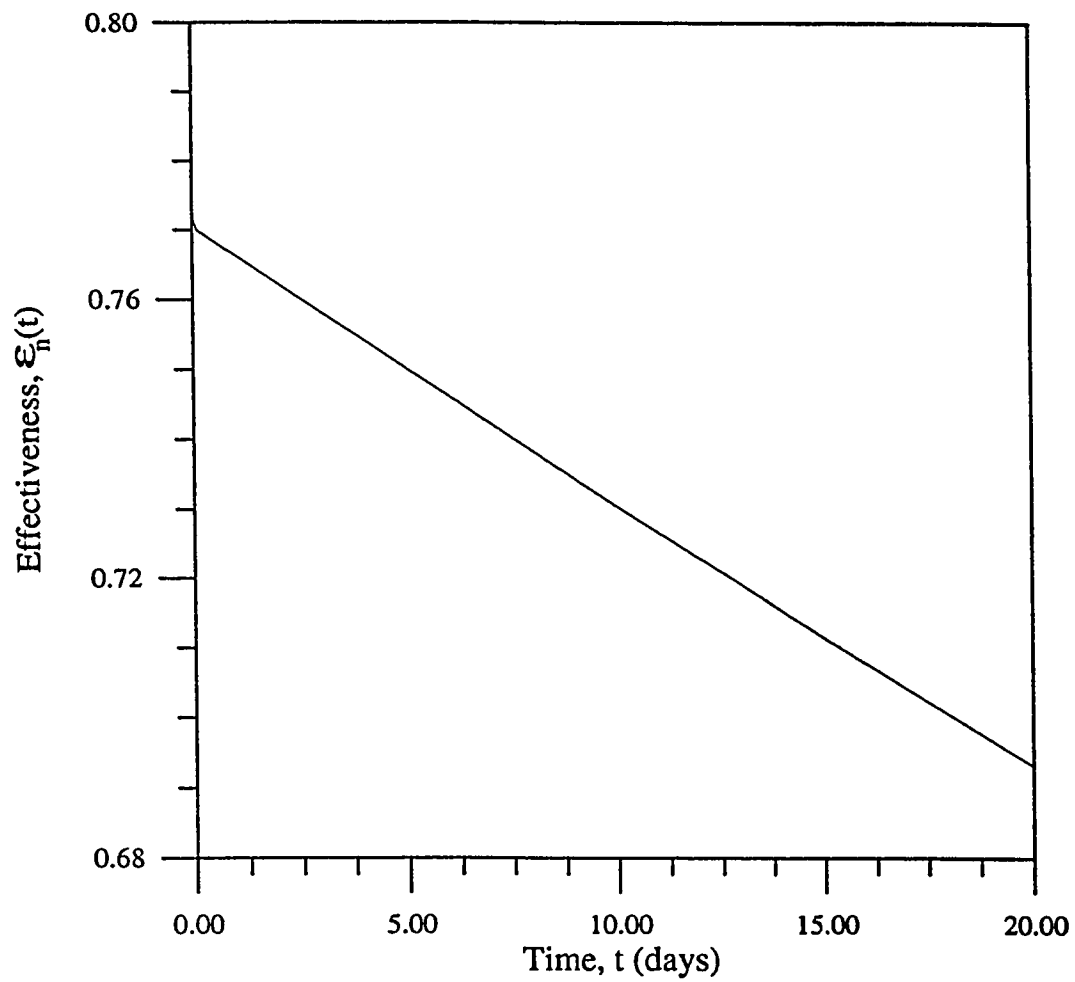


Figure 5.6: Decrease in effectiveness of heat exchanger, with an increase in operating time, undergoing linear deterministic fouling (based on data in Table 5.1 [71]).

5.2.2 Economic Analysis

The operating costs associated with fouling of heat exchanger for the case considered can be subdivided into various elements as discussed hereunder [71]:

Additional consumption of fuel in the fired heater, because of effectiveness drop in the exchanger

For a continuous operation between 0 and t_p days, where t_p represent a planned maintenance cycle corresponding to a risk level p , the costs associated with additional fuel consumption can be expressed as

$$C_H(t_p) = \frac{2400 C_{FOEB}}{e FOEB} \int_0^{t_p} \Delta Q(t) dt \quad (5.19)$$

where C_{FOEB} , e and $FOEB$ are the cost of fuel oil equivalent barrel, fired heater efficiency and fuel oil equivalent barrel, respectively. Also $\Delta Q(t_p) = Q_{max}(\epsilon_n^\circ - \epsilon_n(t_p))$ and introducing another constant k_H ($U.S\$/Btu$) to yield Eq.(5.20) as

$$C_H(t_p) = k_H Q_{max} [\epsilon_n^\circ t_p - \int_0^{t_p} \epsilon_n(t) dt] \quad (5.20)$$

Additional atomization steam needed because of rise in fuel oil consumption

If the rate of atomization steam holds a constant relationship with the fuel oil consumption, and the costs associated with additional atomization steam can be

written as

$$C_S(t_p) = \frac{2400 F_{O/T} F_{S/O} C_{st}}{e NHV} \int_0^{t_p} \Delta Q(t) dt \quad (5.21)$$

$$\text{or } C_S(t_p) = k_S Q_{max} [\epsilon_n^\circ t_p - \int_0^{t_p} \epsilon_n(t) dt], \quad (5.22)$$

where $F_{O/T}$ is weight fraction for fuel oil and fuel gas, $F_{S/O}$ is the weight fraction for steam and oil, C_{st} is the cost of atomization steam and NHV is the net heating value of the fuel oil.

Antifoulant

If antifoulant is used at constant rate then its associated cost is given by

$$C_{AF}(t_p) = 1.498 \times 10^{-3} ppm \rho_c q C_{ad} A_o t_p \quad (5.23)$$

$$C_{AF}(t_p) = C_{AF}' t_p. \quad (5.24)$$

Where ppm are the parts per million of antifoulant, ρ_f is specific gravity of crude oil and q is volumetric flow rate. It is generally observed that the antifoulant cost, C_{ad} is expressed in $U.S \$/lbft^2$ of the total surface of the protected exchangers, to distribute the consumption proportionally to each exchanger.

Cleaning cost

If C_c' is the daily cleaning cost, then the total cost becomes

$$C_c(t_p) = C_c' t_{down}. \quad (5.25)$$

Where t_{down} is the shutdown time for the heat exchanger.

Additional consumption of fuel in the fired heater during exchanger cleaning

If the exchanger's process unit is not stopped (i.e., the exchanger is bypassed), the fired heater will burn an additional amount of fuel necessary to release the heat equivalent to the clean exchanger. This cost may be expressed as:

$$C_A = \frac{2400 C_{FOEB}}{e FOEB} Q_o t_{down} \quad (5.26)$$

$$\text{or } C_A = C_A' t_{down} \quad (5.27)$$

Miscellaneous costs

Finally, other costs related indirectly to fouling are included here as C_M . These include the cleaning program, the shutdown and startup of the process unit, the crude oil filters maintenance, the antifoulant injection system maintenance, and so on. It may be important part in the total fouling costs; however, it is difficult to estimate it with good accuracy.

5.2.3 Derivation of dimensionless cost function

The operating cycle of the heat exchanger consists of the uptime, t_p and downtime, t_{down} , i.e.,

$$t_{cyc} = t_p + t_{down} \quad (5.28)$$

Also, the total fouling cost through an operation cycle can be written as

$$C_{cyc}(t_p) = C_H(t_p) + C_S(t_p) + C_{AF}(t_p) + C_c + C_A + C_M \quad (5.29)$$

Then the total costs through "D" calendar days is

$$C_T(t_p) = \frac{C_{cyc}(t_p) D}{(t_p + t_{down})}. \quad (5.30)$$

Making substitutions and calculating for daily costs, we get

$$\begin{aligned} \frac{C_T(t_p)}{D} = \frac{1}{t_p + t_{down}} \{ & k_H Q_{max} (\epsilon_n \circ t_p - \int_0^{t_p} \epsilon_n(t) dt) + k_S Q_{max} (\epsilon_n \circ t_p - \\ & \int_0^{t_p} \epsilon_n(t) dt) + C_{AF}' t_p + C_c' t_{down} + C_A' t_{down} + C_M \} \end{aligned} \quad (5.31)$$

The curve for the total daily costs for the case by Casado [71] (i.e., $\sqrt{\alpha} = 0$) can be drawn using the above equation as shown in Fig. 5.7. The impact of scatter in fouling reflected by $\sqrt{\alpha}$, for different risk levels is plotted in Figs. 5.8 to 5.10. The effect of increase in the risk level for a particular value of $\sqrt{\alpha}$ is reflected by an increase in the planned maintenance interval t_p and reduced costs. In addition, the curve corresponding to $p = 0.5$ in these figures also represent the deterministic case as discussed by Casado [71].

We can differentiate the above equation with respect to time t_p' and put equal to zero to determine the time period for which costs are minimum to get

$$B(t_p) = \frac{d}{dt} \left(\frac{C_T(t_p)}{D} \right) = \int_0^{t_p} \epsilon_n(t) dt - \epsilon_n(t_p)(t_p + t_{down}) + t_{down} \epsilon_n' = 0 \quad (5.32)$$

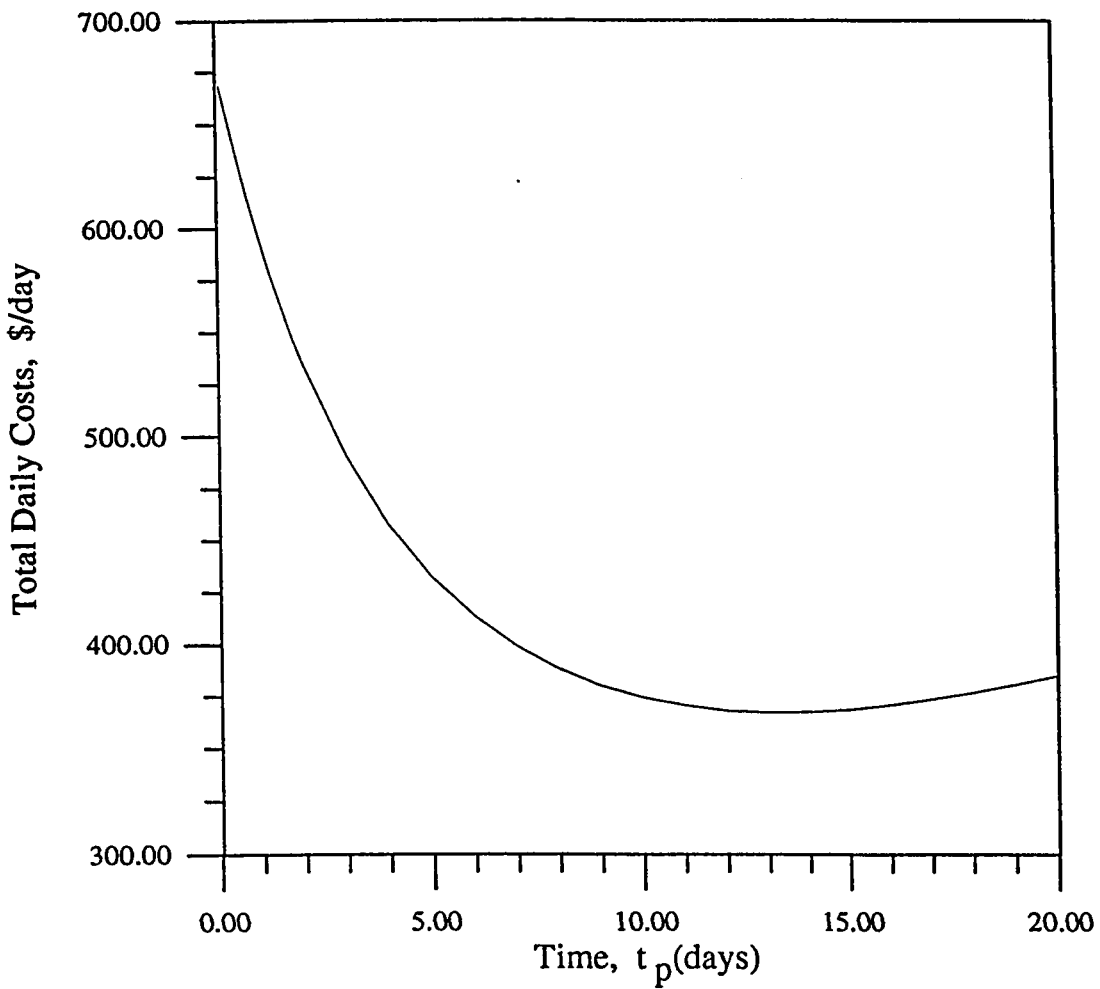


Figure 5.7: Total daily cost for data by Casado[71] (plot of Eq.(5.31) for $\beta=0$, or for $p = 0.5$ for any $\sqrt{\alpha}$.)

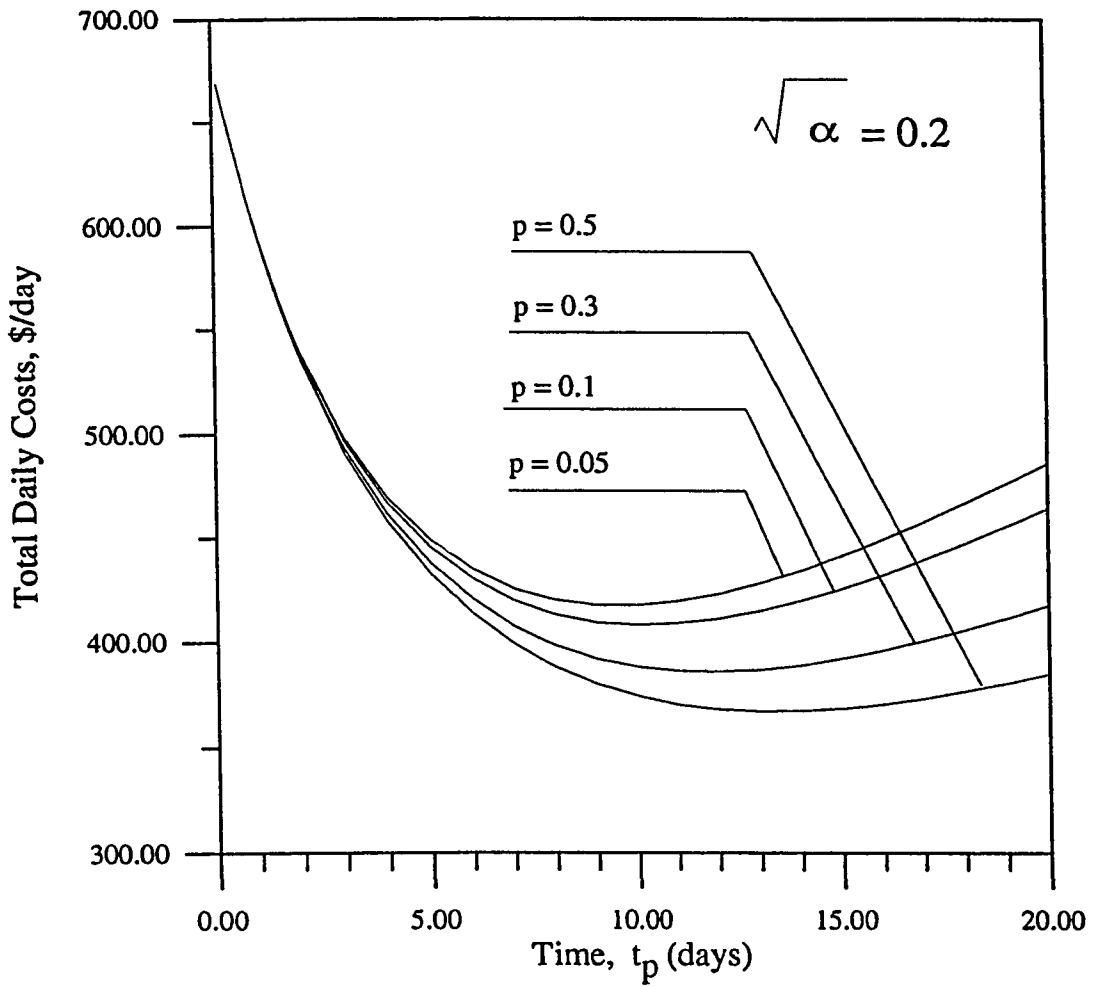


Figure 5.8: Total daily costs at varying risk level p and scatter parameter $\sqrt{\alpha}$.

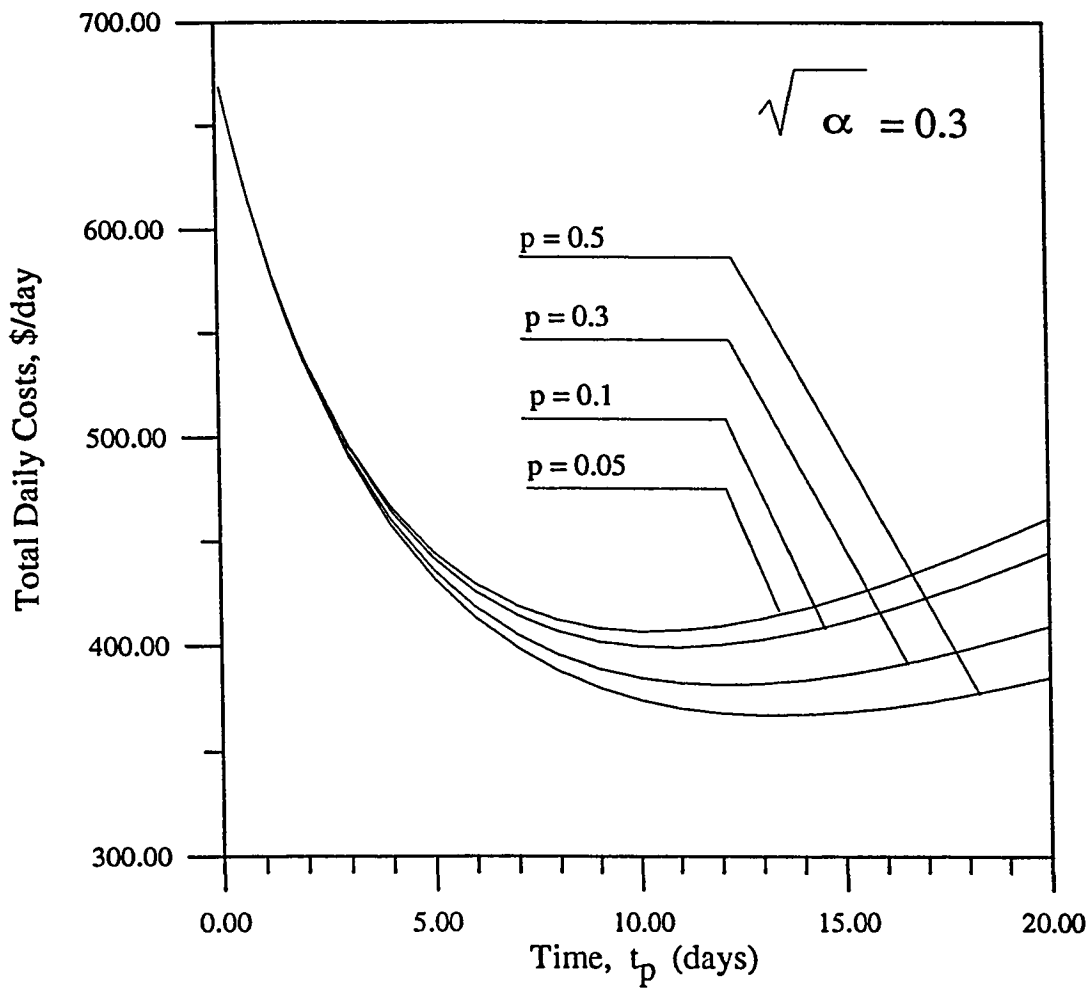


Figure 5.9: Total daily costs at varying risk level p and scatter parameter $\sqrt{\alpha}$.

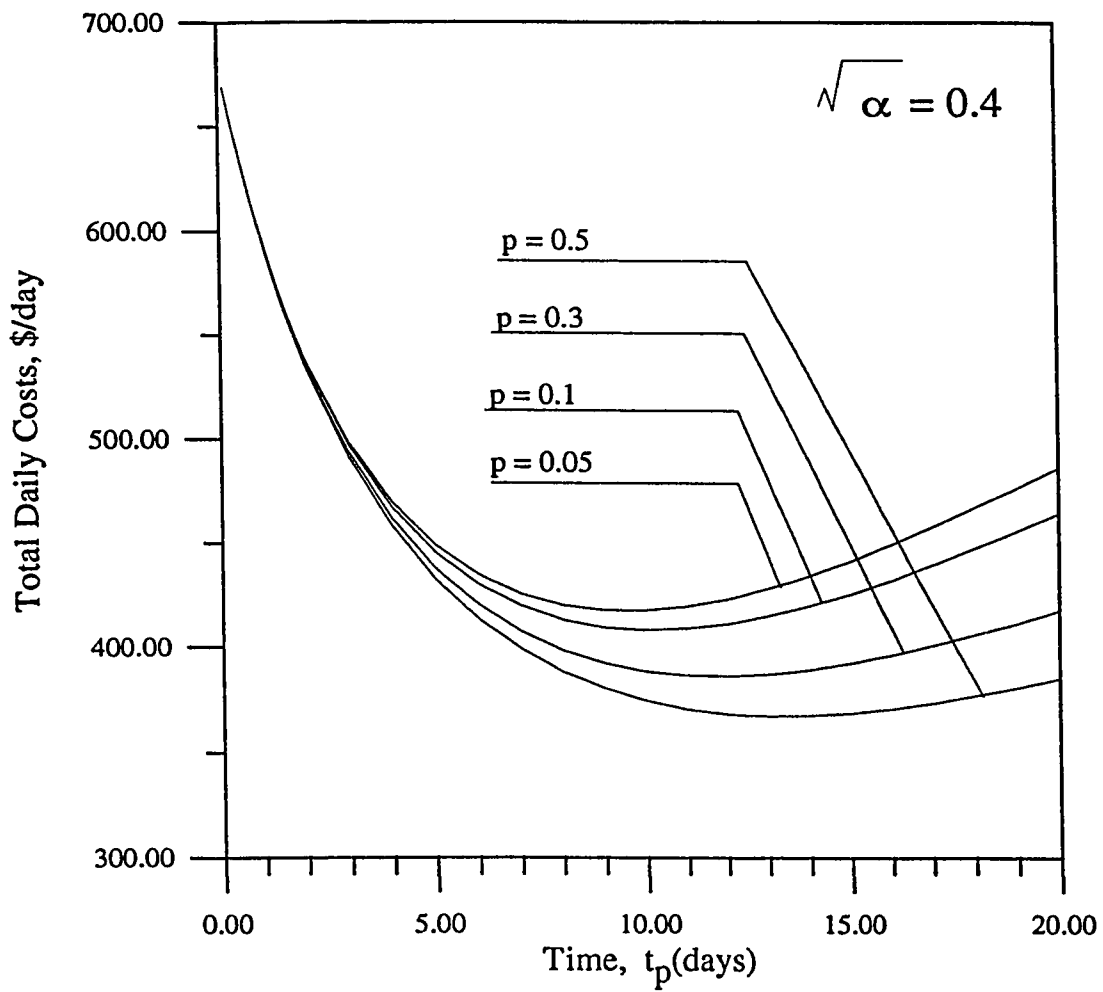


Figure 5.10: Total daily costs at varying risk level p and scatter parameter $\sqrt{\alpha}$.

where

$$\epsilon' = \epsilon_n^\circ + \frac{C_{AF}' - (C_c' + C_A' + C_M/t_{down})}{(k_H + k_S) Q_{max}} \quad (5.33)$$

The solution of Eq.(5.32) for a general case can be facilitated by a graphical approach. For the deterministic case by Casado [71] the graphical approach is illustrated in Fig. 5.11.

Simplifying the above equation for daily costs and dividing throughout by $(C_c' + C_A')$ to convert the equation into dimensionless form, we get

$$\begin{aligned} \Gamma(C) = & \gamma_1 \left[\frac{24}{t_p + t_{down}} (\epsilon_n^\circ t_p - \int_0^{t_p} \epsilon_n(t) dt) \right] \\ & + \gamma_2 \left(\frac{t_p}{t_p + t_{down}} \right) + \gamma_3 \left(\frac{t_{down}}{t_p + t_{down}} \right) \end{aligned} \quad (5.34)$$

Where

$$\gamma_1 = \frac{Q_{max}(k_H + k_S)}{24(C_c' + C_A')} \quad (5.35)$$

$$\gamma_2 = \frac{C_{AF}'}{(C_c' + C_A')} \quad (5.36)$$

$$\gamma_3 = 1 + \frac{C_M}{(C_c' + C_A')t_{down}} \quad (5.37)$$

The variation in the dimensionless cost $\Gamma(C)$ with dimensionless time $t_p/(t_p + t_{down})$ depends upon the values of the dimensionless variables γ_1 , γ_2 and γ_3 and risk level p , and distribution parameters \hat{C} and $\sqrt{\alpha}$. This dimensionless total cost for various values of $\sqrt{\alpha}$, is plotted in Figs. 5.12, 5.13 and 5.14 for different risk levels.

The variation of the dimensionless cost with respect to the cost parameters γ_1 , γ_2 and γ_3 has been shown in Figs. 5.15, 5.16 and 5.17 by fixing the two variables and changing the third.

The sensitivity analysis of dimensionless cost function to variables γ_1 , γ_2 and γ_3 can be assessed by differentiating $\Gamma(C)$ w.r.t γ_1 , γ_2 and γ_3 respectively to get

$$\frac{\partial \Gamma(C)}{\partial \gamma_1} = \frac{24}{t_p + t_{down}} (\epsilon_n \circ t_p - \int_0^{t_p} \epsilon_n(t) dt), \quad (5.38)$$

$$\frac{\partial \Gamma(C)}{\partial \gamma_2} = \frac{t_p}{t_p + t_{down}}, \quad (5.39)$$

$$\frac{\partial \Gamma(C)}{\partial \gamma_3} = \frac{t_{down}}{t_p + t_{down}}, \quad (5.40)$$

The resulting equations are plotted against the dimensionless time as shown in Figs. 5.18, 5.19 and 5.20 respectively. It can be seen that for smaller values of time, the effect of γ_1 is low but for larger values of time, its effect is significant. The effect of γ_2 on dimensionless cost function is linearly increasing. Finally, $\Gamma(C)$ is sensitive to γ_3 in the beginning but its effect diminishes with time.

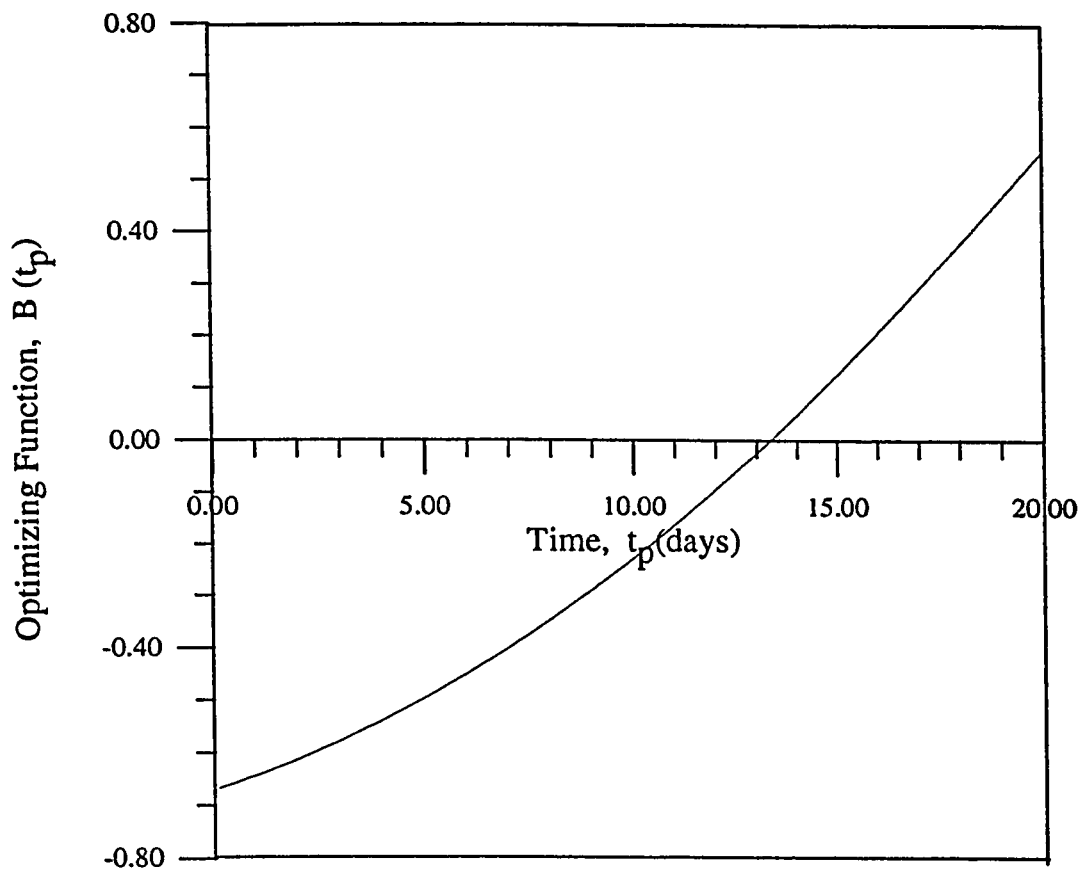


Figure 5.11: Cost optimizing function.

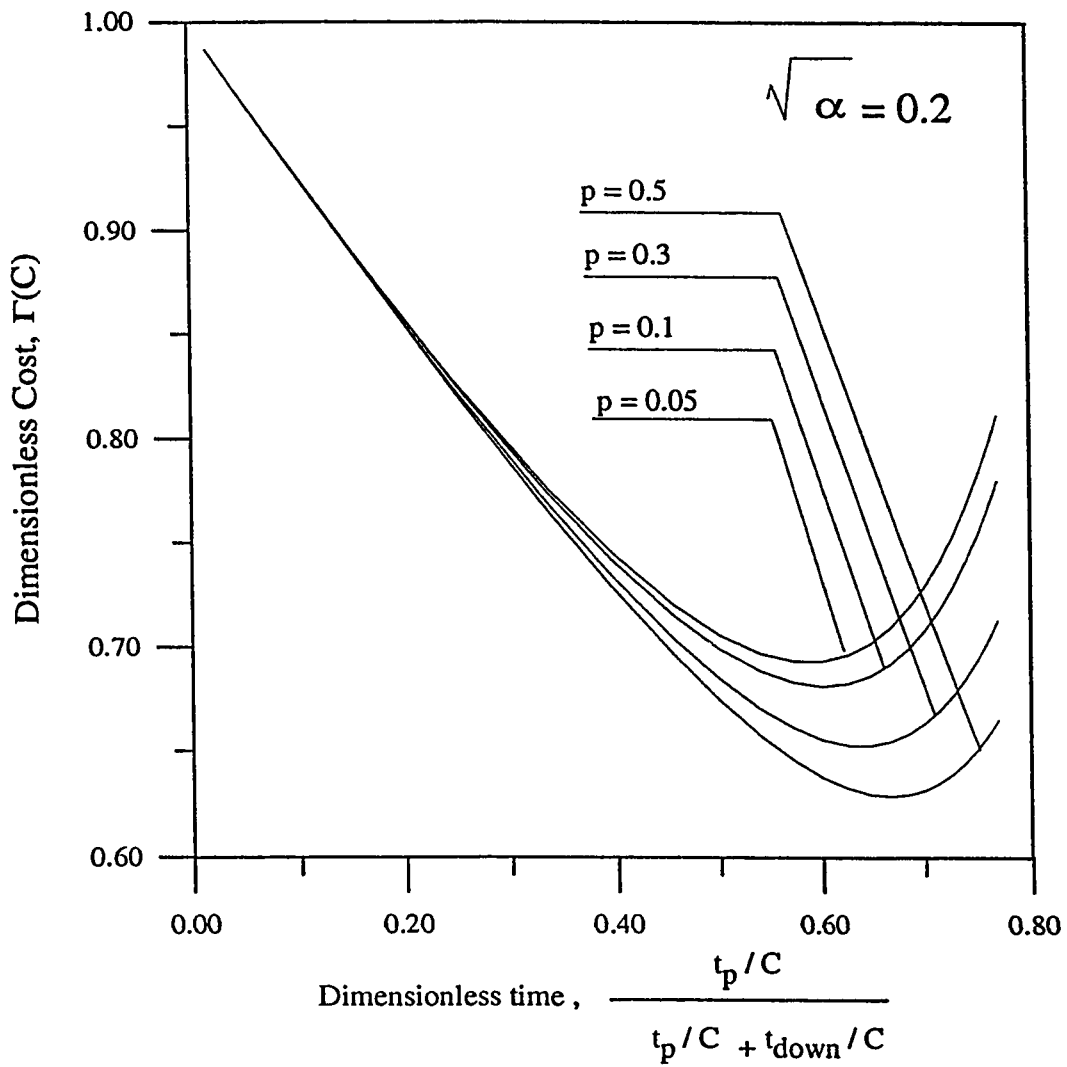


Figure 5.12: Dimensionless cost as a function of dimensionless time, for different risk level p and scatter parameter $\sqrt{\alpha} = 0.2$. The cost parameters γ_1, γ_2 and γ_3 are 0.32914, 0.13042 and 1.0 respectively

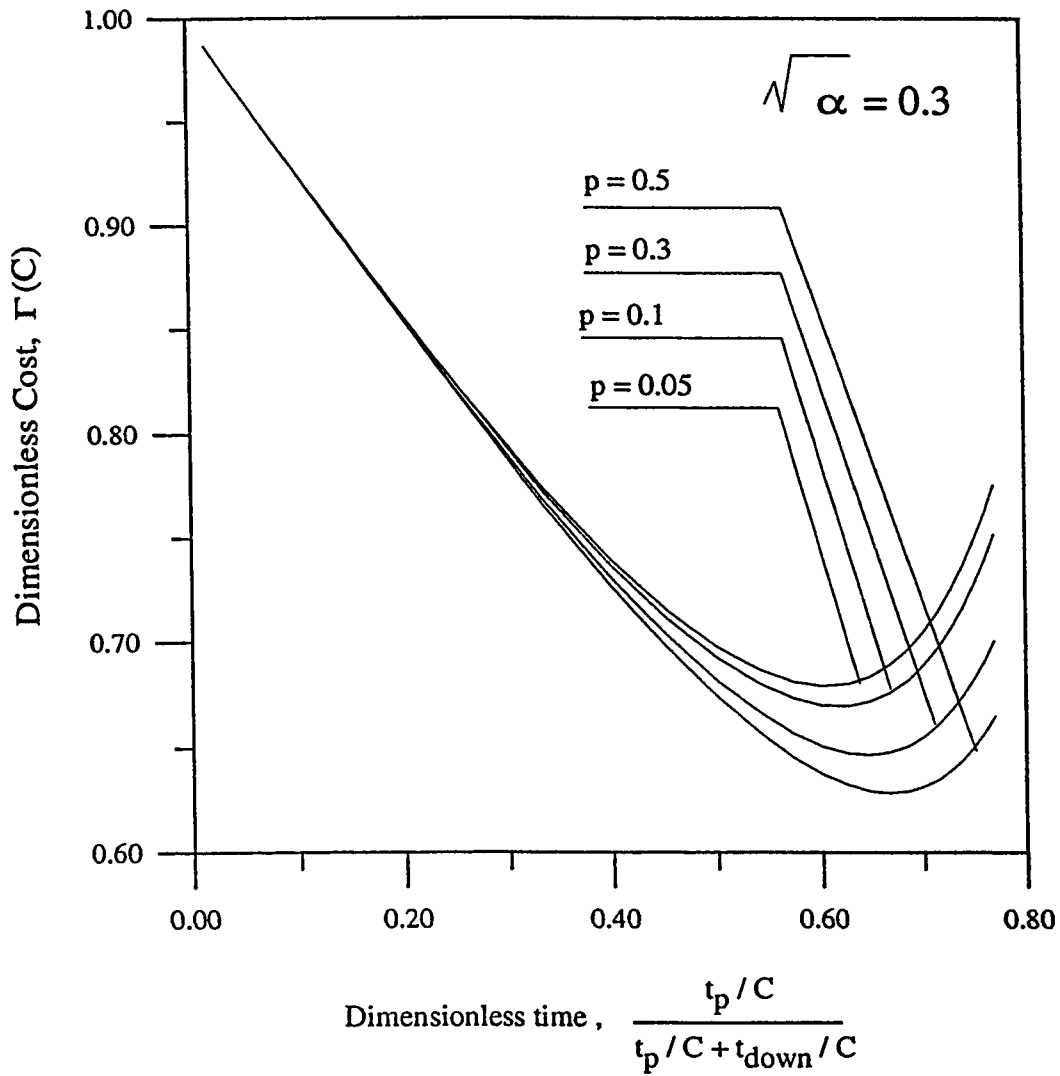


Figure 5.13: Dimensionless cost as a function of dimensionless time, for different risk level p and scatter parameter $\sqrt{\alpha}=0.3$. The cost parameters γ_1, γ_2 and γ_3 are 0.32914, 0.13042 and 1.0 respectively

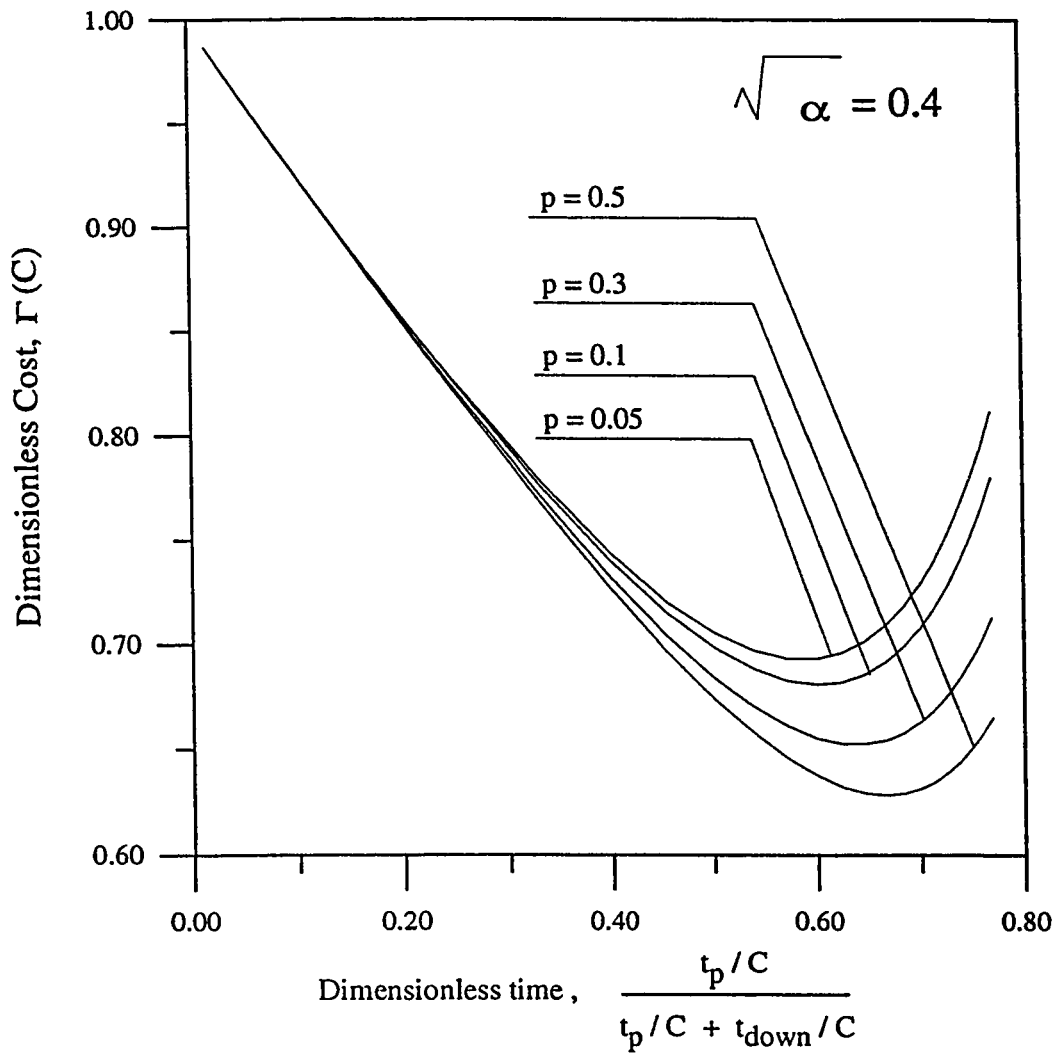


Figure 5.14: Dimensionless cost as a function of dimensionless time, for different risk level p and scatter parameter $\sqrt{\alpha} = 0.4$. The cost parameters γ_1 , γ_2 and γ_3 are 0.32914, 0.13042 and 1.0 respectively

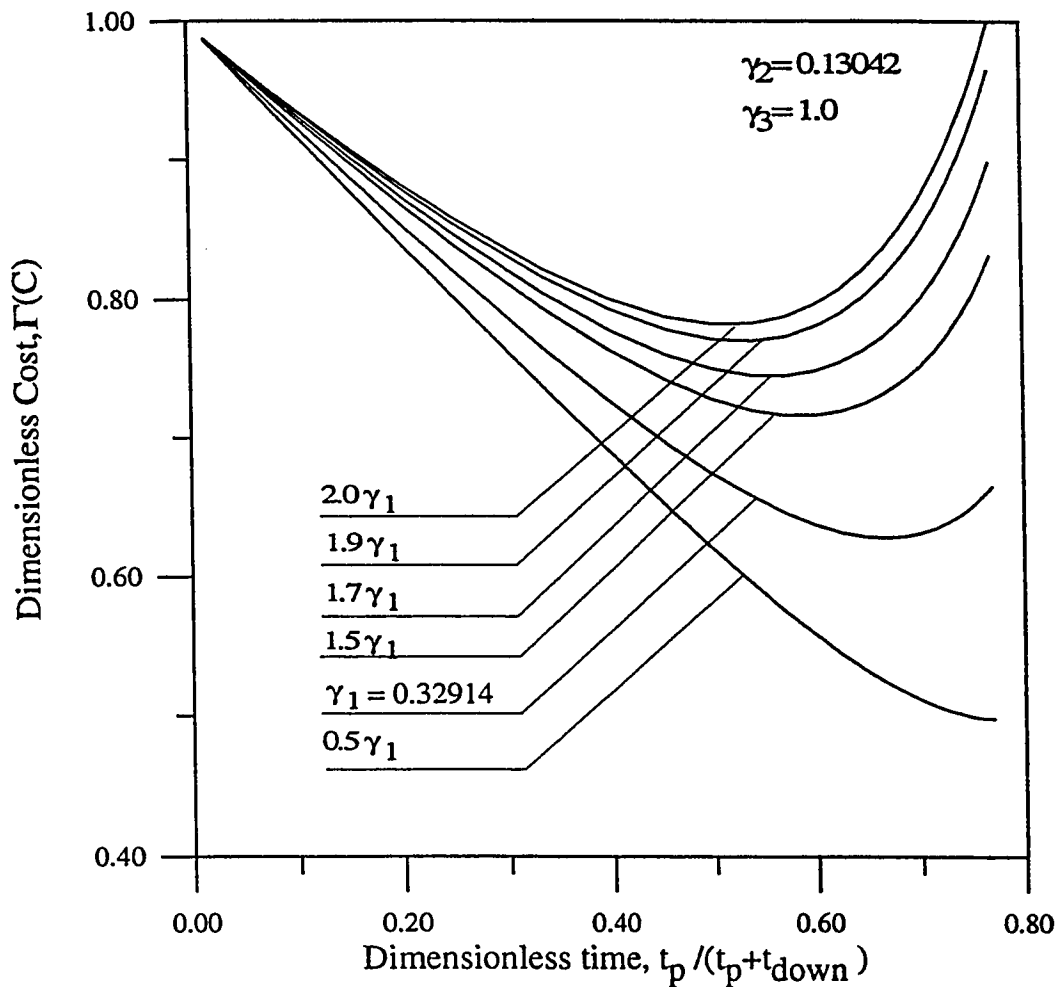


Figure 5.15: The effect of cost parameter γ_1 on the dimensionless cost. These curves represent either a deterministic case $\sqrt{\alpha} = 0$, or cost corresponding to $p = 0.5$ for any value of $\sqrt{\alpha}$. The case by Casado [71] is represented by curve with $\gamma_1 = 0.32914$.

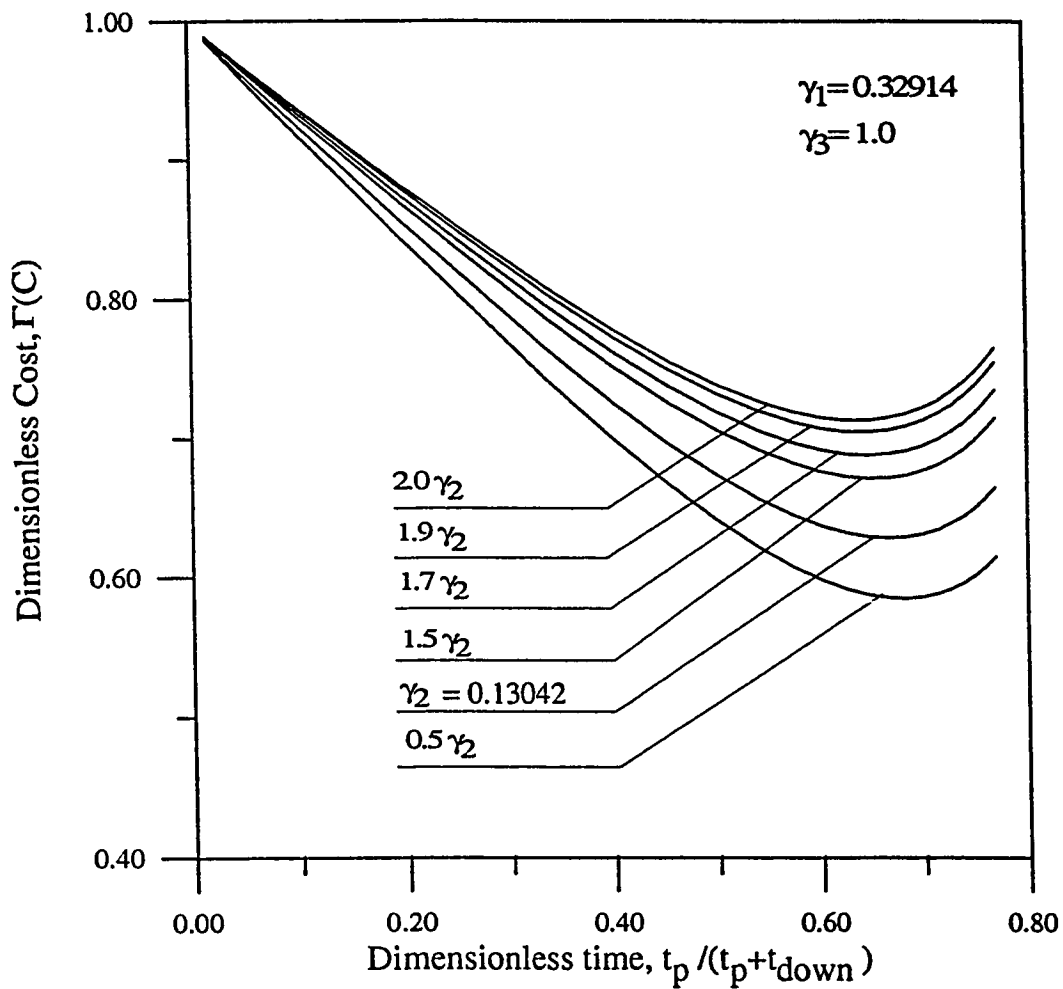


Figure 5.16: The effect of cost parameter γ_2 on the dimensionless cost. These curves represent either a deterministic case $\sqrt{\alpha} = 0$, or cost corresponding to $p = 0.5$ for any value of $\sqrt{\alpha}$. The case by Casado[71] is represented by curve with $\gamma_2 = 0.13042$.

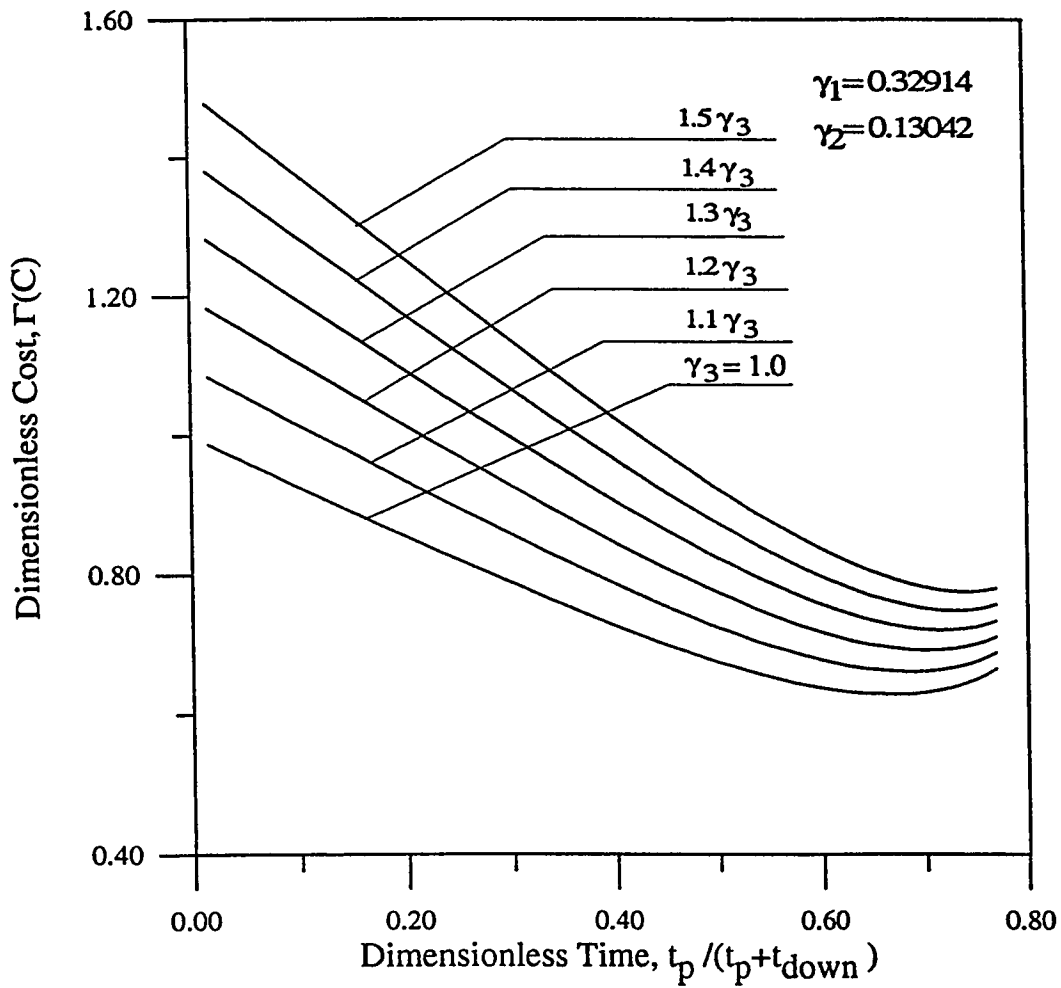


Figure 5.17: The effect of cost parameter γ_3 on the dimensionless cost. These curves represent either a deterministic case $\sqrt{\alpha} = 0$, or cost corresponding to $p = 0.5$ for any value of $\sqrt{\alpha}$. The case by Casado [71] is represented by curve with $\gamma_3 = 1.0$.

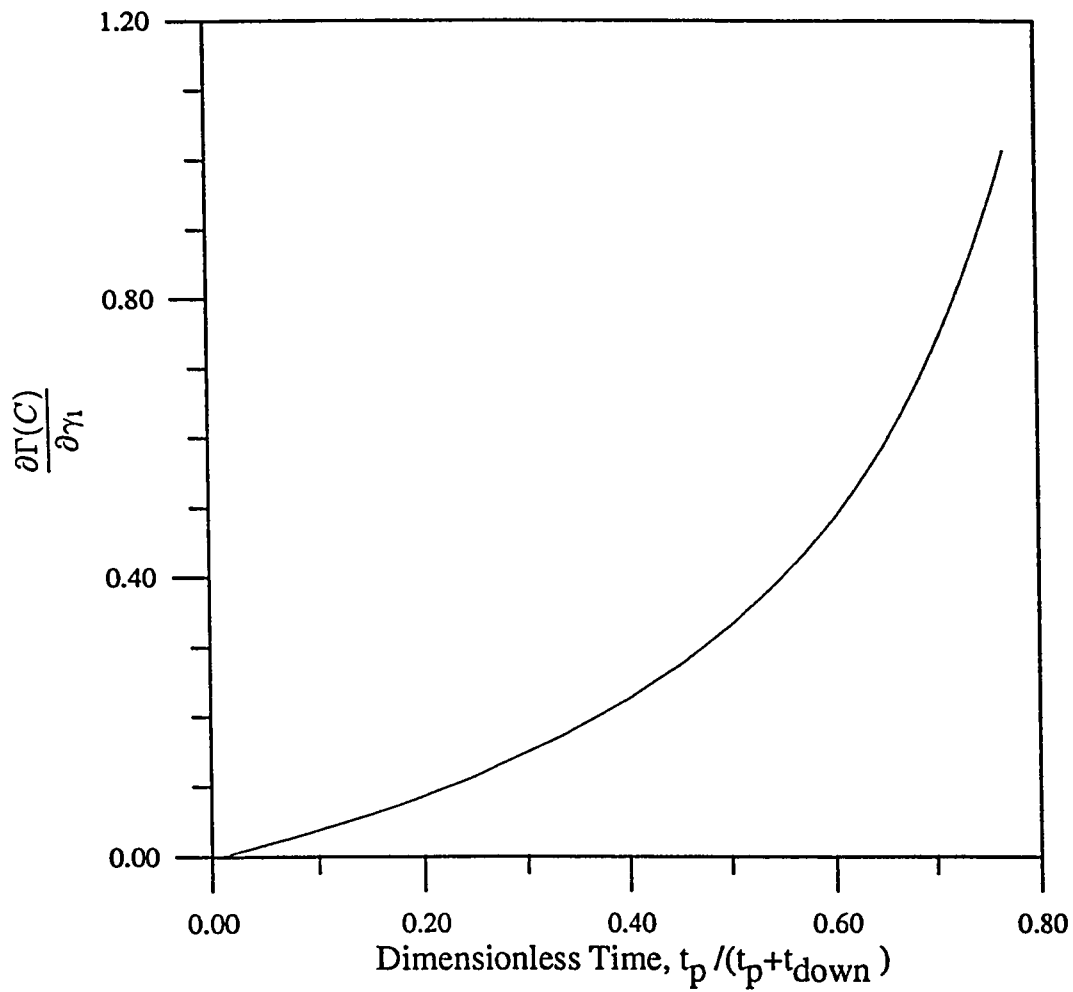


Figure 5.18: The sensitivity of dimensionless cost function w.r.t γ_1 . This curve represent either a deterministic case $\sqrt{\alpha} = 0$, or cost corresponding to $p = 0.5$ for any value of $\sqrt{\alpha}$.

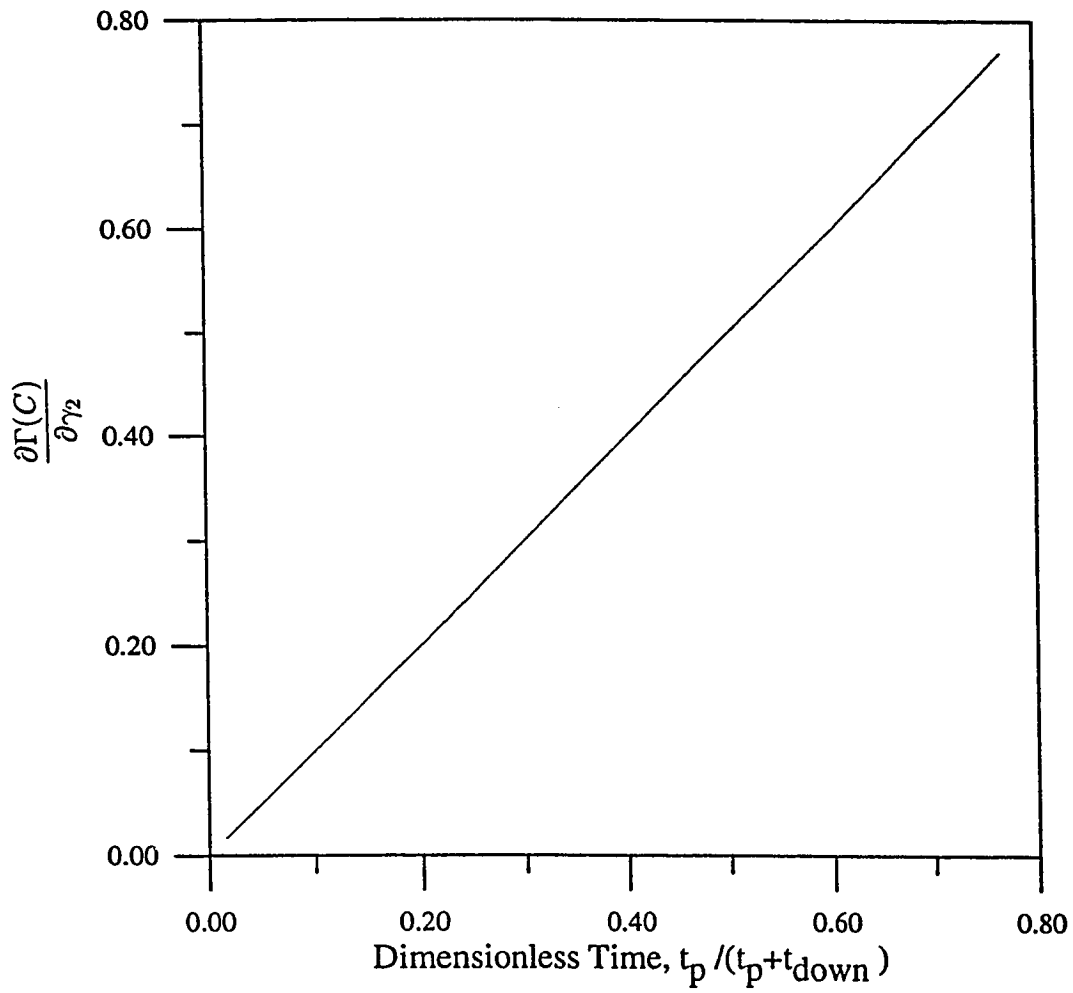


Figure 5.19: The sensitivity of dimensionless cost function w.r.t γ_2 . This curve represent either a deterministic case $\sqrt{\alpha} = 0$, or cost corresponding to $p = 0.5$ for any value of $\sqrt{\alpha}$.

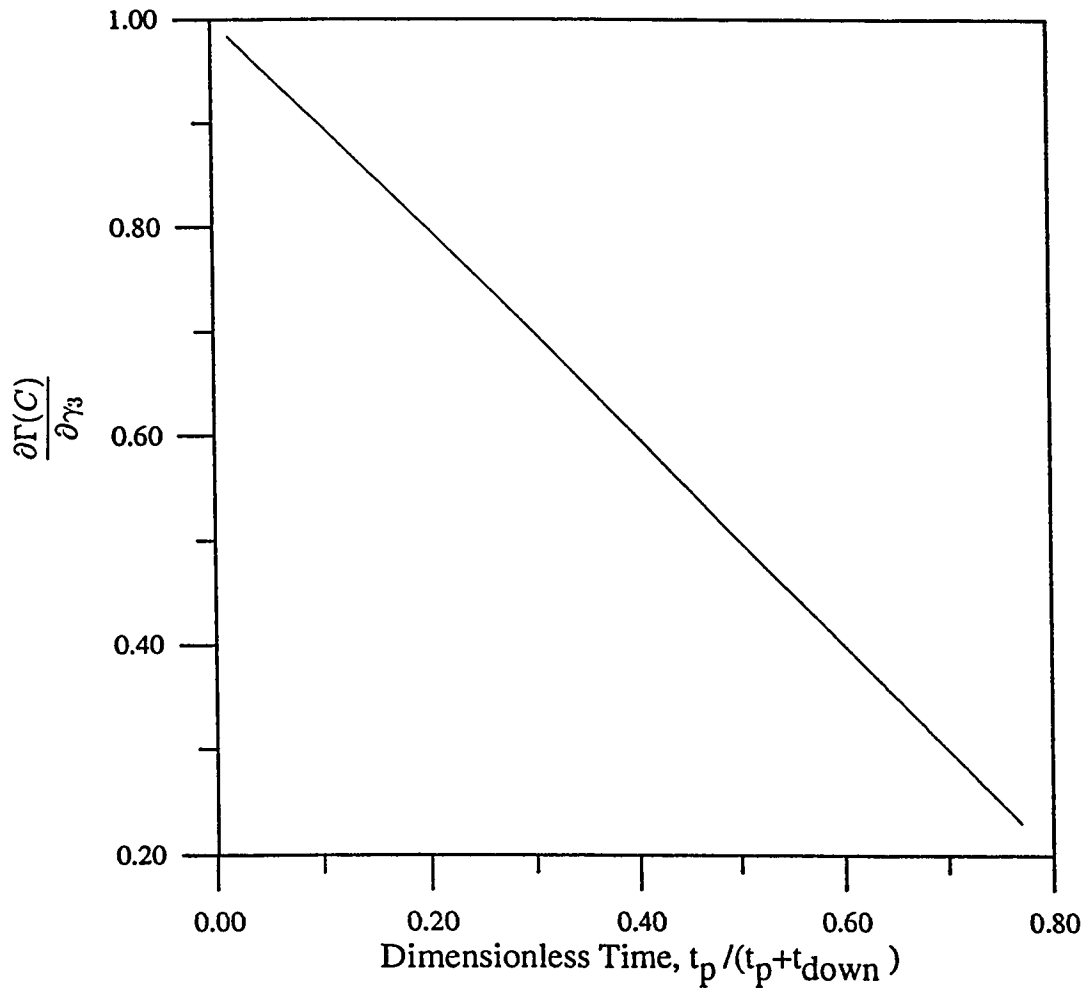


Figure 5.20: The sensitivity of dimensionless cost function w.r.t γ_3 . This curve represent either a deterministic case $\sqrt{\alpha} = 0$, or cost corresponding to $p = 0.5$ for any value of $\sqrt{\alpha}$.

Chapter 6

Conclusions and Recommendations

1. The experimental work regarding $CaCO_3$ scaling has shown that the scale deposit was maximum in the beginning sections and tube bends. In addition, it was observed that the fouling resistance varies from point to point along a horizontal tube and also for the same point it varies from replicate to replicate, i.e., the fouling resistance can be considered as a random variable and the scale formation is a random process. The experimental work can further be extended to study the fouling phenomenon under various simulated conditions of heat transfer, e.g., a double tube can be used and the effect, of a cooling stream in the exterior tube in counter, parallel or cross flow direction, on the scale deposit in the inner tube can be studied.

2. SEM analysis have indicated that the preferential sites for the crystals growth are scratches, polishing marks and other similar surface irregularities on the tube. This suggests that smoother the tube surface is kept during operation, the lesser would be the chances for early crystals growth and therefore the fouling of heat exchange equipment.
3. The data analysis regarding $CaCO_3$ scaling have shown that the distribution of time for tubes to reach a critical level of fouling is inverted normal or α -distribution, whereas the distribution of time to reach a critical level of corrosion fouling is modified version of α -distribution. A similar statistical analysis can be carried out for the fouling data of heat exchangers gathered from the field application for any type of fouling.
4. The statistical and thermoeconomic analysis of heat exchange equipment provides a mathematical basis for their maintenance/cleaning schedules.
5. The economic analysis for the specific heat exchanger used in the preheat train of crude oil refining process have shown that the daily operating costs would be minimum if a regular maintenance/cleaning is carried out every thirteen(13) days, which is found to be the same as discussed by [71] for a similar problem. Similarly for any other heat exchanger, the optimum cleaning cycle can be obtained by using the proposed algorithm.
6. The parametric study of the dimensionless cost function, derived for a partic-

ular case, has indicated that the total operating and maintenance costs (i.e., *Fuel Consumption + Antifoulant + Miscellaneous*) and optimum cleaning/maintenance period very sensitive to $\gamma_1 (= Q_{max}(k_H + k_S)/24(C_c' + C_A'))$, i.e., increasing the value of γ_1 substantially decreases the optimum period for maintenance/cleaning and increases the total costs. On the other hand, the variation in $\gamma_2 (= C_{AF}'/(C_c' + C_A'))$ and $\gamma_3 (= 1 + C_M/(C_c' + C_A')t_{down})$ have a relatively moderate effect on the total operating and maintenance costs and optimum cleaning/maintenance period.

7. The proposed cost model has been treated in a probabilistic domain by introducing the risk level p and the scatter parameter α in the expression for the fouling resistance. The resulting plots highlighted the impact of p and α on the total costs, optimum costs and optimum cleaning/maintenance period. It is observed that decreasing the risk level from 50% increases the total operating costs for the heat exchanger, and shifts the optimum solution to the left (reduction in cleaning period).

Appendix A

Statistical Characterization of Fouling Data

Let t be a random variable denoting the time to reach a critical level of fouling of a heat-exchanger. If ' N ' identical tubes are put in operation at some time $t = 0$, and operated till a critical level of fouling resistance then, in general, all of the tubes will experience a different time to reach a predetermined critical level of fouling resistance. These ' N ' observations of time $(t_1, t_2, t_3, \dots, t_N)$ to reach the critical level represent a set of realizations or an outcome of the random variable t . For example, this set of values of " t " can be determined from the set of sample functions of fouling growth curves. From these curves, at a critical-fouling level, the corresponding values of t_i can be obtained by linear interpolation between the available data points.

We note that the main indicators of the random variable t are [85]:

The mean time, \bar{t} , (often expressed as $E(t)$, $\mu(t)$ or μ), given by

$$\bar{t} = \frac{t_1 + t_2 + \dots + t_k + \dots + t_N}{N} = \frac{1}{N} \sum_{i=1}^N t_i \quad (\text{A.1})$$

The median time t_k , usually expressed as C , is the middle value of the ordered data and standard deviation $\sigma(t)$ given by:

$$\sigma(t) = \sqrt{\frac{(t_1 - \bar{t})^2 + (t_2 - \bar{t})^2 + \dots + (t_i - \bar{t})^2}{(N - 1)}} \quad (\text{A.2})$$

where the variance of time to reach a critical level of fouling is represented as $\sigma^2(t)$.

The coefficient of the time to reach a critical level of fouling can be expressed as

$$K = \frac{\sigma(t)}{\bar{t}} \quad (\text{A.3})$$

A.1 Empirical Distribution of Random Variable

” t ”

Empirical distribution of ” t ” is determined by a non-parametric approach [85]. In this approach, the experimental data obtained from field or laboratory experiments are usually treated in an ungrouped form. This data after ranking in increasing order is given by $t_1 > t_2 > t_3 > \dots > t_i > \dots > t_N$ for N units in a test. In

statistical nomenclature the t_i are referred to as the rank statistics of the test. We may estimate the fraction of the tubes to reach the critical level of fouling by time t_i , to be given by [85]:

Cumulative Distribution Function (cdf) expressed as

$$\hat{F}(t_i) = \frac{i}{N+1} \quad (\text{A.4})$$

The fraction of the tubes which have not yet reached the critical level of fouling by t_i , is defined by a complementary function of *CDF*, defined as *Reliability function* given by

$$\hat{R}(t_i) = \frac{N+1-i}{N+1} \quad (\text{A.5})$$

The *Probability Density Function (pdf)* defined by $dF(t)/dt = -dR(t)/dt$ is given by

$$\hat{f}(t) = \frac{1}{(t_{i+1} - t_i)(N+1)} \quad t_i < t < t_{i+1} \quad (\text{A.6})$$

The caret symbol is used to indicate estimates as opposed to true values.

A.2 The Postulated Distribution for $CaCO_3$ Scaling

The distribution of time to reach a critical level of fouling in the case of $CaCO_3$ scaling (precipitation fouling) is postulated as Inverted Normal (or α -distribution)

and is discussed in detail by Ahmed and Sheikh [79] and was later used in fouling analysis by Shaik [77]. The related functions are

$$R(t; \hat{\alpha}, \hat{C}) = 1 - \Phi \left[\frac{t - \hat{C}}{\sqrt{\hat{\alpha}} t} \right], \quad (\text{A.7})$$

$$f(t; \hat{\alpha}, \hat{C}) = \frac{\hat{C}}{\sqrt{2\pi\hat{\alpha}} t^2} \exp\left[-\frac{1}{2} \left(\frac{t - \hat{C}}{\sqrt{\hat{\alpha}} t}\right)^2\right] \quad (\text{A.8})$$

where $\Phi(z)$ is the Gaussian function or standardized normal *CDF*, given by

$$\Phi(z) = \frac{1}{\sqrt{2\pi}} \int_{-\infty}^z e^{-t^2/2} dt \quad (\text{A.9})$$

This function has a mean zero and standard deviation of 1. The total area under this function's curve is 1. The \hat{C} and $\hat{\alpha}$ represents the estimated parameters of the distribution. It should be noted that \hat{C} is the estimated value of median time to reach the critical fouling (i.e., $\hat{C} = t_{0.5}$), and $\sqrt{\hat{\alpha}}$ is the scatter parameter.

A.2.1 Estimation of Parameters C and α

There are two approaches to find the estimated parameters C and α from the data and are discussed below [79]:

From fouling growth curves

The parameters α and C in the case of linear fouling can be estimated from the slopes of the linearly fitted lines [77, 79]. These are:

$$\hat{\alpha} = \frac{V(m)}{[E(m)]^2} = \frac{\sum_{k=1}^N (m_k - \frac{1}{N} \sum_{i=1}^N m_i)^2 / (N - 1)}{(\frac{1}{N} \sum_{i=1}^N m_i)^2}, \quad (\text{A.10})$$

$$\hat{C} = \frac{R_{f,c}}{\frac{1}{N} \sum_{i=1}^N m_i} = \frac{R_{f,c}}{\bar{m}}, \quad (\text{A.11})$$

where m_i represent the slope of the i th fitted curve, $E(m)$ is the average of all the slopes, and $V(m)$ is the variance of the slope in a given set. This procedure is also called the damage function approach.

From times to reach a critical level of fouling

The equations for estimating the distribution parameters from N observations of time (i.e., t_1, t_2, \dots, t_N) to reach a critical level of fouling by maximum likelihood method are given by [79]

$$\hat{C} = \frac{1}{\frac{1}{N} \sum_{i=1}^N \frac{1}{t_i}}, \quad (\text{A.12})$$

$$\hat{\alpha} = \left[\frac{1}{N} \sum_{i=1}^N \left(\frac{1}{t_i} - \frac{1}{\hat{C}} \right)^2 \right] \hat{C}^2. \quad (\text{A.13})$$

It is important to emphasize that t_i are either direct values to reach the critical level of fouling or they could be linearly interpolated values between the data points. This procedure is also termed as maximum likelihood estimator approach.

A.3 Corrosion Fouling

The times to reach a critical level of the fouling resistance $R_{f,c}$ in the case of corrosion fouling was found to be represented by a modified version of α -distribution as proposed by Sheikh [78] and was later used by Shaik [77]. It's respective distribution

functions are given by [78]

$$R(t; \hat{\alpha}, \hat{C}) = 1 - \Phi\left[\frac{\sqrt{t} - \hat{C}}{\sqrt{\hat{\alpha}t}}\right], \quad (\text{A.14})$$

$$f(t; \hat{\alpha}, \hat{C}) = \frac{\hat{C}}{\sqrt{8\pi\hat{\alpha}t^3}} \exp\left[-\frac{1}{2}\left(\frac{\sqrt{t} - \hat{C}}{\sqrt{\hat{\alpha}t}}\right)^2\right]. \quad (\text{A.15})$$

where

$$\hat{\alpha} = \frac{V(m)}{[E(m)]^2} = \frac{\sum_{k=1}^N (m_k - \frac{1}{N} \sum_{i=1}^N m_i)^2 / (N-1)}{(\frac{1}{N} \sum_{i=1}^N m_i)^2}, \quad (\text{A.16})$$

and

$$\hat{C} = \frac{R_{f,c}}{\frac{1}{N} \sum_{i=1}^N m_i} = \frac{R_{f,c}}{\bar{m}}. \quad (\text{A.17})$$

Appendix B

Tabulated Results of

Reliability-Based Statistical Data

Analysis

The distribution functions calculated on the basis of time to reach a critical level of fouling by using equations (A.4) through (A.6) are shown in the attached tables B.1 through B.3 for sections 1, 2 & 3, respectively for $CaCO_3$ scaling and parameters calculated using both damage function approach as well as maximum likelihood estimator approach. Whereas results in the case of corrosion fouling are given in table B.4.

Table B.1: Parameters and non-parametric results for $CaCO_3$ scaling - Section #1.

Sr. No.	Slope m	Sr. No.	Slope m
1	6.42493E-06	4	9.35814E-06
2	8.67443E-06	5	9.75171E-06
3	9.60271E-06	6	1.01993E-05
m		9.00187E-06	
σ		1.35882E-06	

Fouling resistance		0.00003		m^2K/W	
Damage Function			Maximum Likelihood Est.		
$\sqrt{\alpha}$	0.150948277	$\sqrt{\alpha}$	0.077364661		
C (hrs)	3.332640559	C (hrs)	6.583797024		
Sr. No.	Rep. #	t_i	R(t_i)	f(t_i)	
1		0	1	0.023419	
2	2A	6.1	0.857142857	0.952381	
3	5	6.1	0.714285714	0.952381	
4	4	6.25	0.571428571	0.25974	
5	3	6.8	0.428571429	1.098901	
6	2	6.93	0.285714286	0.223214	
7	1	7.57	0.142857143	-	

Fouling resistance		0.00005		m^2K/W	
Damage Function			Maximum Likelihood Est.		
$\sqrt{\alpha}$	0.150948277	$\sqrt{\alpha}$	0.116897207		
C (hrs)	5.554400931	C (hrs)	8.925973985		
Sr. No.	Rep. #	t_i	R(t_i)	f(t_i)	
1		0	1	0.017358	
2	2A	8.23	0.857142857	0.510204	
3	5	8.23	0.714285714	0.510204	
4	4	8.51	0.571428571	1.298701	
5	3	8.62	0.428571429	0.460829	
6	2	8.93	0.285714286	0.047304	
7	1	11.95	0.142857143	-	

Fouling resistance		0.00007		m^2K/W	
Damage Function			Maximum Likelihood Est.		
$\sqrt{\alpha}$	0.150948277	$\sqrt{\alpha}$	0.086839555		
C (hrs)	7.776161304	C (hrs)	10.71878855		
Sr. No.	Rep. #	t_i	R(t_i)	f(t_i)	
1		0	1	0.014215	
2	5	10.05	0.857142857	0.714286	
3	2A	10.25	0.714285714	1.428571	
4	4	10.25	0.571428571	1.428571	
5	3	10.35	0.428571429	0.332226	
6	2	10.78	0.285714286	0.059032	
7	1	13.2	0.142857143	-	

Table B.2: Parameters and non-parametric results for $CaCO_3$ scaling - Section #2.

Sr. No.	Slope m	Sr. No.	Slope m
1	3.84572E-07	4	5.77579E-07
2	6.49345E-07	5	2.68976E-07
3	3.63716E-07	6	5.2076E-07
m		6.04655E-06	
σ		5.8213E-07	

Fouling resistance		0.00002		m^2K/W	
Damage Function			Maximum Likelihood Est.		
$\sqrt{\alpha}$	0.096274806	$\sqrt{\alpha}$	0.058335807		
C (hrs)	3.307672605	C (hrs)	5.996912081		
Sr. No.	Rep. #	t_i	$R(t_i)$	$f(t)$	
1		0	1	0.026455026	
2	2A	5.4	0.857142857	0.303951368	
3	3	5.87	0.714285714	0.840336134	
4	4	6.04	0.571428571	0.408163265	
5	5	6.04	0.428571429	0.408163265	
6	2	6.25	0.285714286	0.571428571	
7	1	6.5	0.142857143	-	

Fouling resistance		0.00004		m^2K/W	
Damage Function			Maximum Likelihood Est.		
$\sqrt{\alpha}$	0.096274806	$\sqrt{\alpha}$	0.062045471		
C (hrs)	6.61534521	C (hrs)	9.142717904		
Sr. No.	Rep. #	t_i	$R(t_i)$	$f(t)$	
1		0	1	0.016966407	
2	2A	8.42	0.857142857	0.793650794	
3	3	8.6	0.714285714	0.25974026	
4	2	9.15	0.571428571	0.285714286	
5	5	9.15	0.428571429	0.285714286	
6	4	9.65	0.285714286	0.317460317	
7	1	10.1	0.142857143	-	

Fouling resistance		0.00006		m^2K/W	
Damage Function			Maximum Likelihood Est.		
$\sqrt{\alpha}$	0.096274806	$\sqrt{\alpha}$	0.068347807		
C (hrs)	9.923017815	C (hrs)	12.11258233		
Sr. No.	Rep. #	t_i	$R(t_i)$	$f(t)$	
1		0	1	0.012755102	
2	2A	11.2	0.857142857	0.621118012	
3	3	11.43	0.714285714	0.386100386	
4	5	11.8	0.571428571	0.714285714	
5	2	12	0.428571429	0.155279503	
6	4	12.92	0.285714286	0.187969925	
7	1	13.68	0.142857143	-	

Table B.3: Parameters and non-parametric results for $CaCO_3$ scaling - Section #3.

Sr. No.	Slope m	Sr. No.	Slope m
1	3.88461E-06	4	4.97682E-06
2	4.08788E-06	5	5.3886E-06
3	4.65939E-06	6	5.64295E-06
m		4.77338E-06	
σ		6.99834E-07	

Fouling resistance		0.000045		m^2K/W	
Damage Function			Maximum Likelihood Est.		
$\sqrt{\alpha}$	0.14661204	$\sqrt{\alpha}$	0.091433164		
C (hrs)	4.189907156	C (hrs)	6.639699123		
Sr. No.	Rep. #	t_i	R(t_i)	f(t)	
1		0	1	0.024845	
2	5	5.75	0.857142857	0.190476	
3	4	6.5	0.714285714	0.510204	
4	2A	6.5	0.571428571	0.510204	
5	2	6.78	0.428571429	0.131062	
6	3	6.78	0.285714286	0.131062	
7	1	7.87	0.142857143	-	

Fouling resistance		0.0000325		m^2K/W	
Damage Function			Maximum Likelihood Est.		
$\sqrt{\alpha}$	0.14661204	$\sqrt{\alpha}$	0.086054748		
C (hrs)	6.808599128	C (hrs)	9.074559411		
Sr. No.	Rep. #	t_i	R(t_i)	f(t)	
1		0	1	0.017702	
2	5	8.07	0.857142857	0.269542	
3	4	8.6	0.714285714	0.47619	
4	2A	8.9	0.571428571	1.428571	
5	3	9	0.428571429	0.21978	
6	2	9.65	0.285714286	0.142857	
7	1	10.65	0.142857143	-	

Fouling resistance		0.00002		m^2K/W	
Damage Function			Maximum Likelihood Est.		
$\sqrt{\alpha}$	0.14661204	$\sqrt{\alpha}$	0.094844219		
C (hrs)	9.427291101	C (hrs)	11.53923702		
Sr. No.	Rep. #	t_i	R(t_i)	f(t)	
1		0	1	0.013897	
2	5	10.28	0.857142857	0.3861	
3	4	10.65	0.714285714	0.210084	
4	2A	11.33	0.571428571	0.104275	
5	3	11.33	0.428571429	0.104275	
6	2	12.7	0.285714286	0.15873	
7	1	13.6	0.142857143	-	

Table B.4: Parameters and non-parametric results for corrosion fouling.

Sr. No.	Slope m	Sr. No.	Slope m
1	0.000037	4	0.000013
2	0.000031	5	0.000012
3	0.000018	6	0.000022
m		0.000022	
σ		0.0000098	

Fouling Resistance 0.00014625 m ² K/W				
Damage Function				
$\sqrt{\alpha}$		0.44223		
C (hrs)		6.6064		
(t _i) ^{1/2}	Sp #	t _i	R(t)	f(t)
0		0	1	0.01102
3.6	4	12.96	0.85714	0.00292
3.6	5	12.96	0.71429	0.00294
7.85	6	61.6225	0.57143	0.00903
8.8	7	77.44	0.42857	0.00911
9.65	9	93.1225	0.28571	0.00179
13.15	8	172.923	0.14286	-

Fouling Resistance 0.00022 m ² K/W				
Damage Function				
$\sqrt{\alpha}$		0.44223		
C (hrs)		9.93783		
(t _i) ^{1/2}	Sp #	t _i	R(t)	f(t)
0		0	1	0.00667
5	4	25	0.83333	0.00211
5	5	25	0.66667	0.00211
10.2	9	104.04	0.5	0.00507
11.7	6	136.89	0.333333	0.00391
13.4	7	179.56	0.16667	-

Appendix C

Method for Determination of Enthalpy of Petroleum Fractions

The following equations are recommended [86] for estimating the enthalpy of petroleum fractions in liquid phase with $T_r \leq 0.8$ and $P_r \leq 1.0$

$$H_L = A_1(T - 259.7) + A_2(T^2 + 259.7^2) + A_3(T^3 + 259.7^3) \quad (C.1)$$

Where

$$H_L = \text{enthalpy of liquid petroleum fraction with } T_r \leq 0.8 \\ \text{and } P_r \leq 1.0, \text{ in british thermal units per pound} \quad (C.2)$$

$$A_1 = 10^{-3}[-1171.26 + (23.722 + 24.907 \text{ sp gr}) K + \frac{(1149.82 - 46.535 K)}{\text{sp gr}}] \quad (C.3)$$

$$A_2 = 10^{-6}[(1.0 + 0.82463 K)(56.086 - \frac{13.817}{sp\ gr})] \quad (C.4)$$

$$A_2 = 10^{-9}[(1.0 + 0.82463 K)(9.6757 - \frac{2.3653}{sp\ gr})] \quad (C.5)$$

$$P_r = \text{reduced pressure} = P/P_{pc} \quad (C.6)$$

$$P = \text{pressure, pounds per square inch absolute} \quad (C.7)$$

$$P_{pc} = \text{pseudocritical pressure, pounds per square inch absolute} \quad (C.8)$$

$$T_r = \text{reduced temperature} = T/T_{pc} \quad (C.9)$$

$$T = \text{temperature, degrees Rankine} \quad (C.10)$$

$$T_{pc} = \text{pseudocritical temperature, degrees Rankine} \quad (C.11)$$

$$K = \text{Watson characterization factor} \quad (C.12)$$

$$sp\ gr = \text{specific gravity, } 60F/60F \quad (C.13)$$

No correction for pressure effects is needed for the liquid phase below a reduced temperature of 0.8 and reduced pressure of 1.0.

Nomenclature

A_o	external surface area for heat transfer, ft^2 (m^2)
C	specific heat ratio, <i>dimensionless</i>
D	calendar <i>days</i>
e	fired heater efficiency, <i>dimensionless</i>
F	weight fraction, <i>dimensionless</i>
$FOEB$	fuel oil equivalent barrel
G	solute concentration of supersaturated solution
I	electrical current, <i>amp</i>
ΔH	change in enthalpy Btu/lb (kJ/kg)
k	thermal conductivity of $CaCO_3$, $Btu/h^\circ R ft^2$ ($W/m^2 K$)
l	length of a test section, <i>in</i> (m)
m	slope of the fitted curve
N	number of time values corresponding to a critical level of fouling
NHV	net heat value of fuel oil, Btu/lb (kJ/kg)
NTU	number of transfer units, <i>dimensionless</i>
p	risk factor, <i>dimensionless</i>
ppm	parts per million

q	volumetric flow rate, ft^3/hr (m^3/hr)
Q	amount of heat transferred, Btu/hr (<i>watts</i>)
r	radius of the tube section, <i>in</i> (m)
R	thermal resistance, $h^\circ F ft^2/Btu$ (m^2K/W)
t	time, <i>hrs</i> , <i>days</i>
T	Temperature, $^\circ R$ ($^\circ K$)
U	overall heat transfer coefficient, $Btu/h^\circ R ft^2$ (W/m^2K)
W	mass of flowing fluid, <i>lb</i> (kg)
A_1, A_2, A_3	constants for the petroleum fraction
\hat{C}	median time, <i>hrs</i> or <i>days</i>
C_p	specific heat value for a fluid, $Btu/lb^\circ R$ ($J/Kg^\circ K$)
k_H	cost of additional burned fuel, $U.S \$/Btu$ ($U.S \$/kJ$)
k_S	cost of additional atomization steam, $U.S \$/Btu$ ($U.S \$/kJ$)
R_f°	fouling resistance at time $t = 0$, $h^\circ F ft^2/Btu$ (m^2K/W)

Greek Symbols

α	scatter parameter, <i>dimensionless</i>
γ	weight density of $CaCO_3$, lb/ft^3 (kg/m^3)
γ_1	dimensionless unit cost reflecting the effect of fuel cost
γ_2	dimensionless unit cost reflecting the effect of antifoulant cost
γ_3	dimensionless unit cost reflecting the effect of miscellaneous costs

Γ	dimensionless total cost
ϵ	effectiveness of heat-exchanger, <i>dimensionless</i>
ρ	specific gravity of crude oil, <i>dimensionless</i>
ϵ_n°	effectiveness of heat-exchanger at time $t = 0$

Subscripts

A	additional fuel
ad	additional steam
AF	antifoulant
c	cold
ci	cold fluid at inlet
co	cold fluid at outlet
cyc	cycle
$down$	shutdown
f	fouling
f,c	critical fouling
h	hot
hi	hot fluid at inlet
ho	hot fluid at outlet
H	heat
min	minimum

<i>max</i>	maximum
<i>M</i>	miscellaneous
<i>n</i>	number of shell passes
<i>O/T</i>	fuel oil/(fuel oil+ fuel gas)
<i>S/O</i>	steam/fuel oil
<i>S</i>	steam

References

- [1] E. F. C. Somerscales and J. G. Knudsen, eds. *Fouling of Heat Transfer Equipment*. Hemisphere, Washington D.C., 1981.
- [2] B. A. Garrett-Price, S. A. Smith, R. L. Watts, J. G. Knudsen, W. J. Marner, and J. W. Sutor, eds. *Fouling of Heat Exchangers*. Noyes, New Jersey, 1985.
- [3] J. Taborek, T. Aoki, R.B. Ritter, J.W. Palen, and J.G. Knudsen. Fouling: The major unresolved problem in heat transfer. *Chemical Engineering Progress*, Vol.68(2); pp.59–67, 1972.
- [4] J. G. Knudsen. Fouling in heat-exchangers. *Seventh International Fouling Conference*, 1982.
- [5] J. G. Knudsen. Fouling of heat exchangers: Are we solving the problem? *21st National Heat Transfer Conference*, July 1983.
- [6] D. Q. Kern and R. E. Seaton. A theoretical analysis of thermal surface fouling. *British Chemical Engineering*, Vol.4(5); pp.258–262, 1959.

- [7] J. M. Chenoweth. Final report of the HTRI/TEMA committee to review the fouling section of the TEMA standards. *Heat Transfer Engineering*, Vol.11(1); pp.73–107, 1990.
- [8] J. Taborek and G. Aurioles. Effect of 1988 TEMA standards on mechanical and thermo-hydraulic design of shell and tube heat-exchangers. *AIChE Symposium Series*, Vol.85(269); pp.79–83, 1989.
- [9] P. A. Pilavachi and J. D. Isdale. European community R&D strategy in the field of heat exchanger fouling: Projects. *Heat Recovery Systems & CHP*, Vol.13(2); pp.133–138, 1993.
- [10] J. E. Hesselgreaves. The effect of system parameters on the fouling performance of heat exchangers. *ICHEME Symposium Series No. 129*, pp.995–1006, 1992.
- [11] A. M. Konings. Guide values for the fouling resistances of cooling water with different types of treatment for design of shell-and-tube heat exchangers. *Heat Transfer Engineering*, Vol.10(4); pp.54–61, 1989.
- [12] A. P. Watkinson. Fouling of augmented heat transfer tubes. *Heat Transfer Engineering*, Vol.11(3); pp.57–65, 1990.
- [13] D. C. Thompson and Bridgwater. Plant demonstration of a technique to measure the local fouling resistance. *ICHEME Symposium Series No. 129*, pp.979–985, 1992.

- [14] B. D. Crittenden and E. H. Khater. Economic fouling resistance selection. In E. F. C. Somerscales and J. G. Knudsen, eds, *Fouling of Heat Transfer Equipment*, pp.645–652, Washington D.C., 1981. Hemisphere.
- [15] T. R. Bott, ed. *Fouling Notebook*. Institution of Chemical Engineers, Rugby, England, 1990.
- [16] H. M. Steinhagen and R. Blochl. Particulate fouling in heat exchangers. *Transactions EMCh - Institution of Professional Engineers, New Zealand*, Vol.15; pp.109–118, 1988.
- [17] N. H. Kim and R. L. Webb. Particulate fouling of water in tubes having a two-dimensional roughness geometry. *International Journal of Heat and Mass Transfer*, 34(11); pp.2727–2738, 1991.
- [18] H. M. Steinhagen, F. Reif, N. Epstein, and A. P. Watkinson. Influence of operating conditions on particulate fouling. *The Canadian Journal of Chemical Engineering*, Vol.66; pp.42–50, February 1988.
- [19] S. H. Chan, H. Rau, C. DeBellis, and K. F. Neusen. Silica fouling of heat transfer equipment-experiments and model. *Journal of Heat Transfer*, Vol.110; pp.841–849, 1988.
- [20] K. F. Neusen, S. H. Chan, and D. Z. Zhou. *Heat Transfer in Geophysical and Geothermal Systems*, Vol. 76, pp.45–50. ASME HTD, New York, 1987.

- [21] L. Oufer and J. G. Knudsen. Modelling chemical reaction fouling under sub-cooled boiling conditions. *AIChE Symposium Series*, Vol.89(289); pp.308–313, 1993.
- [22] C. B. Panchal and A. P. Watkinson. Chemical reaction fouling model for single-phase heat transfer. *AIChE Symposium Series*, Vol.89(289); pp.323–334, 1993.
- [23] P. J. Fryer, P. J. Hobin, and S. P. Mawer. Optimal design of heat exchanger undergoing reaction fouling. *The Canadian Journal of Chemical Engineering*, Vol.66; pp.558–562, August 1988.
- [24] E. F. C. Somerscales. Corrosion fouling. In J. M. Chenoweth and M. Impaggi-
azzo, eds, *Fouling in Heat Exchange Equipment*, Vol. 17, pp.17–27, New York,
1981. ASME HTD.
- [25] F. J. Witt. Corrosion and fouling concerns of service water piping and heat
exchanger components: A regulatory perspective. In J. R. Maurer and A. L.
Steel, eds., *Practical Aspects and Performance of Heat Exchanger Components
and Materials*, Vol. 14, pp. 1–4, New York, 1991. ASME PWR.
- [26] C. B. Panchal and D. S. Saccerc. Biofouling and corrosion fouling of plain
and enhanced Aluminum surfaces. In T. J. Rabas and J. M. Chenoweth, eds.,
Fouling and Enhancement Interactions, Vol. 164, pp.9–15, New York, 1991.
ASME HTD.

- [27] D. H. Lister. Corrosion products in power generating systems. In E. F. C. Somerscales and J. G. Knudsen, eds., *Fouling of Heat Transfer Equipment*, pp.135–200, Washington D.C., 1981. Hemisphere.
- [28] S. K. Beal and R. C. Armstrong. A model to predict the particle size distribution in a system with corrosion fouling. In J. M. Chenoweth and M. Impagliazzo, eds., *Fouling in Heat Exchange Equipment*, Vol. 17, pp.89–95, New York, 1981. ASME HTD.
- [29] E. F. C. Somerscales and M. Kassemi. Fouling due to corrosion products formed on a heat-transfer surface. *Transactions of the ASME, J. of Heat Transfer*, Vol.109; pp.267–271, 1987.
- [30] D. Hasson. Precipitation fouling. In E. F. C. Somerscales and J. G. Knudsen, eds., *Fouling of Heat Transfer Equipment*, pp.527–568, Washington D.C., 1981. Hemisphere.
- [31] H. Roques and A. Girou. Kinetics of formation conditions of carbonate tartars. *Water Research*, Vol.8; pp.907–, 1974.
- [32] H. N. S. Wiechers, P. Sturrock, and G. V. R. Marais. $CaCO_3$ crystallization kinetics. *Water Research*, Vol.9; pp.835, 1975.
- [33] P. J. Fryer. Modelling the behavior of heat exchangers undergoing scaling. *Geothermics*, Vol.18; pp.89–96, 1989.

- [34] R. W. Morse and J. G. Knudsen. Effect of alkalinity on the scaling of simulated cooling tower water. *The Canadian Journal of Chemical Engineering*, Vol.55; pp.272–278, 1977.
- [35] M. Story and J. G. Knudsen. The effect of heat transfer surface temperature on the scaling behavior of simulated cooling tower water. *AIChE Symposium Series*, Vol.74(124); pp.25–30, 1978.
- [36] S. H. Lee and J. G. Knudsen. Scaling characteristics of cooling tower water. *ASHRAE Transactions*, Vol.85(1); pp.281–302, 1979.
- [37] K. E. Coates and J. G. Knudsen. Calcium carbonate scaling characteristics of cooling tower water. *ASHRAE Transactions*, Vol.86(2); pp.68–91, 1980.
- [38] O. V. Tretyakov, V. G. Kristskiy, and P. S. Styazhkin. Improved prediction of the formation of calcium carbonate scale in heat exchangers of secondary loops of conventional thermal and nuclear power plants. *Heat Transfer - Soviet Research*, Vol.23(4); pp.532–538, 1991.
- [39] C. A. Branch and H. M. M. Steinhagen. Influence of scaling on the performance of shell-and-tube heat exchangers. *Heat Transfer Engineering*, Vol.12(2); pp.37–45, 1991.

- [40] E. S. Gaddis and E. U. Schlunder. Temperature distribution and heat exchange in multipass shell-and-tube exchangers with baffles. *Heat Transfer Engineering*, Vol.1(1), 1979.
- [41] S. R. Yang, J. M. Wang, G. D. Zai, and R. H. Kim. Investigation of heat transfer augments as a fouling cleaner and its optimum geometry in the tube side of a condenser. *Experimental, Thermal and Fluid Science*, Vol.5; pp.795–802, 1992.
- [42] R. H. Kim. A new approach to fouling cleaning and heat transfer enhancement and its conceptual implementation. In T. J. Rabas and J. M. Chenoweth, eds., *Fouling and Enhancement Interactions*, Vol. 164, pp.39–45, New York, 1991. ASME HTD.
- [43] G. Dickakian. *Heat Transfer Equipment Fundamentals, Design, Applications and Operating Problems*, Vol. 108, pp.331–336. ASME HTD, New York, 1990.
- [44] B. D. Crittenden, S. T. Kolaczkowski, and T. Takemoto. Use of in-tube inserts to reduce fouling from crude oils. *AIChE Symposium Series*, Vol.89(289); pp.300–307, 1993.
- [45] H. Miyuki, T. Kudo, N. Haruki, T. Kimura, and M. Kuroda. *Practical Aspects and Performance of Heat Exchanger Components and Materials*, Vol. 19, pp.1–8. ASME PWR, New York, 1992.

- [46] R. Schwarz, R. Tombaugh, and D. Papanek. *Practical Aspects and Performance of Heat Exchanger Components and Materials*, Vol. 19, pp.1–8. ASME PWR, New York, 1992.
- [47] J. G. Knudsen. Coping with cooling water fouling in tubular heat exchangers. *AIChE Symposium Series*, Vol.85(269); pp.1–12, 1989.
- [48] A. M. Pritchard. Fouling - science or art. In E. F. C. Somerscales and J. G. Knudsen, eds., *Fouling of Heat Transfer Equipment*, pp.513–523, Washington D.C., 1981. Hemisphere.
- [49] P. A. Thackery. The cost of fouling in heat exchanger plant. In A. M. Pritchard, ed., *Fouling-Science or Art*, Guildford, U.K, March 27-28 1979.
- [50] W. L. Van Nostrand, S. H. Leach, and J. L. Haluska. Economic penalties associated with the fouling of refinery heat transfer equipment. In E. F. C. Somerscales and J. G. Knudsen, eds., *Fouling of Heat Transfer Equipment*, pp.619–643, Washington D.C., 1981. Hemisphere.
- [51] R. Steinhagen, H. M. Steinhagen, and K. Maani. Problems and costs due to heat exchanger fouling in New Zealand industries. *Heat Transfer Engineering*, Vol.14(1); pp.19–30, 1993.

- [52] E. F. Melo, T. R. Bott, and C. A. Bernardo, eds. *Fouling Science and Technology - NATO ASI Series*. Kluwer Academic Publishers, Washington D.C., 1987.
- [53] P. L. Curlett and A. M. Impagliazzo. The impact of condenser tube fouling on power plant design and economics. In J. M. Chenoweth and M. Impagliazzo, eds., *Fouling in Heat Exchange Equipment*, Vol. 17, pp.45-59, New York, 1981. ASME HTD.
- [54] S. S. Penner, S. B. Alpert, J. M. Beer, C. R. Bozzuto, I. Glassman, R. B. Knust, Markert Jr., A. K. Oppenheim, L. D. Smoot, R. E. Sommerland, C. L. Wagoner, I. Wender, W. Wolowowdiuk, and K. E. Yeager. Developing coal-combustion technologies. *Prog. Energy Combust. Sci.*, Vol.10(1); pp.87-144, 1984.
- [55] H. A. Schlesinger. Economics of alternatives for OTEC biofouling protection. In *OTEC Biofouling and Corrosion Symposium*, Seattle, October 1977.
- [56] J. L. Kasper, W. Chow, J. Graham, and Y. G. Musalli. Use and cost of chlorination systems. *Power Engineering*, pp.54-57, October 1983.
- [57] W. A. Hendrix and G. H. Hoyos. Conserving boiler energy. *Chemical Engineering*, Vol.86(28); pp.77-78, 1979.
- [58] Betz Ltd. Water treatment for boilers. *Processing*, July/August 1980.

- [59] R. J. Terrell. The economics of cooling - from birth onwards. In *Fouling and Cleaning of Heat Exchangers*, Liverpool, March 1986.
- [60] P. Hinckley. How to avoid problems of waste heat boilers. *Chemical Engineering*, Vol.82(18); pp.94-98, 1975.
- [61] J. G. Collier. Reliability problems of heat transfer equipment. *Heat Transfer Engineering*, Vol.4(3); pp.51-62, 1983.
- [62] N Epstein. Optimum evaporator cycles with scale formation. In E. F. C. Somerscales and J. G. Knudsen, eds., *Fouling of Heat Transfer Equipment*, pp.653-659, Washington D.C., 1981. Hemisphere.
- [63] G. P. Singh and R. Tweddell. *Practical Aspects and Performance of Heat Exchanger Components and Materials*, Vol. 19, pp.85-91. ASME PWR, New York, 1992.
- [64] S. M. Zubair, A. K. Sheikh, and M. N. Shaik. A probabilistic approach to the maintenance of heat-transfer equipment subject to fouling. *Energy*, Vol.17(8); pp.769-776, 1992.
- [65] J. F. Axsom. Exchanger cleaning method cuts costs, ups throughput. *The Oil and Gas Journal*, pp.71-72, June 1977.
- [66] M. T. Syed, S. A. Sherif, and T. N. Veriroglu. *Solar Energy in 1990's*, Vol. 10, pp.77-87. ASME SED, New York, 1990.

- [67] I. Walker and A. W. Cockerill. Mathematics raises nuclear power plant maintenance efficiency. *Power Engineering*, pp.28–31, December 1989.
- [68] J. Barton. Method improves pyrolysis. *Oil and Gas Journal*, pp.81–84, January 1990.
- [69] W. E Wang and R. H. Ge. Determination of power condenser optimum cleanliness. In J. R. Maurer and A. L. Steel, eds., *Practical Aspects and Performance of Heat Exchanger Components and Materials*, Vol. 14, pp. 57–60, New York, 1991. ASME PWR.
- [70] R. S. T. Ma and N. Epstein. Optimum cycles for falling rate processes. *The Canadian Journal of Chemical Engineering*, Vol.59; pp.631–633, October 1981.
- [71] E. Casado. Model optimizes exchanger cleaning. *Hydrocarbon Processing*, Vol.69(8); pp.71–76, August 1990.
- [72] SAUDI ARAMCO Internal Document - Analysis of scale/deposit in heat exchangers, Rastanura refinery. January 1992.
- [73] J. C. Cowan and D. J. Weiritt, eds. *Water-Formed Scale Deposits*. Gulf Publishing Co., Houston, Texas, 1976.
- [74] A. Bejan. *Heat Transfer*. John Wiley, New York, 1993.
- [75] R. H. Perry and D. Green. *Perry's Chemical Engineer' Handbook*. McGraw-Hill international editions.

- [76] J. O. Bockris and A. K. N. Reddy, eds. *Modern Electrochemistry*, Vol. 2, pp.1177–1182. Macdonalds, London, England, 1970.
- [77] M. N. Shaik, ed. *Reliable Life-Prediction Models for Various Material Damage Processes*. King Fahd University of Petroleum and Minerals, Dhahran, 1990.
- [78] A. K. Sheikh. *Generalized Non-linear Damage Process and Reliability Models*. Unpublished work, 1990.
- [79] M. Ahmed and A. K. Sheikh. Bernstein reliability model: Derivation and estimation of parameters. *Reliability Engineering*, Vol.8; pp.131–148, 1984.
- [80] B. Brixey and T. Eckert. Thermal performance operability. In J. R. Maurer and A. L. Steel, eds., *Practical Aspects and Performance of Heat Exchanger Components and Materials*, Vol. 14, pp. 15–18, New York, 1991. ASME PWR.
- [81] J. L. Hughes Jr. Containment heat exchangers tubeside cleaning program at NRC G.L. 89-13. In J. R. Maurer and A. L. Steel, eds., *Practical Aspects and Performance of Heat Exchanger Components and Materials*, Vol. 14, pp. 1–4, New York, 1991. ASME PWR.
- [82] Y. Musalli, E. G. Hecker, M. Padmanabhan, C. Cooper, and M. Whitt. Improved on-line condenser cleaning ball distribution. In J. R. Maurer and A. L. Steel, eds., *Practical Aspects and Performance of Heat Exchanger Components and Materials*, Vol. 14, pp. 51–56, New York, 1991. ASME PWR.

- [83] M. J. Hager. Selection, operation and maintenance experience with flat plate heat exchangers. In J. R. Maurer and A. L. Steel, eds., *Practical Aspects and Performance of Heat Exchanger Components and Materials*, Vol. 14, pp. 41–45, New York, 1991. ASME PWR.
- [84] B. Hornery, A. Hovland, and K. Mastin. Condenser tube cleaning reduces fuel consumption and greenhouse emissions. In J. R. Maurer and A. L. Steel, eds., *Practical Aspects and Performance of Heat Exchanger Components and Materials*, Vol. 14, pp. 47–49, New York, 1991. ASME PWR.
- [85] K. C. Kapur and L. R. Lamberson, eds. *Reliability in Engineering Design*. John Wiley, New York, 1977.
- [86] *API Data Book - Petroleum Refining Procedure 7B4.7*, pp.133–134. American Petroleum Institute, 1978.

Vita

- Manzoor-ul-Haq
- Born in Lahore, Pakistan
- Received Bachelor's degree in Mechanical Engineering from University of Engineering & Technology, Lahore, Pakistan in January 1988.
- Have served an Engineering Consultancy firm in Pakistan for about four years before starting Master's program in September 1992.
- Completed Master's degree in Mechanical Engineering at King Fahd University of Petroleum and Minerals, Dhahran, Saudi Arabia in April, 1995.